Electronic Supplementary Material (ESI) for Organic Chemistry Frontiers.


# Supporting Information

## Phloroglucinol heterodimers and bis-indolyl alkaloids from the Sponge-Derived Fungus *Aspergillus* sp. SCSIO 41018

Cui Guo,[a,b] Pei Wang,[c] Xiuping Lin,[a] Limbadri Salendra,[a,b] Fandong Kong,[c] Shengrong Liao,[a] Bin Yang,[a] Xuefeng Zhou,[a] Junfeng Wang*,[a] and Yonghong Liu*,[a,b,d]

## Table of Contents


| Contents | page |
|---|---|
| **Experimental Details** | 5 |
| **Table S1**. Stable conformers of **3a**–**3g** | 10 |
| **The strain's (*Aspergillus* sp. SCSIO41018) ITS sequence of the rDNA.** | 11 |
| **Table S2**. $^{1}H$ and $^{13}C$ NMR data in $CDCl_3$ for **4–6** (700, 175 MHz, TMS, $\delta$ ppm) | 12 |
| **Table S3**. $^{1}H$ and $^{13}C$ NMR data in $CDCl_3$ for **7–9** (700, 175 MHz, TMS, $\delta$ ppm) | 13 |
| **Figure S1.** The ORTEP drawing of compound **12** | 15 |
| **Figure S2**. The $^{1}H$ NMR spectrum of gilluone A (**1)** in$CD_3OD$(700 MHZ) | 16 |
| **Figure S3**. The $^{13}C$ NMR spectrum of gilluone A (**1)** in $CD_3OD$(175 MHz) | 16 |
| **Figure S4**. The DEPT spectrum of gilluone A (**1)** in $CD_3OD$(175 MHz) | 17 |
| **Figure S5**. The HSQC spectrum of gilluone A (**1)** in $CD_3OD$ | 17 |
| **Figure S6**. The $^{1}H$-$^{1}H$ COSY spectrum of gilluone A (**1)** in $CD_3OD$ | 18 |
| **Figure S7**. The HMBC spectrum of gilluone A (**1)** in $CD_3OD$ | 18 |
| **Figure S8**. The HRESIMS spectrum ofgilluone A (**1)** | 19 |
| **Figure S9**. The UV spectrum of gilluone A (**1)** | 20 |
| **Figure S10**. The $^{1}H$ NMR spectrum of gilluone B(**2)** inDMSO-$d_6$(700 MHZ) | 21 |
| **Figure S11**. The $^{13}C$ NMR spectrum of gilluone B (**2)** in DMSO-$d_6$(175 MHz) | 21 |
| **Figure S12**. The DEPT spectrum of gilluone B (**2)** in DMSO-$d_6$(175 MHz) | 22 |
| **Figure S13**. The HSQC spectrum of gilluone B(**2)** in DMSO-$d_6$ | 22 |
| **Figure S14**. The $^{1}H$-$^{1}H$ COSY spectrum of gilluone B(**2)** in DMSO-$d_6$ | 23 |
| **Figure S15**. The HMBC spectrum of gilluone B (**2)** in DMSO-$d_6$ | 23 |
| **Figure S16**. The HRESIMS spectrum of gilluone B (**2)** | 24 |
| **Figure S17**.The UV spectrum of gilluone B (**2)** | 25 |
| **Figure S18**. The $^{1}H$ NMR spectrum of gilluone C (**3)** in $CDCl_3$ (700 MHz) | 26 |
| **Figure S19**. The $^{13}C$ NMR spectrum of gilluone C (**3)** in $CDCl_3$ (175 MHz) | 26 |
| **Figure S20**. The DEPT spectrum of gilluone C (**3)** in $CDCl_3$ (175 MHz) | 27 |
| **Figure S21**. The HSQC spectrum of gilluone C (**3)** in $CDCl_3$ | 27 |
| **Figure S22**. The $^{1}H$-$^{1}H$ COSY spectrum of gilluone C (**3)** in $CDCl_3$ | 28 |
| **Figure S23**. The HMBC spectrum of gilluone C (**3)** in $CDCl_3$ | 28 |

**Figure S24**. The NOESY spectrum of gilluone C (**3)** in $CDCl_3$ 29

**Figure S25**. The NOE difference experiments of gilluone C (**3)** in $CDCl_3$ 30

**Figure S26**. The HRESIMS spectrum of gilluone C (**3)** 31

**Figure S27**. The UV spectrum of gilluone C (**3)** 32

**Figure S28**. The $^1$H NMR spectrum of asterriquinone I (**4)** in $CDCl_3$ (700 MHz) 32

**Figure S29**. The $^{13}$C NMR spectrum of asterriquinone I (**4)** in $CDCl_3$ (175 MHz) 33

**Figure S30**. The DEPT spectrum of asterriquinone I (**4)** in $CDCl_3$ (175 MHz) 33

**Figure S31**. The HSQC spectrum of asterriquinone I (**4)** in $CDCl_3$ 34

**Figure S32**. The $^1$H-$^1$H COSY spectrum of asterriquinone I (**4)** in $CDCl_3$ 34

**Figure S33**. The HMBC spectrum of asterriquinone I (**4)** in $CDCl_3$ 35

**Figure S34**. The HRESIMS spectrum of asterriquinone I (**4)** 36

**Figure S35**. The UV spectrum of asterriquinone I (**4)** 37

**Figure S36**. The $^1$H NMR spectrum of asterriquinone J (**5**) in $CDCl_3$ (700 MHz) 37

**Figure S37**. The $^{13}$C NMR spectrum of asterriquinone J (**5**) in $CDCl_3$ (175 MHz) 38

**Figure S38**. The DEPT spectrum of asterriquinone J (**5**) in $CDCl_3$ (175 MHz) 38

**Figure S39**. The HSQC spectrum of asterriquinone J (**5**) in $CDCl_3$ 39

**Figure S40**. The $^1$H-$^1$H COSY spectrum of asterriquinone J (**5**) in $CDCl_3$ 39

**Figure S41**. The HMBC spectrum of asterriquinone J (**5**) in $CDCl_3$ 40

**Figure S42**. The HRESIMS spectrum of asterriquinone J (**5**) 41

**Figure S43**. The UV spectrum of asterriquinone J (**5**) 42

**Figure S44**. The $^1$H NMR spectrum of asterriquinone K (**6**)in $CDCl_3$ (700 MHz) 42

**Figure S45**. The $^{13}$C NMR spectrum of asterriquinone K (**6**) in $CDCl_3$ (175 MHz) 43

**Figure S46**. The DEPT spectrum of asterriquinone K (**6**) in $CDCl_3$ (175 MHz) 43

**Figure S47**. The HSQC spectrum of asterriquinone K (**6**) in $CDCl_3$ 44

**Figure S48**. The $^1$H-$^1$H COSY spectrum of asterriquinone K (**6**) in $CDCl_3$ 44

**Figure S49**. The HMBC spectrum of asterriquinone K (**6**) in $CDCl_3$ 45

**Figure S50**. The HRESIMS spectrum of asterriquinone K (**6**) 46

**Figure S51**. The UV spectrum of asterriquinone K (**6**) 47

**Figure S52**. The $^1$H NMR spectrum of asterriquinol G (**7**) in $CDCl_3$(700 MHz) 47

**Figure S53**. The $^{13}C$ NMR spectrum of asterriquinol G (**7**) in $CDCl_3$(175 MHz) 48

**Figure S54**. The DEPT spectrum of asterriquinol G (**7**) in $CDCl_3$(175 MHz) 48

**Figure S55**. The HSQC spectrum of asterriquinol G (**7**) in $CDCl_3$ 49

**Figure S56**. The $^{1}H$-$^{1}H$ COSY spectrum of asterriquinol G (**7**) in $CDCl_3$ 49

**Figure S57**. The HMBC spectrum of asterriquinol G (**7**) in $CDCl_3$ 50

**Figure S58**. The HRESIMS spectrum of asterriquinol G (**7**) 51

**Figure S59**. The UV spectrum of asterriquinol G (**7**) 52

**Figure S60**. The $^{1}H$ NMR spectrum of asterriquinol H (**8**) in $CDCl_3$ (700 MHz) 52

**Figure S61**. The $^{13}C$ NMR spectrum of asterriquinol H (**8**) in $CDCl_3$ (175 MHz) 53

**Figure S62**. The DEPT spectrum of asterriquinol H (**8**) in $CDCl_3$ (175 MHz) 53

**Figure S63**. The HSQC spectrum of asterriquinol H (**8**) in $CDCl_3$ 54

**Figure S64**. The $^{1}H$-$^{1}H$ COSY spectrum of asterriquinol H (**8**) in $CDCl_3$ 54

**Figure S65**. The HMBC spectrum of asterriquinol H (**8**) in $CDCl_3$ 55

**Figure S66**. The HRESIMS spectrum of asterriquinol H (**8**) 56

**Figure S67**.The UV spectrum of asterriquinol H (**8**) 57

**Figure S68**. The $^{1}H$ NMR spectrum of asterriquinol I (**9**) in $CDCl_3$ (500 MHz) 57

**Figure S69**. The $^{13}C$ NMR spectrum of asterriquinol I (**9**) in $CDCl_3$ (125 MHz) 58

**Figure S70**. The DEPT spectrum of asterriquinol I (**9**) in $CDCl_3$ (125 MHz) 58

**Figure S71**. The HSQC spectrum of asterriquinol I (**9**) in $CDCl_3$ 59

**Figure S72**. The $^{1}H$-$^{1}H$ COSY spectrum of asterriquinol I (**9**) in $CDCl_3$ 59

**Figure S73**. The HMBC spectrum of asterriquinol I (**9**) in $CDCl_3$ 60

**Figure S74**. The HRESIMS spectrum of asterriquinol I (**9**) 61

**Figure S75**. The UV spectrum of asterriquinol I (**9**) 62

## Experimental Details

**General Experimental Procedures.** NMR spectra were obtained on a Bruker Avance spectrometer (Bruker) operating at 500 and 700 MHz for $^{1}$HNMR 125 and 175 MHz for $^{13}$CNMR with TMS as the internal reference. HRESIMS spectra data were measured with a Brukerma Xisquadrupole-time-of-flight mass spectrometer (Bruker). Optical rotations were recorded on a PerkinElmer MPC 500 (Waltham) polarimeter. UV spectra were acquired using a Shimadzu UV-2600 PC spectrometer (Shimadzu). ECD spectra were measured with a Chirascan circular dichroism spectrometer (Applied Photophysics). X-ray diffraction intensity data were collected on a CrysAlis PRO CCD area detector diffractometer with graphite-monochromated Cu K$\alpha$ radiation ($\lambda$ = 1.54184). TLC and column chromatography (CC) were performed on plates precoated with silica gel GF254 (10-40 $\mu$m) and over silia gel (200-300 mesh) (Qingdao Marine Chemical Factory) and Sephadex LH-20 (Amersham Biosciences), respectively. Spots were detected on TLC (Qingdao Marine Chemical Factory) under 254 nm UV light. All solvents employed were of analytical grade (Tianjin Fuyu Chemical and Industry Factory). Semi-preparative HPLC was carried out using an ODS column (YMC-pack ODS-A, YMC Co. Ltd., 10×250 mm, 5 $\mu$m, 2 mL/min). The (*R*)/(*S*)-(-)-$\alpha$-methoxy-$\alpha$-(trifluoromethyl)phenylacetyl chloride (Beijing J&K Scientific) were used as chiral reagent in the Mosher's method. The artificial sea salt was a commercial product (Guangzhou Haili Aquarium Technology Company).

**Fungal Material.** The strain was isolated from sponge (Xuwen Guangdong Provience). This strain was stored on MB ager slants at 4°C and then deposited at the Marine Microbial collection center of CAS Key Laboratory of Tropical Marine Bio-resources and Ecology. It was identified as a member of the genus *Aspergillus* sp. SCSIO41018on the basis of its ITS phylogenetic analyses of the rDNA as described in the Supporting Information. (NCBI Gen Bank accession number MH109740.1).

**Fermentation.** The strain *Aspergillus* sp. SCSIO41018 stored on MB ager slants at 4 °C was cultured on MB ager plants and incubated at 25°C for 7 days. Seed medium (malt extract 15 g, sea salt 10 g, distilled water 1.0 L) inoculated with *Aspergillus* sp. SCSIO41018 and incubated at 25 °C for 2 days on a rotating shaker (180 rpm, 25 °C). Then, large-scale fermentation in a solid rice medium of 1000 mL flasks (rice 200 g, sea salt 2.5 g, distilled water 200 mL) (n=48) was

inoculated with 10 mL of seed solution. Flasks were incubated at 25 °C under static condition and fermented for 60 days.

**Extraction and Isolation.** Strain cultures were harvested after 60 days. Then fungal mycelium was cut into small pieces and immersed into acetone for 2 days, sonicated for 10min and filtered using gauze, yielding the rice solid medium and water phases, which were extracted with EtOAC (6*1L and 6*10L, respectively). Both organic extracts were combined to gain 220 g of crude extract. The all of crude EtOAC extract was subjected to silica gel column chromatography and eluted with petroleum ether/$CH_2Cl_2$ in gradient eluent (100:0–0:100), and followed by $CH_2Cl_2$/MeOH in gradient eluent (99:1–0:100) to yield eight fractions (fractions 1–8). Fraction 3 (38.0 g) was applied to C-18 reversed-phase column ($H_2O$/MeCN, 95:5-0:100), gaining seventeen subfractions ($Fr._{3-1}$–$Fr._{3-17}$). $Fr._{3-12}$ was further purified by semi-preparative reversed-phase HPLC (40% MeCN/$H_2O$, 2 mL/min) to yield **7** (3.2 mg, $t_R$ 22 min). $Fr._{3-14}$ was separated by semi-preparative reversed-phase HPLC (80% MeOH/$H_2O$, 2 mL/min) to yield **8** (8.3 mg, $t_R$20 min), and **10** (59.3 mg, $t_R$25 min). $Fr._{3-15}$ was separated by semi-preparative reversed-phase HPLC (75% MeOH/$H_2O$, 2 mL/min) to yield **3** (3.6 mg, $t_R$11 min). Fraction 4 (15.4 g) was applied to C-18 reversed-phase column ($H_2O$/MeOH, 95:5–0:100), gaining eighteen subfractions ($Fr._{4-1}$–$Fr._{4-18}$). $F_{4-4}$ was further purified by semi-preparative reversed-phase HPLC (45% MeCN/$H_2O$, 2 mL/min) to yield **2** (20 mg, $t_R$ 24 min). $Fr._{4-9}$ was further purified by semi-preparative reversed-phase HPLC (60% MeOH/$H_2O$, 2 mL/min) to yield **1** (2.8 mg, $t_R$18 min). $Fr._{4-13}$ was further purified by semi-preparative reversed-phase HPLC (56% MeOH/$H_2O$, 2 mL/min) to yield **14** (1.5 mg, $t_R$ 23 min). $Fr._{4-14}$ was purified by HPLC (72% MeOH/$H_2O$, 2 mL/min) to yield **12** (38.9 mg, $t_R$40 min). $Fr._{4-15}$ was directly separated by HPLC (70% MeOH/$H_2O$, 2 mL/min) to yield **13** (3.3 mg, $t_R$34 min), **4** (3 mg, $t_R$42 min) and **6** (8.7 mg, $t_R$45 min). $Fr._{4-16}$ was purified by HPLC (68% MeCN/$H_2O$, 2 mL/min) to yield **9** (35.8 mg, $t_R$21 min). $Fr._{4-18}$ was further separated by HPLC (78% MeOH/$H_2O$, 2 mL/min) to yield **5** (8.0 mg, $t_R$17 min) and **11** (2 mg, $t_R$19 min).

*Gilluone A **(1)***: yellow orthorhombic (MeOH); mp 184-185 °C; $[\alpha]^{25}_D$ +14.5 (*c* 0.1 MeOH); UV (MeOH) $\lambda_{max}$ (log $\varepsilon$) 253 (3.95), 204 (3.96); ECD (0.4 mg/mL, MeOH) $\lambda_{max}$ ($\Delta\varepsilon$): 307 (-2.57), 262 (3.75), 226 (0.82), 205 (4.26) nm; $^1$H NMR ($CD_3OD$, 700MHZ) and $^{13}$C NMR ($CD_3OD$, 175MHZ) data, Table 1; HRESIMS at *m/z* 435.2011 $[M+H]^+$ (calcd for $C_{23}H_{31}O_8$, 435.2013).

X-ray Crystallographic Data of **1**. Gilluone A (**1**) was crystallized from methanol to give yellow crystal. Crystal data: orthorhombic, space group $P2_12_12_1$ with $a$ = 8.0029 (10) Å, $b$ = 15.3468 (3) Å, $c$ = 17.8042 (3) Å, V = 2186.69 (6) Å$^3$, Z = 4, $P_{calc}$= 1.320 g/cm$^3$, $R$ = 0.0361, $wR_2$ = 0.0907. The absolute configuration was determined on the basis of a Flack parameter of 0.01 (7). Crystallographic data (excluding structure factors) for structure **1** in this paper have been deposited with Cambridge Crystallographic Data Centre as supplementary publication number CCDC 1885045. Copies of the data can be obtained, free of charge, on application to CCDC, 12 Union Road, Cambridge CB21EZ, UK [fax: +44 (0)-1223-336033 or e-mail: deposit@ccdc.cam.ac.uk].

*Gilluone B (**2**)*: yellow crystal; mp177-178 °C; $[\alpha]^{25}_D$ +34.2 (*c* 0.1 MeOH); UV (MeOH) $\lambda_{max}$ (log $\varepsilon$): 394 (3.57), 314 (3.78), 246 (4.12), 203 (4.09) nm; ECD (0.4 mg/mL, MeOH) $\lambda_{max}$ ($\Delta\varepsilon$) 390 (+6.27), 310 (-12.18), 279 (-4.50), 249 (-6.32), 206 (+10.55) nm; $^1$H and $^{13}$C NMR data, Table 1; HRESIMS at *m/z* 519.2585 $[M+H]^+$ (calcd for $C_{28}H_{39}O_9$, 519.2589).

X-ray Crystallographic Data of **2**. Gilluone B (**2**) was crystallized from methanol to give yellow crystal. Crystal data: orthorhombic, space group $P2_12_12_1$ with $a$ = 8.0907 (8) Å, $b$ = 25.4976 (3) Å, $c$ = 41.3088 (4) Å, V = 8521.69 (15) Å$^3$, Z = 4, $P_{calc}$= 1.271 g/cm$^3$, $R$ = 0.0370, $wR_2$ = 0.0941. The absolute configuration was determined on the basis of a Flack parameter of 0.03 (5). Crystallographic data (excluding structure factors) for structure **2**in this paper have been deposited with Cambridge Crystallographic Data Centre as supplementary publication number CCDC 1900153. Copies of the data can be obtained, free of charge, on application to CCDC, 12 Union Road, Cambridge CB21EZ, UK [fax: +44 (0)-1223-336033 or e-mail: deposit@ccdc.cam.ac.uk].

*Gilluone C (**3**)*: yellow powder; $[\alpha]^{25}_D$ -23.1 (*c* 0.1 MeOH); UV (MeOH) $\lambda_{max}$ (log $\varepsilon$): 274 (3.24), 218 (3.73), 203 (3.91) nm; ECD (0.3 mg/mL, MeOH) $\lambda_{max}$ ($\Delta\varepsilon$) 371 (+0.15), 336 (+0.03), 311 (+0.20), 260 (-0.46), 243 (+0.10), 201 (-2.52) nm; $^1$H and $^{13}$C NMR data, Table1; HRESIMS at *m/z* 534.2685 $[M+H]^+$ (calcd for $C_{28}H_{40}NO_9$, 534.2698).

*Asterriquinone I (**4**)*: dark purple powder; $[\alpha]^{25}_D$+20.0, (*c* 0.04 MeOH); UV (MeOH) $\lambda_{max}$ (log $\varepsilon$): 218 (3.84), 221 (4.26), 203 (4.25); $^1$H and $^{13}$C NMR data, TableS2; (+)-HRESIMS at *m/z* 573.2359 $[M+Na]^+$ (calcd for $C_{34}H_{34}N_2NaO_5$, 573.2360).

*Asterriquinone J (**5**)*: dark purple powder; $[\alpha]^{25}_{D}$-96.0, (*c* 0.03 MeOH); UV (MeOH) $\lambda_{max}$ (log $\varepsilon$): 290 (4.10), 282 (4.13), 221 (4.51); $^{1}$H and $^{13}$C NMR data, TableS2; HRESIMS at *m/z* 585.2170 $[M-H]^-$ (calcd for $C_{34}H_{34}ClN_2O_5$, 585.2162).

*Asterriquinone K (**6**)*: dark purple powder; $[\alpha]^{25}_{D}$ +4.6 (*c* 0.03 MeOH); UV (MeOH) $\lambda_{max}$ (log $\varepsilon$): 290 (3.96), 282 (3.98), 221 (4.38), 205 (4.30); $^{1}$H and $^{13}$C NMR data, TableS2; HRESIMS at *m/z* 583.2829 $[M+H]^+$ (calcd for $C_{35}H_{39}N_2O_6$, 583.2803).

*Asterriquinol G (**7**)*: dark purple powder; $[\alpha]^{25}_{D}$ -18.73 (*c* 0.1 MeOH); UV (MeOH) $\lambda_{max}$ (log $\varepsilon$): UV (MeOH) $\lambda_{max}$ (log $\varepsilon$): 283 (4.40), 223 (4.83), 206 (4.75);$^{1}$H and $^{13}$C NMR data, TableS3; HRESIMS at *m/z* 599.3119 $[M+H]^+$ (calcd for $C_{36}H_{43}N_2O_6$, 599.3116).

*Asterriquinol H (**8**)*: yellow powder; UV (MeOH) $\lambda_{max}$ (log $\varepsilon$): 281 (4.37), 222 (4.84); $^{1}$H and $^{13}$C NMR data, TableS3; HRESIMS at *m/z* 551.2903 $[M+H]^+$(calcd for $C_{35}H_{39}N_2O_4$, 551.2904).

*Asterriquinol H (**9**)*: yellow powder; UV (MeOH) $\lambda_{max}$ (log $\varepsilon$): 291 (4.19), 283 (4.21), 224 (4.71); $^{1}$H and $^{13}$C NMR data, TableS3; HRESIMS at *m/z* 505.2099 $[M+Na]^+$ (calcd for $C_{30}H_{30}N_2NaO_4$, 505.2098).

X-ray Crystallographic Data of **12**. Asterriquinone-C-1(**12**) was crystallized from methanol to give yellow crystal. Crystal data: monoclinic, space group Cc with *a* = 14.3037 (10) Å, *b* = 14.0845 (10) Å, *c* = 23.7866 (2) Å, V = 4789.36 (6) Å$^3$, Z = 4, $P_{calc}$= 1.319 g/cm$^3$, *R* = 0.0412, $wR_2$ = 0.1109. Crystallographic data (excluding structure factors) for structure **12**in this paper have been deposited with Cambridge Crystallographic Data Centre as supplementary publication number CCDC 1900155. Copies of the data can be obtained, free of charge, on application to CCDC, 12 Union Road, Cambridge CB21EZ, UK [fax: +44 (0)-1223-336033 or e-mail: deposit@ccdc.cam.ac.uk].

**Preparation of MTPA Ester of 4 by Modified Mosher's Method.**

Asterriquinone I (**4**): (0.6 mg for each) was reacted with either *R*/*S*-(+)-MTPA chloride (2.0 $\mu$L) in 200 $\mu$L of anhydrous pyridine for 12h at room temperature. The reaction mixture was separated by semi-preparative HPLC on ODS (82% MeCN/$H_2O$, V/V) to afford the *S*-MTPA ester **4a** (1.6 mg, $t_R$ 23 min) and *R*-MTPA ester **4b** (1.3 mg, $t_R$ 23 min), respectively.

***Compound 4a***: $^{1}$H NMR ($CDCl_3$, 700 MHz) $\delta_H$ 9.66 (d, *J* =12.0, 1H, H-1'), 8.14 (s, 1H, H-1"), 7.52 (d, *J* =7.6, 1H, H-2'), 7.47 (d, *J* =8.0, 1H, H-4'), 7.34 (d, *J* =8.19, 1H, H-7"), 7.30 (d, *J* =7.7, 1H, H-4"), 7.18 (t, *J* =7.6, 1H, H-6"), 7.11 (t, *J* =7.5, 1H, H-5'), 7.10 (t, *J* =7.5, 1H, H-5"),

6.93 (d, $J$ =7.1, 1H,H-6'), 6.14, (dd, $J$ =17.4, 10.5, 2H, $H_2$-11''), 5.66 (t, $J$ =4.8, 1H,H-11'), 5.22 (d, $J$ =17.5, 1H, $H_a$-12''), 5.16 (d, $J$ =10.6, 1H, $H_b$-12''), 4.95 (s, 1H, $H_a$-13'), 4.82 (s, 1H, $H_b$-13'), 3.80 (d, $J$ =5.3, 3H, $H_3$-7), 3.70 (s, 3H, $H_3$-8), 3.42 (dt, $J$ =14.3, 2.8, 1H, $H_a$-10'), 3.16 (dd, $J$ =14.1, 8.5, 1H, $H_b$-10'), 1.83 (s, 3H, $H_3$-14'), 1.51 (s, 3H, $H_3$-13''), 1.51 (s, 3H, $H_3$-14''). ESIMS at *m/z* 767.2 $[M+H]^+$.

***Compound 4b***: $^1$H NMR ($CDCl_3$, 700 MHz) $\delta_H$ 9.38 (d, $J$ =11.7, 1H, H-1'), 8.14 (s, 1H, H-1''), 7.48 (d, $J$ =7.8, 1H, H-2'), 7.48 (d, $J$ =7.8, 1H, H-4'), 7.34 (d, $J$ =8.1, 1H, H-7''), 7.30 (d, $J$ =7.7, 1H, H-4''), 7.18 (t, $J$ =8.1, 1H, H-6''), 7.11 (t, $J$ =8.8, 1H, H-5'), 7.09 (t, $J$ =2.2, 1H, H-5''), 7.00 (d, $J$ =7.1, 1H,H-6'), 6.14, (dd, $J$ =17.4, 10.5, 2H, $H_2$-11''), 5.61 (t, $J$ =8.7, 1H,H-11'), 5.22 (d, $J$ =18.1, 1H, $H_a$-12''), 5.17 (d, $J$ =10.6, 1H, $H_b$-12''), 4.95 (s, 1H, $H_a$-13'), 4.82 (s, 1H, $H_b$-13'), 3.80 (d, $J$ =5.3, 3H, $H_3$-7), 3.70 (s, 3H, $H_3$-8), 3.38 (dt, 1H, $H_a$-10'), 3.19 (dd, $J$ =14.3, 6.9, 1H, $H_b$-10'), 1.83 (s, 3H, $H_3$-14'), 1.51 (s, 3H, $H_3$-13''), 1.51 (s, 3H, $H_3$-14''). ESIMS at *m/z* 767.2 $[M+H]^+$.

**Biological Assay**

**Antibacterial assays**. The antibacterial activities against three gram-positive bacteria, *Methicillin-resistant Staphyloccocusaureus*, *Staphyloccocusaureus*, *Enterococcus faecalis* and three gram-negative bacteria, *Acinetobacter baumannii*, *Escherichia coli*, *Klebsiellapneumonia* were evaluated by an agar dilution method.[S1] The tested strains were cultivated in LB agar plates for bacteria and in YPD agar plates for C. albicans at 37 °C. Compounds **1**–**3** and positive control (ciprofloxacin lactate) were dissolved in MeOH at the concentration of 100 μg/mL. A 10μL quantity of test solution was absorbed by a paper disk (5 mm diameter) and placed on the assayplates. After 24 h incubation, zones of inhibition (mm in diameter) were recorded. If the inhibitionzone was observed, the compounds diluted to different concentrations by the continuous 2-folddilution methods. The minimum inhibitory concentrations (MICs) were defined as the lowestconcentration at which no microbial growth could be observed.

**Cytotoxic assays**. Cytotoxic activities (five human cancer cell Lines, K562, BEL-7042, SGC-7901, A549 and Hela cells) were evaluatedusing the CCK-8 method as described previously.[S2] In the CCK-8 assay, cancer cell Lines were grown in RPMI-1640 supplemented with 10% FBS under a humidified atmosphere of 5% $CO_2$ and 95% air at 37 °C. Cell suspension, 100 $\mu$L, at a density of 5 × $10^5$ cell mL-1 was plated in 96-well microtiter plates and then exposed to varying concentrations ($10^{-5}$–$10^{-12}$ M) of compounds after cultivation for 24 h. Three days later,

10 $\mu$L of CCK-8 solution was added 4 h before detection. Then the absorbency (A450 value) was measured, and the growth rates of cells were computed.

**Table S1**. Stable conformers of **3a**–**3g**

| Conformer | Conformation | E (Hartree) | Energy (kcal/mol) | Percent (%) |
|---|---|---|---|---|
| **3a** | 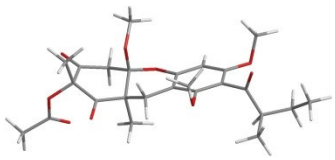 | -1648.9240293 | -1034715.32827 | 5.73 |
| **3b** | 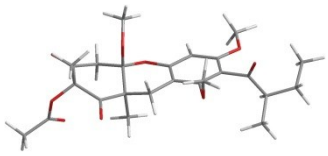 | -1648.9266285 | -1034716.95929 | 90.13 |
| **3c** | 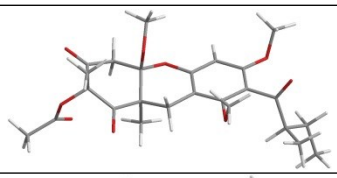 | -1648.9214478 | -1034713.70836 | 0.37 |
| **3d** | 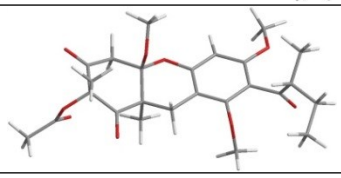 | -1648.9234386 | -1034714.95761 | 3.06 |
| **3e** | 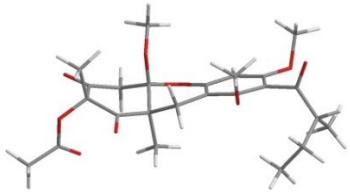 | -1648.9200699 | -1034712.84731 | 0.09 |
| **3f** | 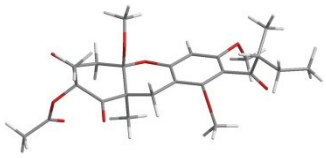 | -1648.9198166 | -1034712.68476 | 0.07 |
| **3g** | 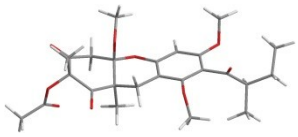 | -1648.9218252 | -1034713.94518 | 0.55 |

**Theory and Calculation Details.** The calculations were performed by using the density functional theory (DFT) as carried out in the Gaussian 09.[S3] The preliminary conformational distributions search were performed by HyperChem 7.5 software. All ground-state geometries were optimized at theB3LYP/6-31G(d) level. Conformers within a 2 kcal/mol energy threshold from the global minimum were selected to calculate the electronic transitions.[S4] The overall theoretical ECD spectra were obtained according to the Boltzmann weighting of each conformers.

The percentage of each conformer for **3a**–**3g** was calculated from the energy combined with the ratio between them. Solvent effects of methanol solution were evaluated at the same DFT level by using the SCRF/PCM method.[S5]

**References**


S1. Wang, J. F., Wei, X. Y., Qin, X. C., Lin, X. P., Zhou, X. F., Liao, S. R., Yang, B., Liu, J., Tu, Z. C., Liu, Y. H. *Org. Lett.* **2015**, 17: 656–659.

S2. Wang, J. F., He, W. J., Huang, X. L., Tian, X. P., Liao, S. R., Yang, B., Wang, F. Z., Zhou, X. J., Liu, Y. H. *J. Agric. Food Chem.* **2016**, 64: 2910–2916.

S3. Gaussian 03, Revision E.01, M. J. Frisch, G. W. Trucks, H. B. Schlegel, G. E. Scuseria, M. A. Robb, J. R. Cheeseman, J. A.Montgomery, Jr., T. Vreven, K. N. Kudin, J. C. Burant, J. M. Millam, S. S. Iyengar, J. Tomasi, V. Barone, B. Mennucci, M. Cossi, G.Scalmani, N. Rega, G. A. Petersson, H. Nakatsuji, M. Hada, M. Ehara, K. Toyota, R. Fukuda, J. Hasegawa, M. Ishida, T. Nakajima, Y.Honda, O. Kitao, H. Nakai, M. Klene, X. Li, J. E. Knox, H. P. Hratchian, J. B. Cross, V. Bakken, C. Adamo, J. Jaramillo, R. Gomperts,R. E. Stratmann, O. Yazyev, A. J. Austin, R. Cammi, C. Pomelli, J. W. Ochterski, P. Y. Ayala, K. Morokuma, G. A. Voth, P. Salvador, J.J. Dannenberg, V. G. Zakrzewski, S. Dapprich, A. D. Daniels, M. C. Strain, O. Farkas, D. K. Malick, A. D. Rabuck, K. Raghavachari,J. B. Foresman, J. V. Ortiz, Q. Cui, A. G. Baboul, S. Clifford, J. Cioslowski, B. B. Stefanov, G. Liu, A. Liashenko, P. Piskorz, I.Komaromi, R. L. Martin, D. J. Fox, T. Keith, M. A. Al-Laham, C. Y. Peng, A. Nanayakkara, M. Challacombe, P. M. W. Gill, B. Johnson,W. Chen, M. W. Wong, C. Gonzalez, and J. A. Pople, Gaussian, Inc., Wallingford CT, 2004.

S4. (a) Casida, M. E. In Recent Advances in Density Functional Methods, part I; Chong, D. P., Eds.; World Scientific: Singapore, **1995**; pp 155–192. (b) Gross, E. K. U.; Dobson, J. F.; Petersilka, M. Top. *Curr. Chem.* **1996**, *181*, 81–172. (c) Gross, E. K. U.; Kohn, W. *Adv.Quantum Chem.* **1990**, *21*, 255–291. (d) Runge, E.; Gross, E. K. U. *Phys. Rev. Lett.* **1984**, *52*, 997–1000.

S5. (a) Miertus, S.; Tomasi, J. *Chem. Phys.* **1982**, *65*, 239–245. (b) Tomasi, J.; Persico, M. *Chem. Rev.* **1994**, *94*, 2027–2094. (c) Cammi,R.; Tomasi, J. *J. Comp. Chem.* **1995**, *16*, 1449–1458.


**The strain's (*Aspergillus* sp. SCSIO 41018) ITS sequence of the rDNA.**

CCTGCGGAAGGATCATTACTGAGTGAGGGTTCCTTCGGGGCCCAACCTCCCACCCTTG

TATACTGTACCAAGTTGCTTCGGCGGGCCCGCCGTTCGCGCGGCCGCCGGGGGGGAA

CCCCTCCCCCCGGGCGAGCGCCCGCCGGAGACCCCAACGTGAACACTGTCTGAAGTT

TTGTCGTCTGAGTTCGATTGTATCGCAATCAGTTAAAACTTTCAACAATGGATCTCTT

GGTTCCGGCATCGATGAAGAACGCAGCGAAATGCGATAATTAATGTGAATTGCAGAA

TTCAGTGAATCATCGAGTCTTTGAACGCACATTGCACCCCCTGGTATTCCGGGGGGTA

TGCCTGTCCGAGCGTCATTGCTGCCCTCAAGCCCGGCTTGTGTGTTGGGTCCTCGTCC

CCCCCGGGGGACGGGCCCGAAAGGCAGCGGCGGCACCGCGTCCGGTCCTCGAGCGTA

TGGGGCTTTGTCACACCGCTCTCGTAGGCCCGGCCGGCGCTGGCCGACGCTGAAAAG

CAACCATTATTTCTCCAGGTTGACCTCGGATCAGGTAGGGATACCCGCTGAACTTAAG

CATATCAATA

**Table S2**. $^{1}H$ and $^{13}C$ NMR data in $CDCl_3$ for **4–6** (700, 175 MHz, TMS, $\delta$ ppm)

| ***no.*** | **4** | | **5** | | **6** | |
|---|---|---|---|---|---|---|
| | $\delta_C$ | $\delta_H$ ($J$, Hz) | $\delta_C$ | $\delta_H$ ($J$, Hz) | $\delta_C$ | $\delta_H$ ($J$, Hz) |
| **1** | 183.9 | | 184.2 | | 184.2 | |
| **2** | 154.4 | | 154.5 | | 154.3 | |
| **3** | 120.7 | | 122.6 | | 120.7 | |
| **4** | 183.8 | | 183.7 | | 183.8 | |
| **5** | 156.4 | | 156.3 | | 156.4 | |
| **6** | 122.3 | | 122.1 | | 122.4 | |
| **7** | 60.9 | 3.80, s | 60.9 | 3.81, d (2.7) | 60.8 | 3.79, d (3.3) |
| **8** | 60.2 | 3.70, s | 60.2 | 3.69, s | 60.2 | 3.69, s |
| **1'** | | 9.82, brs | | 9.75, brs | | 10.31, brs |
| **2'** | 128.2 | 7.62, d (1.89) | 128.2 | 7.61, s | 128.3 | 7.62, q (1.4) |
| **3'** | 105.5 | | 105.6 | | 105.3 | |
| **4'** | 120.2 | 7.47, d (8.05) | 120.4 | 7.48, d (7.8) | 120.1 | 7.47, d (8.1) |
| **5'** | 120.4 | 7.11, t (7.21) | 120.4 | 7.11, m | 120.3 | 7.10, t (7.2) |
| **6'** | 123.6 | 7.02, d (7.0) | 123.3 | 7.02, d (6.9) | 123.1 | 6.99, d (7.0) |
| **7'** | 122.7 | | 122.6 | | 123.4 | |
| **8'** | 136.0 | | 135.8 | | 135.8 | |
| **9'** | 127.0 | | 127.1 | | 127.1 | |
| **10'** | 39.5 | 3.18, dd (14.7, 8.5)<br>3.09, dt (17.7, 2.9) | 35.7 | 3.17, d (14.6)<br>3.04, dd (9.0, 9.2) | 36.1 | 2.99, m |
| **11'** | 77.5 | 4.46, t (6.8) | 80.7 | 3.93, m | 78.2 | 3.83, qd (5.6,1.6) |
| **12'** | 147.6 | | 75.5 | | 77.7 | |
| **13'** | 111.0 | 5.04, s<br>4.89, s | 28.6 | 1.68, s | 18.9 | 1.25, s |

| | | | | | | |
|---|---|---|---|---|---|---|
| **14'** | 18.5 | 1.87, s | 26.9 | 1.75, s | 20.4 | 1.29, s |
| **15'** | | | | | 49.4 | 3.28, s |
| **1''** | | 8.13, brs | | 8.16, brs | | 8.14, brs |
| **2''** | 142.2 | | 142.3 | | 142.2 | |
| **3''** | 101.9 | | 101.8 | | 101.9 | |
| **4''** | 118.9 | 7.29, d (7.8) | 118.8 | 7.29, d (7.9) | 118.9 | 7.30, d (7.9) |
| **5''** | 120.5 | 7.09, t (7.7) | 120.5 | 7.11, m | 120.4 | 7.10, t (7.2) |
| **6''** | 122.2 | 7.16, t (7.1) | 122.2 | 7.16, t (7.9) | 122.2 | 7.17, m |
| **7''** | 110.8 | 7.32, d (8.0) | 110.8 | 7.32, m | 110.8 | 7.33, d (8.1) |
| **8''** | 134.6 | | 134.6 | | 134.6 | |
| **9''** | 130.0 | | 130.0 | | 130.0 | |
| **10''** | 39.5 | | 39.4 | | 39.5 | |
| **11''** | 145.6 | 6.13, dd (17.4, 10.6) | 145.6 | 6.13, dd (17.4,10.5) | 145.6 | 6.13, dd (17.4,10.5) |
| **12''** | 112.5 | 5.21, d (17.4) | 112.4 | 5.21, d (17.4) | 112.4 | 5.21, d (0.6) |
| | | 5.16, d (11.3) | | 5.15, d (10.6) | | 5.15, d (0.7) |
| **13''** | 27.0 | 1.50, d (2.6) | 27.2 | 1.50, s | 26.9 | 1.50, s |
| **14''** | 27.2 | 1.50, d (2.6) | 27.2 | 1.50, d (2.6) | 27.2 | 1.50, s |

**Table S3**. $^{1}H$ and $^{13}C$ NMR data in $CDCl_3$ for **7–9** (TMS, $\delta$ ppm)

| ***no*** | 7[a] | | 8[a] | | 9[b] | |
|---|---|---|---|---|---|---|
| | $\delta_C$ | $\delta_H$ (*J*, Hz) | $\delta_C$ | $\delta_H$(*J*, Hz) | $\delta_C$ | $\delta_H$(*J*, Hz) |
| **1** | 145.70 | | 148.1 | | 145.7 | 8.45, brs |
| **2** | 142.13 | | 145.7 | | 148.1 | |

| | | | | | | |
|---|---|---|---|---|---|---|
| **3** | 115.66 | | 115.4 | | 115.2 | |
| **4** | 143.34 | | 142.1 | | 143.3 | |
| **5** | 148.10 | | 143.3 | | 142.1 | |
| **6** | 122.76 | | 120.7 | | 122.8 | |
| **7** | 61.15 | 3.49, s | 61.1 | 3.56, s | 60.2 | 3.51, s |
| **8** | 60.78 | 3.42, s | 61.0 | 3.50, s | 60.8 | 3.55, s |
| **9** | 60.95 | 3.50, s | 60.8 | 3.41, s | 60.9 | 3.42, s |
| **1'** | | 10.08, brs | | 8.43, brs | | 8.45, brs |
| **2'** | 125.10 | 7.50, d (2.31) | 124.5 | 7.46, d (2.2) | 124.9 | 7.48, s |
| **3'** | 107.55 | | 108.3 | | 108.0 | |
| **4'** | 119.73 | 7.53, dd (7.77, 3.15) | 119.1 | 7.50, d (7.8) | 121.2 | 7.67, d (7.9) |
| **5'** | 119.62 | 7.09, m | 120.2 | 7.12, t (7.1) | 120.0 | 7.19, q (7.8) |
| **6'** | 122.89 | 7.00, d (6.93) | 121.6 | 7.08, m | 122.3 | 7.26, m |
| **7'** | 123,63 | | 124.1 | | 111.3 | 7.46, d (8.1) |
| **8'** | 136.27 | | 135.5 | | 136.2 | |
| **9'** | 127.22 | | 127.0 | | 127.1 | |
| **10'** | 36.14 | 3.03, m | 31.0 | 3.65, d (7.1) | | |
| **11'** | 78.19 | 3.90, dd (8.33, 1.40) | 122.5 | 5.51, t (7.1) | | |
| **12'** | 77.78 | | 133.50 | | | |
| **13'** | 19.05 | 1.27, s | 25.9 | 1.83, s | | |
| **14'** | 20.42 | 1.30, s | 18.2 | 1.87, s | | |
| **15'** | 49.39 | 3.30, s | | | | |
| **1''** | | 8.04, s | | 8.06, brs | | 8.04, brs |
| **2''** | 140.70 | | 140.7 | | 140.7 | |
| **3''** | 104.53 | | 104.4 | | 104.4 | |
| **4''** | 119.62 | 7.33, d (8.33) | 119.4 | 7.34, t (7.1) | 110.3 | 7.35, d (8.5) |
| **5''** | 119.61 | 7.09, m | 119.6 | 7.08, m | 121.7 | 7.19, q (7.8) |
| **6''** | 121.60 | 7.17, td | 122.0 | 7.17, m | 119.65 | 7.08, t (7.6) |
| **7''** | 110.22 | 7.34, d (8.33) | 110.3 | 7.34, t (7.1) | 119.58 | 7.33, d (8.5) |

| | | | | | | |
|---|---|---|---|---|---|---|
| **8''** | 134.77 | | 134.8 | | 130.4 | |
| **9''** | 130.47 | | 130.4 | | 134.8 | |
| **10''** | 39.26 | | 39.9 | | 39.9 | |
| **11''** | 146.72 | 6.17, dd (17.43, | 146.7 | 6.17, dd (17.4, 10.5) | 146.6 | 6.18, dd (17.5, 10.6) |
| **12''** | 111.67 | 5.21, d (17.43) | 111.7 | 5.21, dd (17.4, 1.1) | 111.7 | 5.22, dd (17.5, 0.9) |
| | | 5.11, d (10.57) | | 5.11, dd (10.5, 1.1) | | 5.12, dd (10.6, 1.0) |
| **13''** | 26.66 | 1.45, s | 26.6 | 1.45, s | 26.66 | 1.46, s |
| **14''** | 26.60 | 1.44, s | 26.7 | 1.44, s | 26.58 | 1.45, s |

[a]700, 175 MHz.[b]500, 125 MHz.

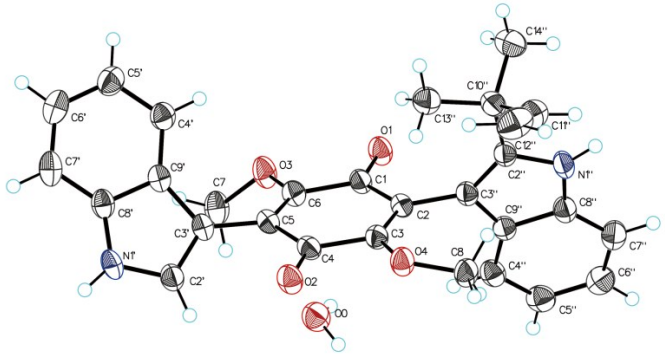


**Figure S1**. The ORTEP drawing of compound**12**

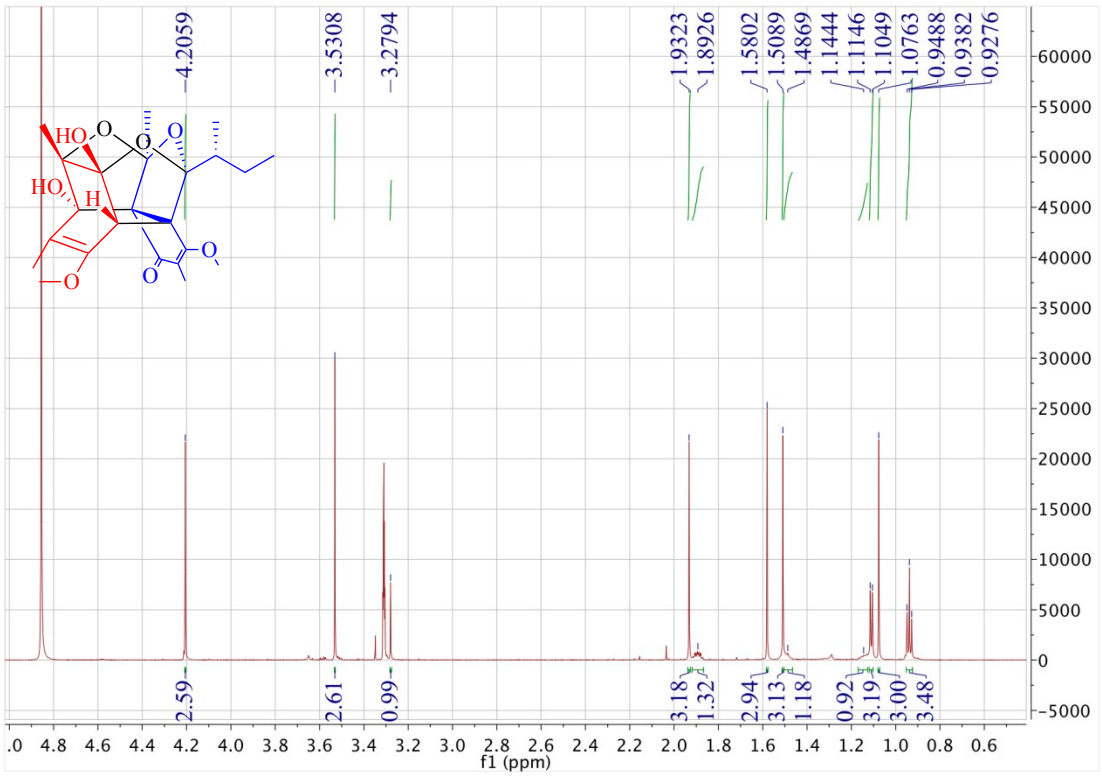


**Figure S2**. The $^{1}H$ NMR spectrum of gilluone A (**1**) in $CD_3OD$ (700 MHZ)

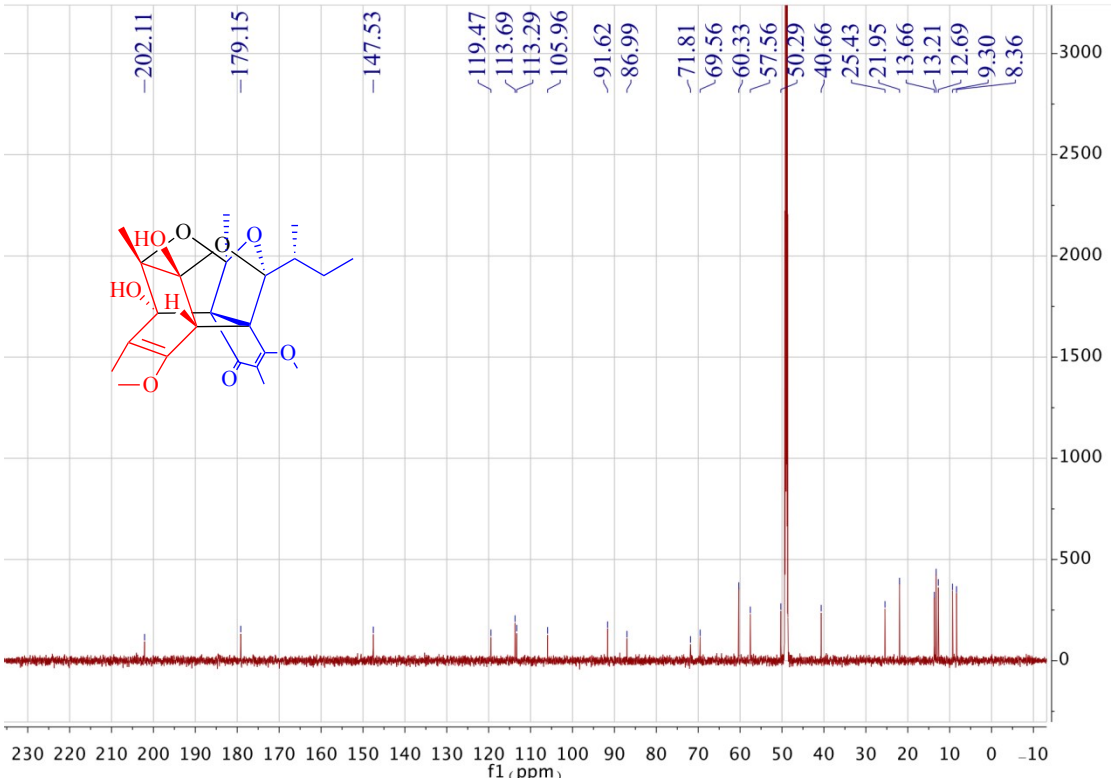


**Figure S3**. The $^{13}C$ NMR spectrum of gilluone A (**1**) in $CD_3OD$ (175 MHz)

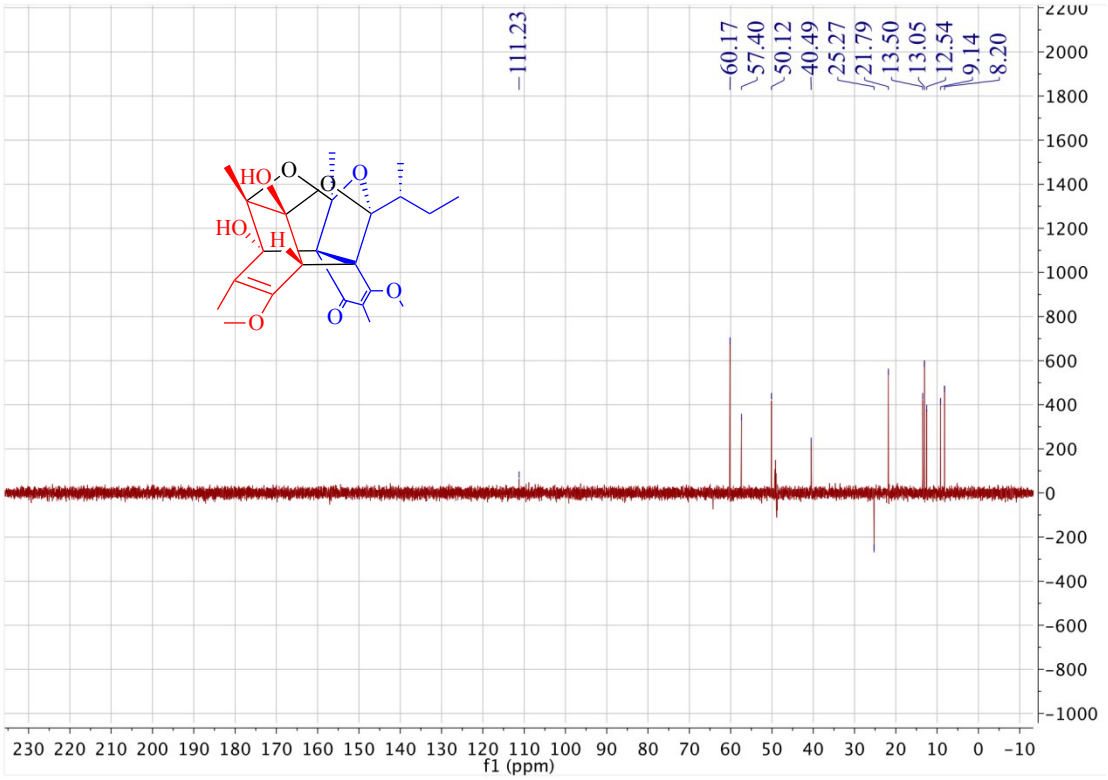


**Figure S4**. The DEPT spectrum of gilluone A (**1**) in $CD_3OD$ (175 MHz)

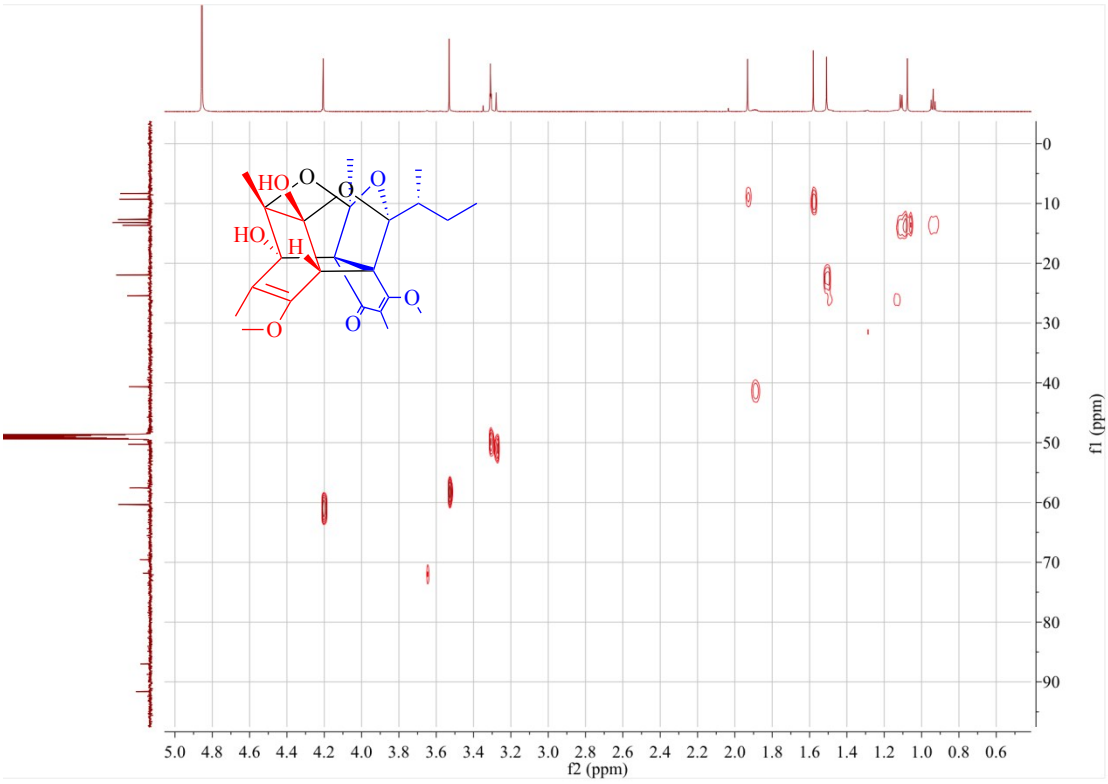


**Figure S5**. The HSQC spectrum ofgilluone A (**1**) in $CD_3OD$

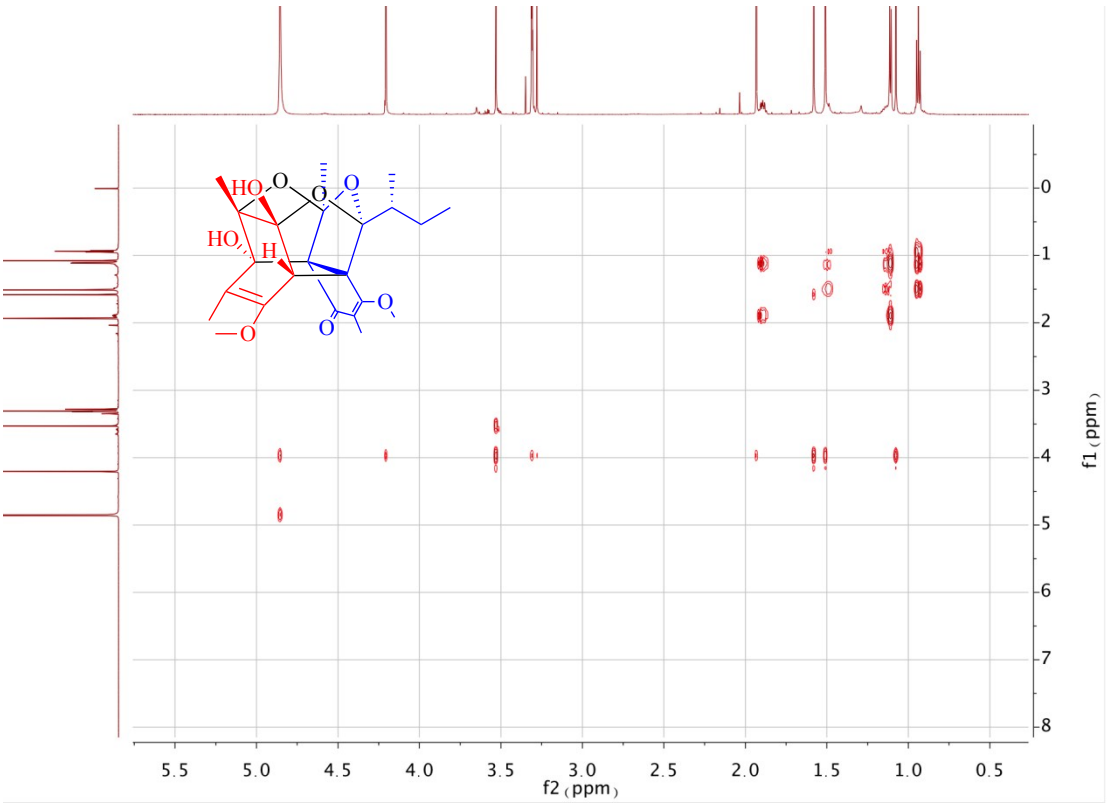


**Figure S6**. The $^{1}$H-$^{1}$H COSY spectrum of gilluone A (**1**) in $CD_3OD$

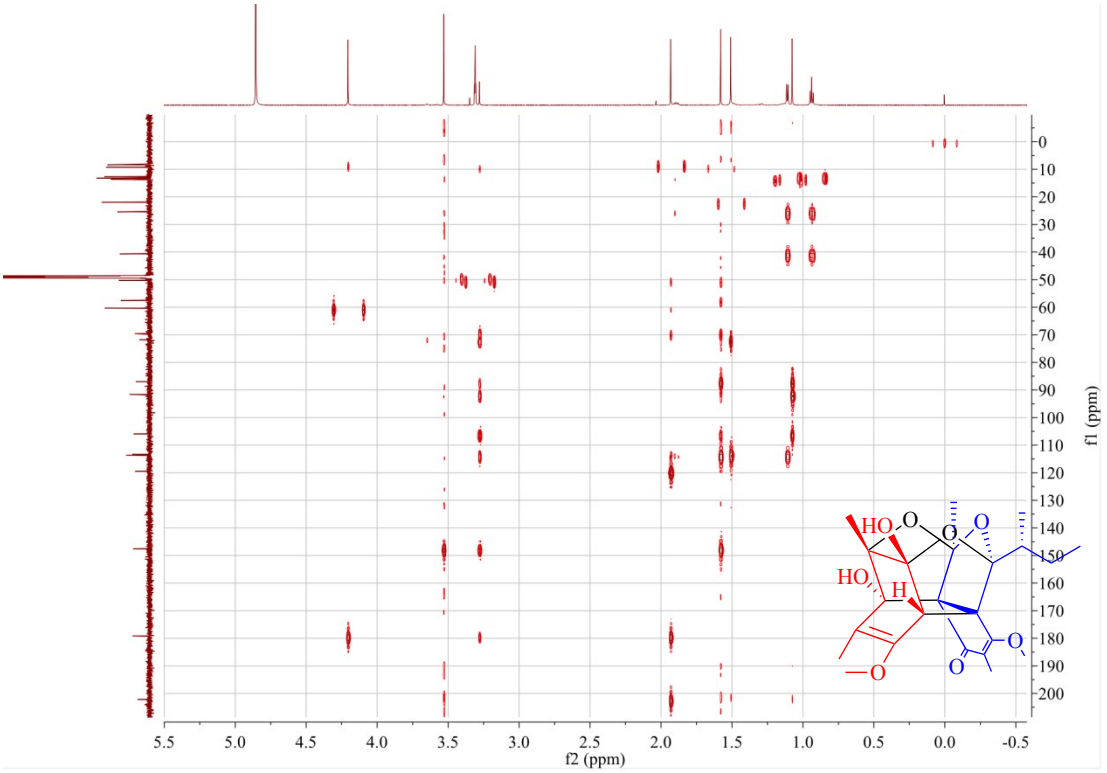


**Figure S7**. The HMBC spectrum of gilluone A (**1**) in $CD_3OD$

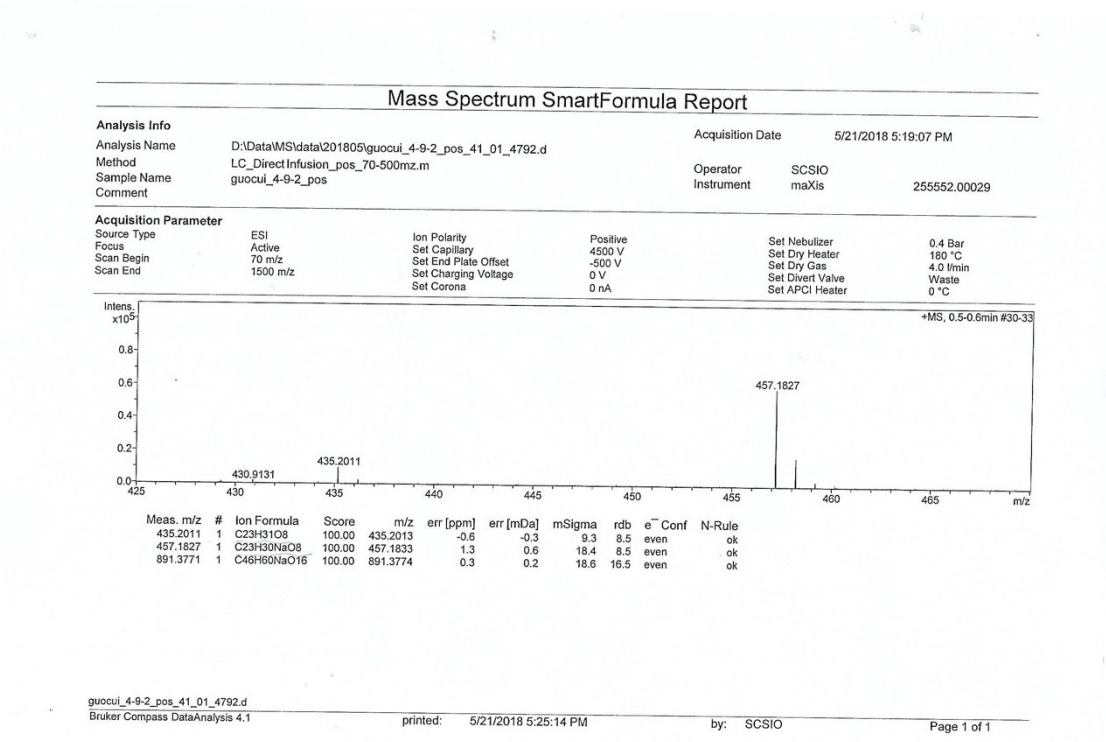


**Figure S8**. The HRESIMS spectrum of gilluone A (**1**)

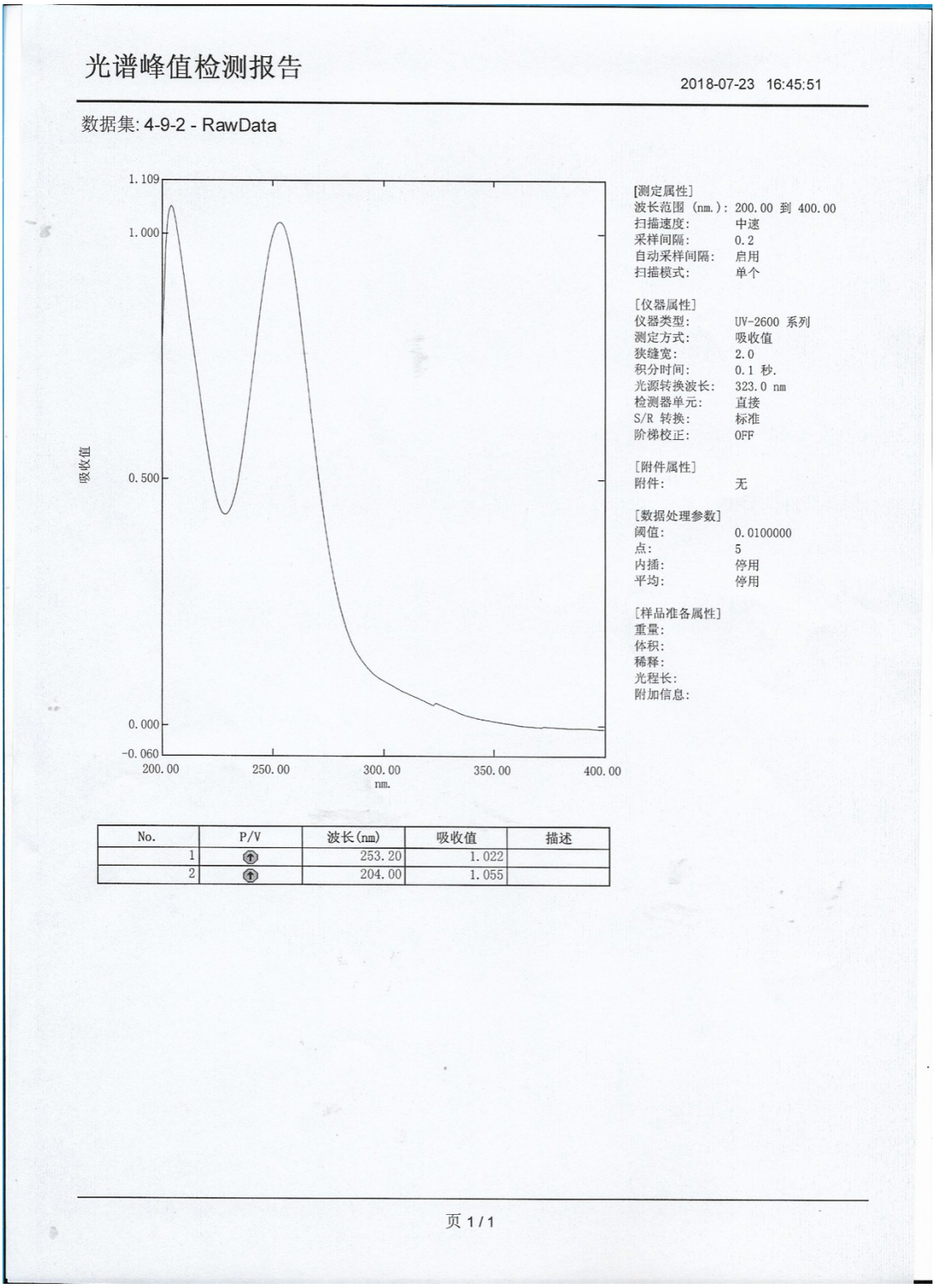


**Figure S9**. The UV spectrum of gilluone A (**1**)

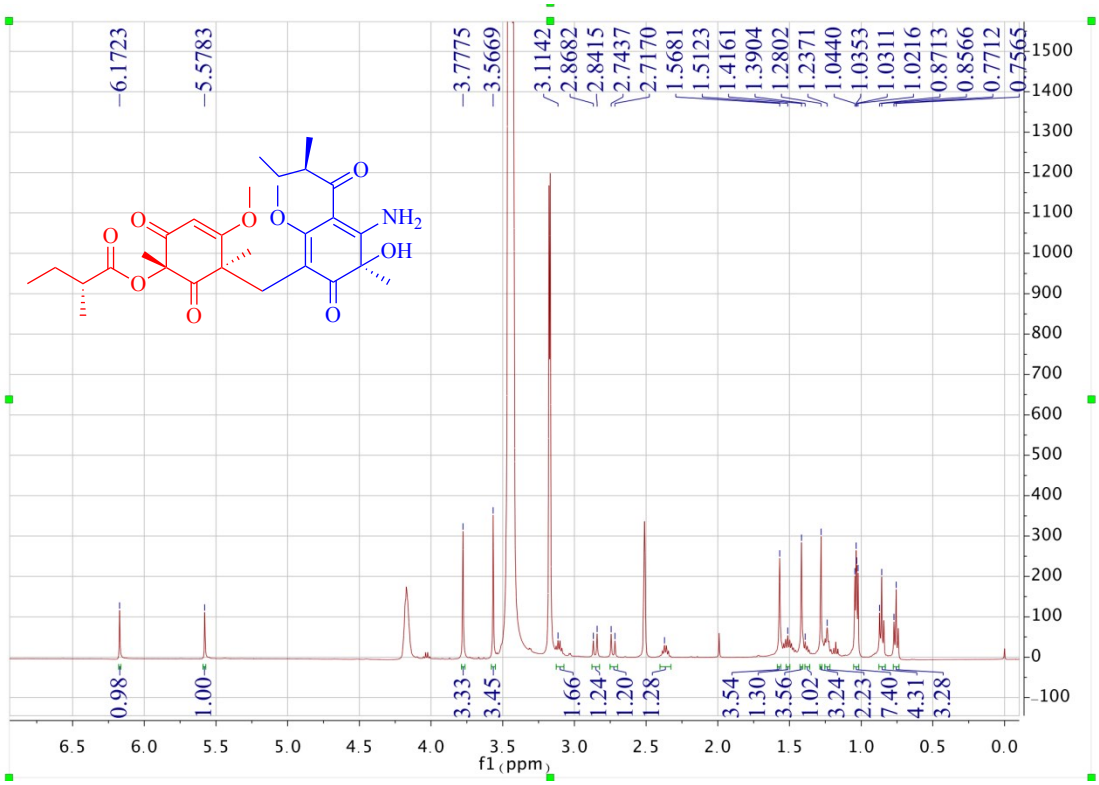


**Figure S10**. The $^{1}$H NMR spectrum of gilluoneB (**2**) inDMSO-$d_6$ (700 MHz)

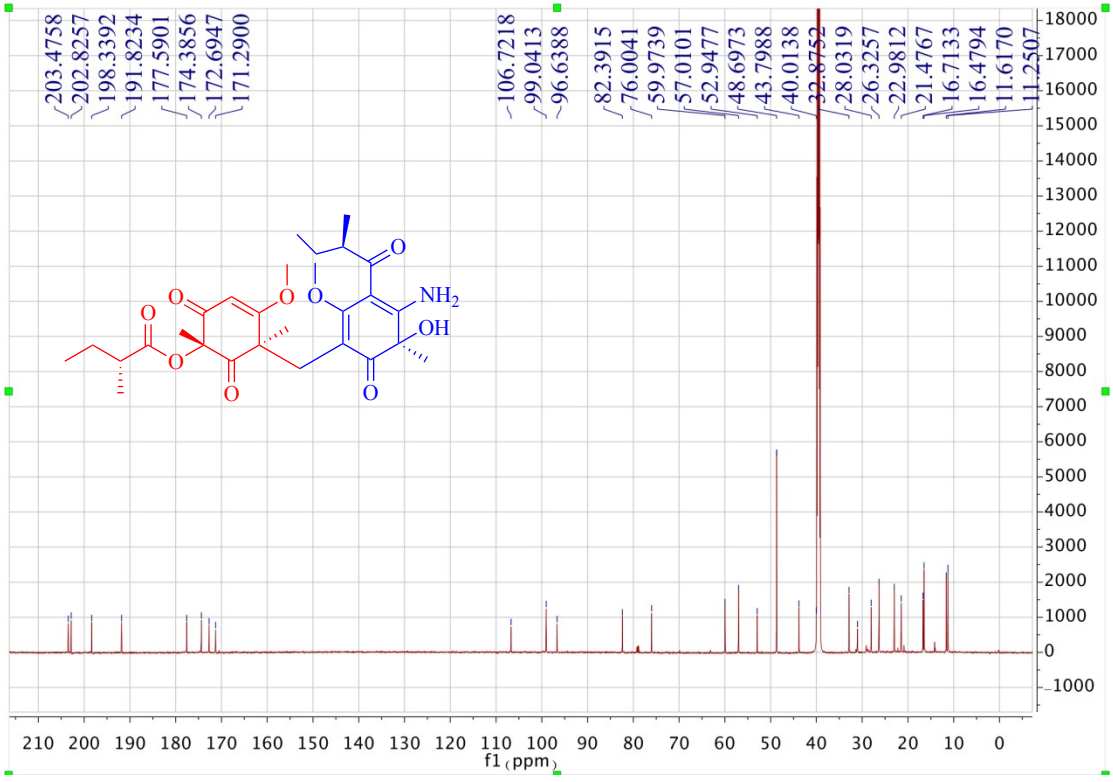


**Figure S11**. The $^{13}$C NMR spectrum of gilluone B (**2**) in DMSO-$d_6$ (175 MHz)

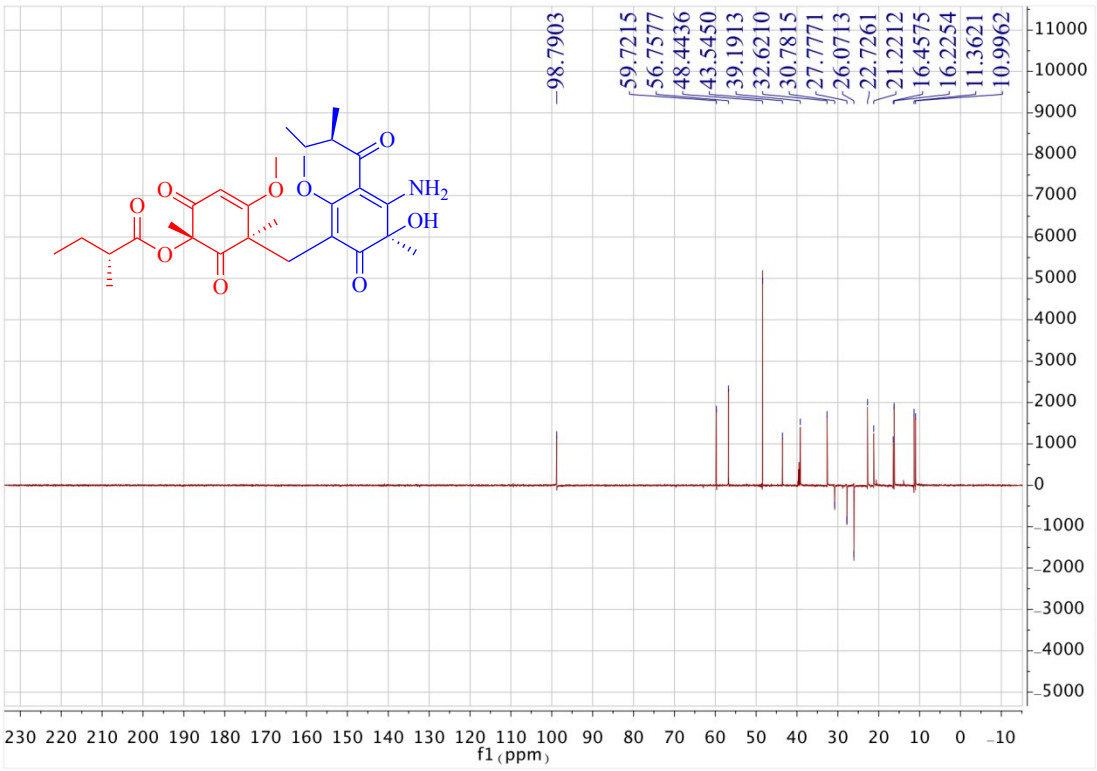


**Figure S12**. The DEPT spectrum of gilluone B (**2**) in DMSO-$d_6$ (175 MHz)

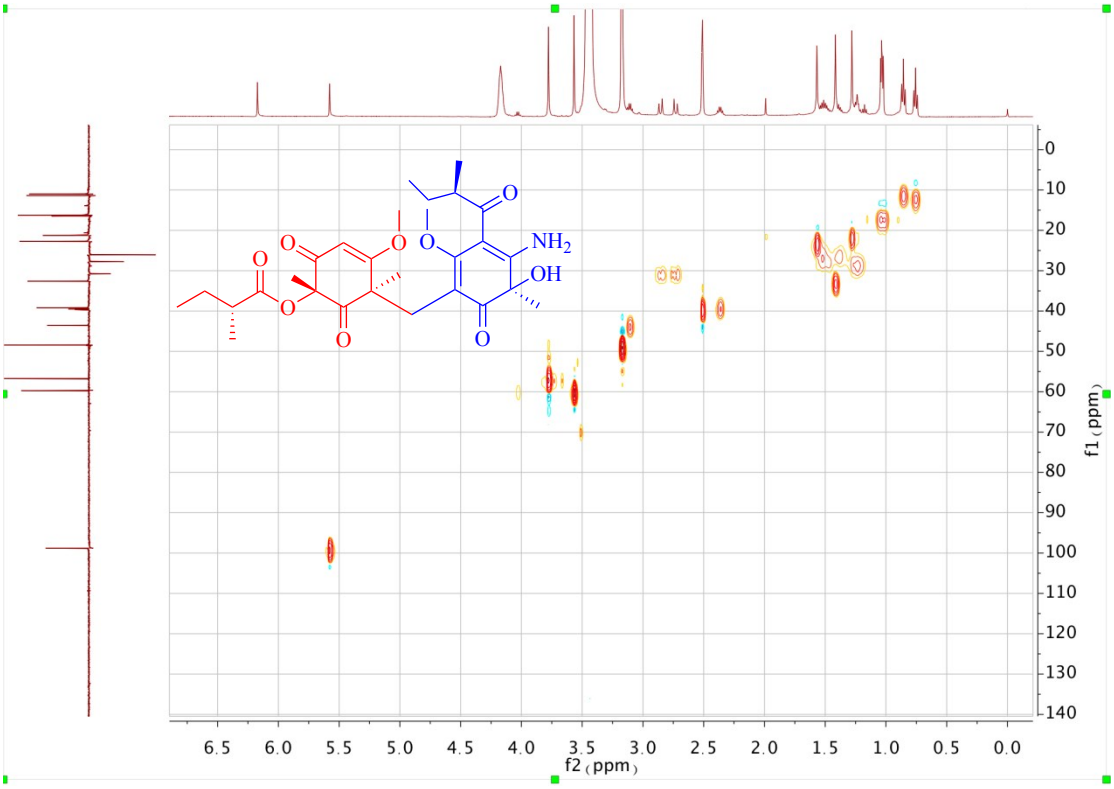


**Figure S13**. The HSQC spectrum of gilluoneB (**2**) in DMSO-$d_6$

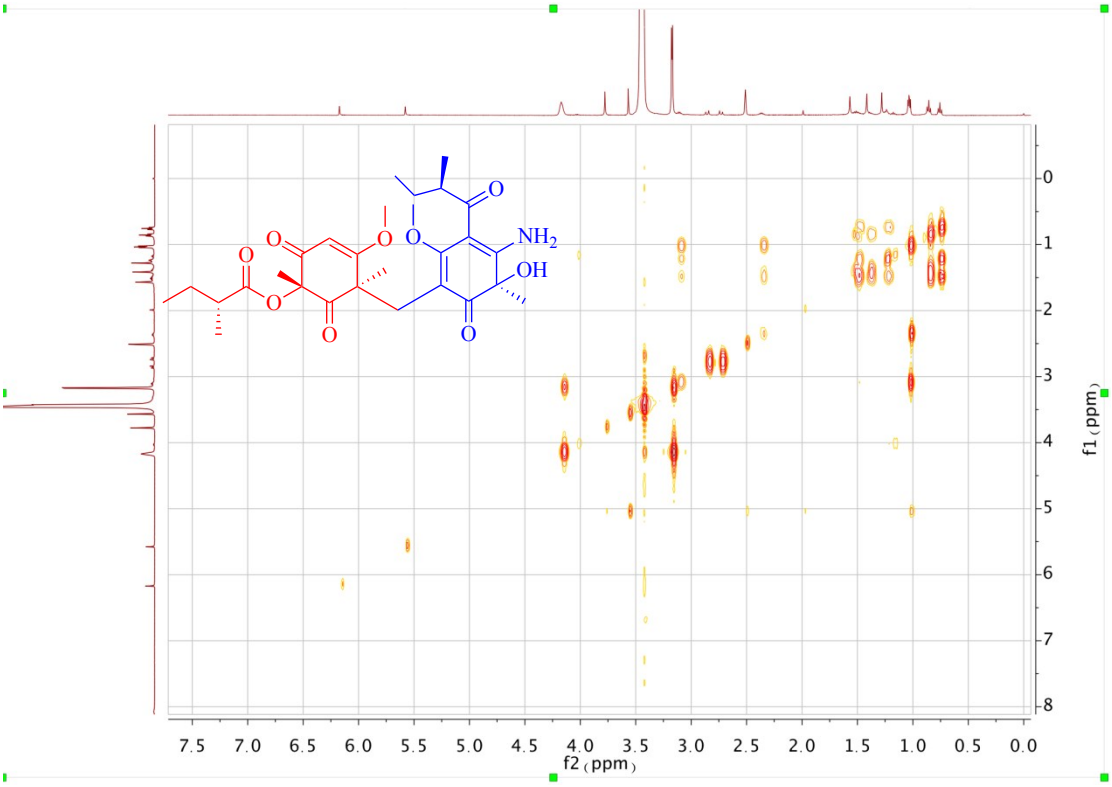


**Figure S14**. The $^{1}$H-$^{1}$H COSYspectrum of gilluoneB (**2**) in DMSO-$d_6$

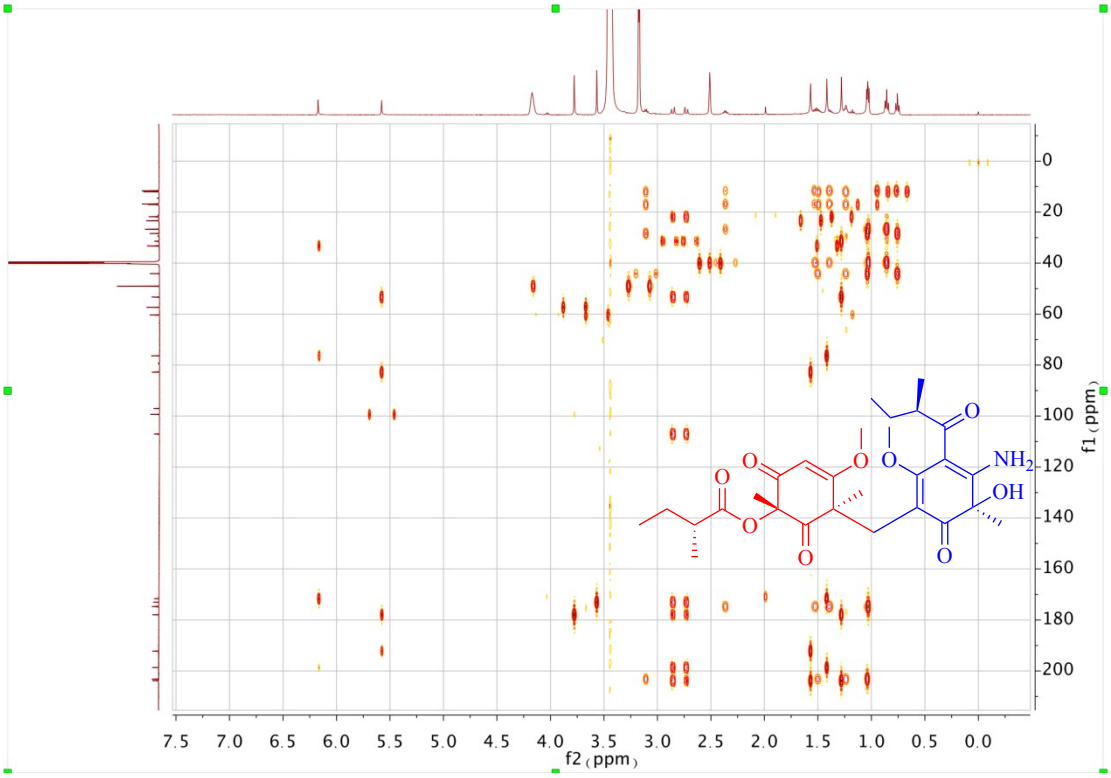


**Figure S15**. The HMBC spectrum of gilluoneB (**2**) in DMSO-$d_6$

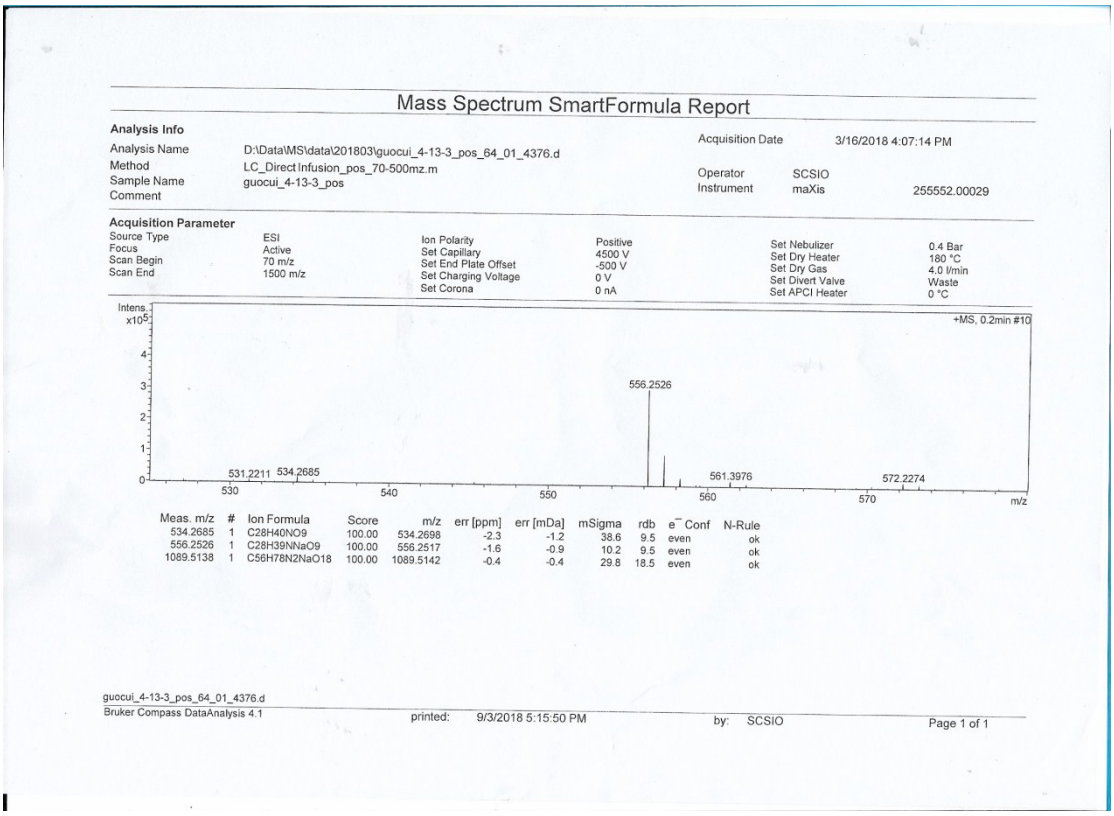

Mass Spectrum SmartFormula Report

**Analysis Info**

| | | | |
|---|---|---|---|
| Analysis Name | D:\Data\MS\data\201803\guocui_4-13-3_pos_64_01_4376.d | Acquisition Date | 3/16/2018 4:07:14 PM |
| Method | LC_Direct Infusion_pos_70-500mz.m | | |
| Sample Name | guocui_4-13-3_pos | Operator | SCSIO |
| Comment | | Instrument | maXis 255552.00029 |

**Acquisition Parameter**

| | | | | | |
|---|---|---|---|---|---|
| Source Type | ESI | Ion Polarity | Positive | Set Nebulizer | 0.4 Bar |
| Focus | Active | Set Capillary | 4500 V | Set Dry Heater | 180 °C |
| Scan Begin | 70 m/z | Set End Plate Offset | -500 V | Set Dry Gas | 4.0 l/min |
| Scan End | 1500 m/z | Set Charging Voltage | 0 V | Set Divert Valve | Waste |
| | | Set Corona | 0 nA | Set APCI Heater | 0 °C |



| Meas. m/z | # | Ion Formula | Score | m/z | err [ppm] | err [mDa] | mSigma | rdb | e⁻ Conf | N-Rule |
|---|---|---|---|---|---|---|---|---|---|---|
| 534.2685 | 1 | C28H40NO9 | 100.00 | 534.2698 | -2.3 | -1.2 | 38.6 | 9.5 | even | ok |
| 556.2526 | 1 | C28H39NNaO9 | 100.00 | 556.2517 | -1.6 | -0.9 | 10.2 | 9.5 | even | ok |
| 1089.5138 | 1 | C56H78N2NaO18 | 100.00 | 1089.5142 | -0.4 | -0.4 | 29.8 | 18.5 | even | ok |



**Figure S16**. The HRESIMS spectrum of gilluoneB (**2)**

# 光谱峰值检测报告

2018-06-19 16:59:36

数据集: 4-13-3 - RawData

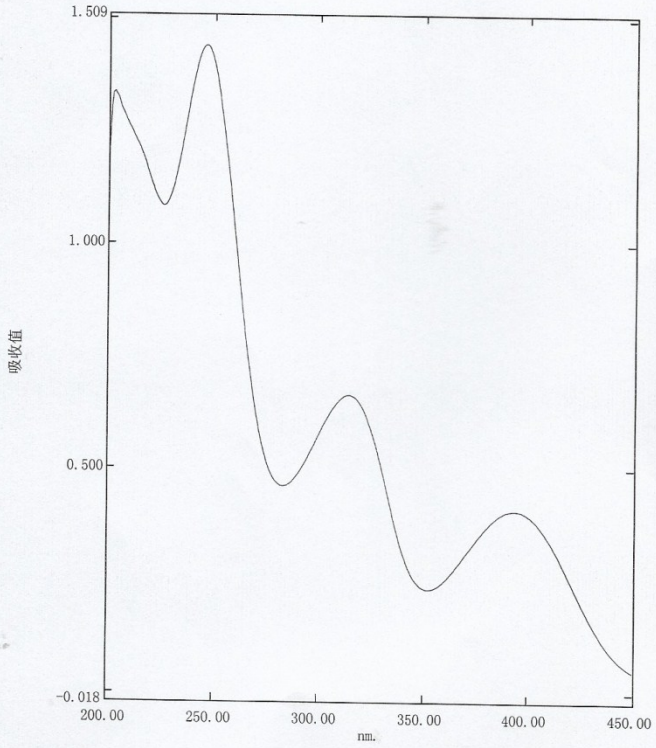


[测定属性]
波长范围 (nm.): 200.00 到 450.00
扫描速度: 中速
采样间隔: 0.2
自动采样间隔: 启用
扫描模式: 单个

[仪器属性]
仪器类型: UV-2600 系列
测定方式: 吸收值
狭缝宽: 2.0
积分时间: 0.1 秒.
光源转换波长: 323.0 nm
检测器单元: 直接
S/R 转换: 标准
阶梯校正: OFF

[附件属性]
附件: 无

[数据处理参数]
阈值: 0.0100000
点: 5
内插: 停用
平均: 停用

[样品准备属性]
重量:
体积:
稀释:
光程长:
附加信息:

| No. | P/V | 波长(nm) | 吸收值 | 描述 |
|---|---|---|---|---|
| 1 | ↑ | 393.60 | 0.408 | |
| 2 | ↑ | 314.40 | 0.663 | |
| 3 | ↑ | 246.20 | 1.440 | |
| 4 | ↑ | 202.80 | 1.336 | |
| 5 | ↓ | 352.00 | 0.233 | |
| 6 | ↓ | 283.40 | 0.461 | |
| 7 | ↓ | 226.60 | 1.083 | |



**Figure S17**. The UV spectrum of gilluoneB (**2)**

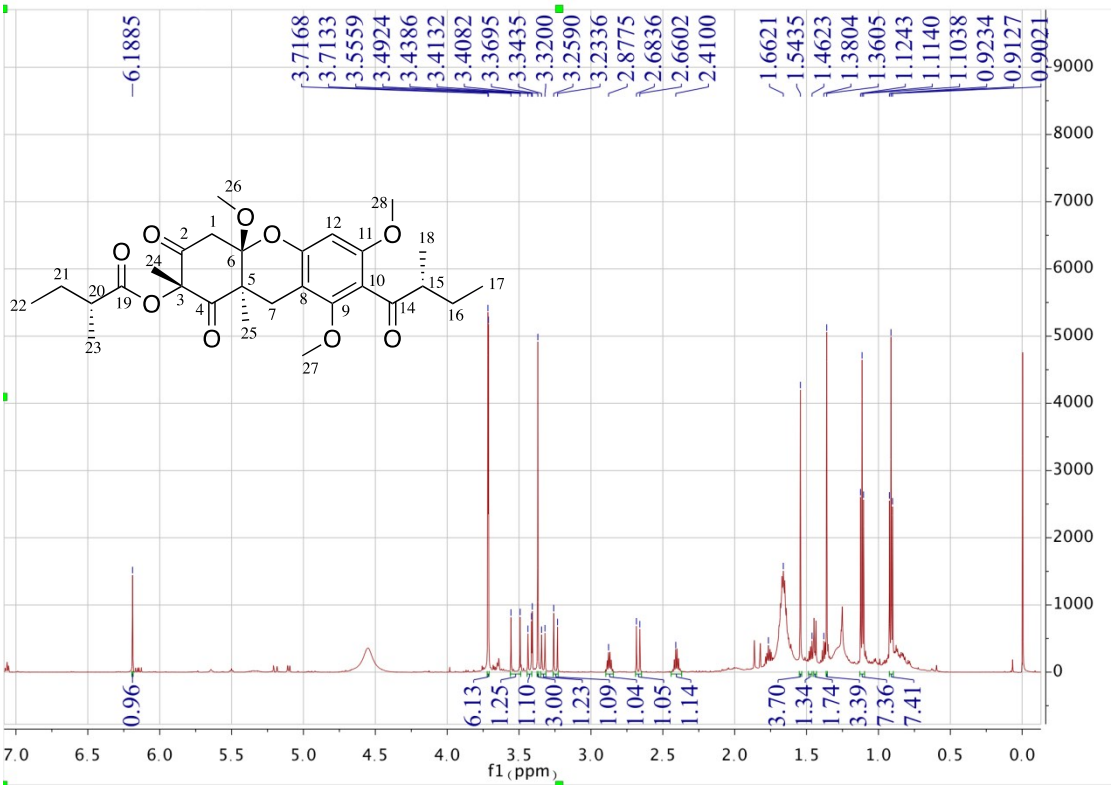


**Figure S18**. The $^{1}H$ NMR spectrum of gilluone C(**3**) in $CDCl_3$ (700 MHz)

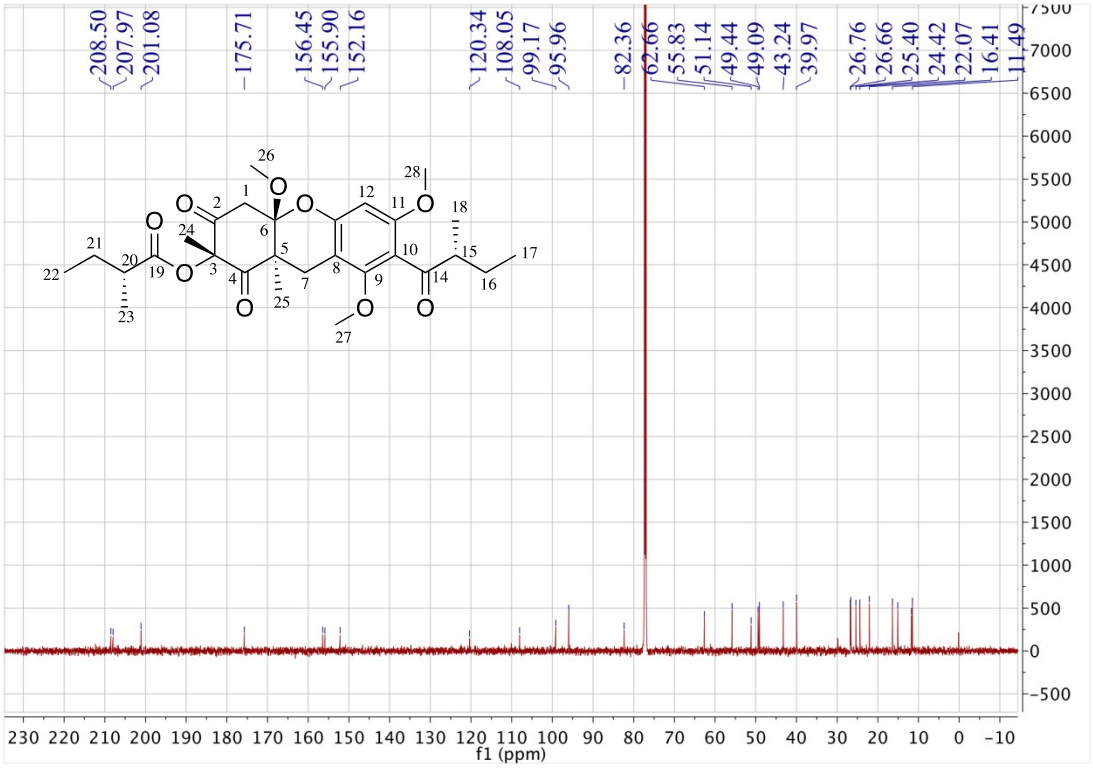


**Figure S19**. The $^{13}C$ NMR spectrum of gilluone C (**3**) in $CDCl_3$ (175 MHz)

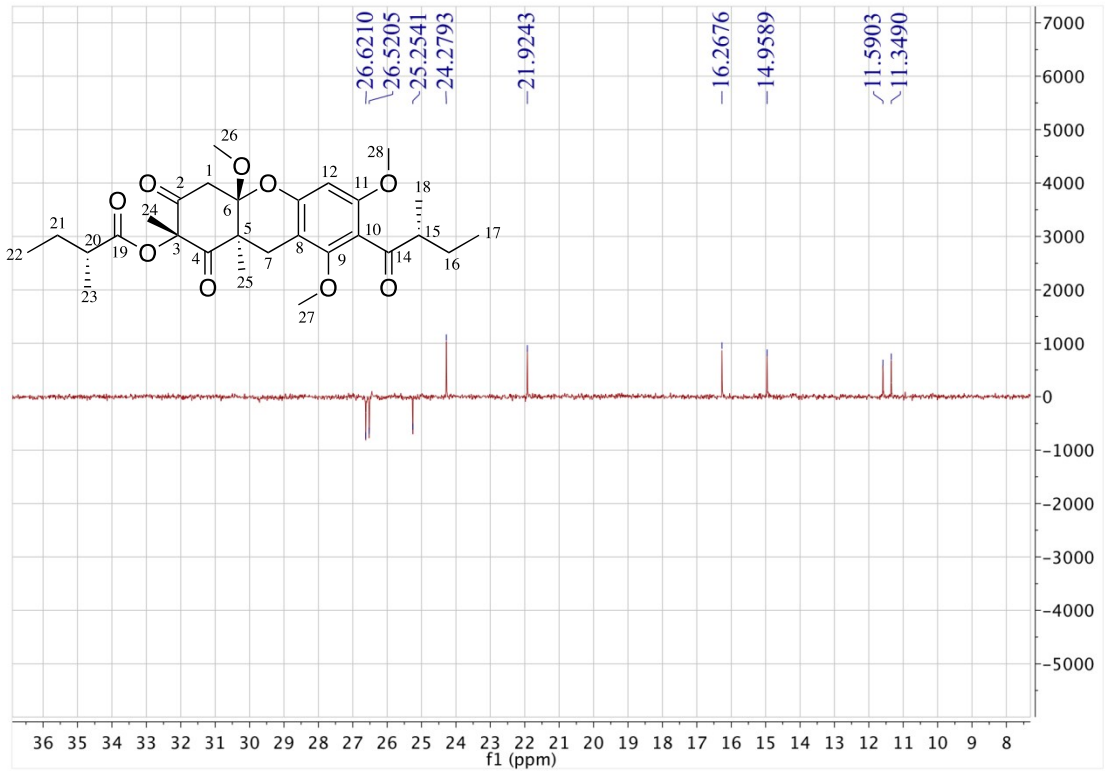


**Figure S20**. The DEPT spectrum of gilluone C (**3**) in $CDCl_3$ (175 MHz)

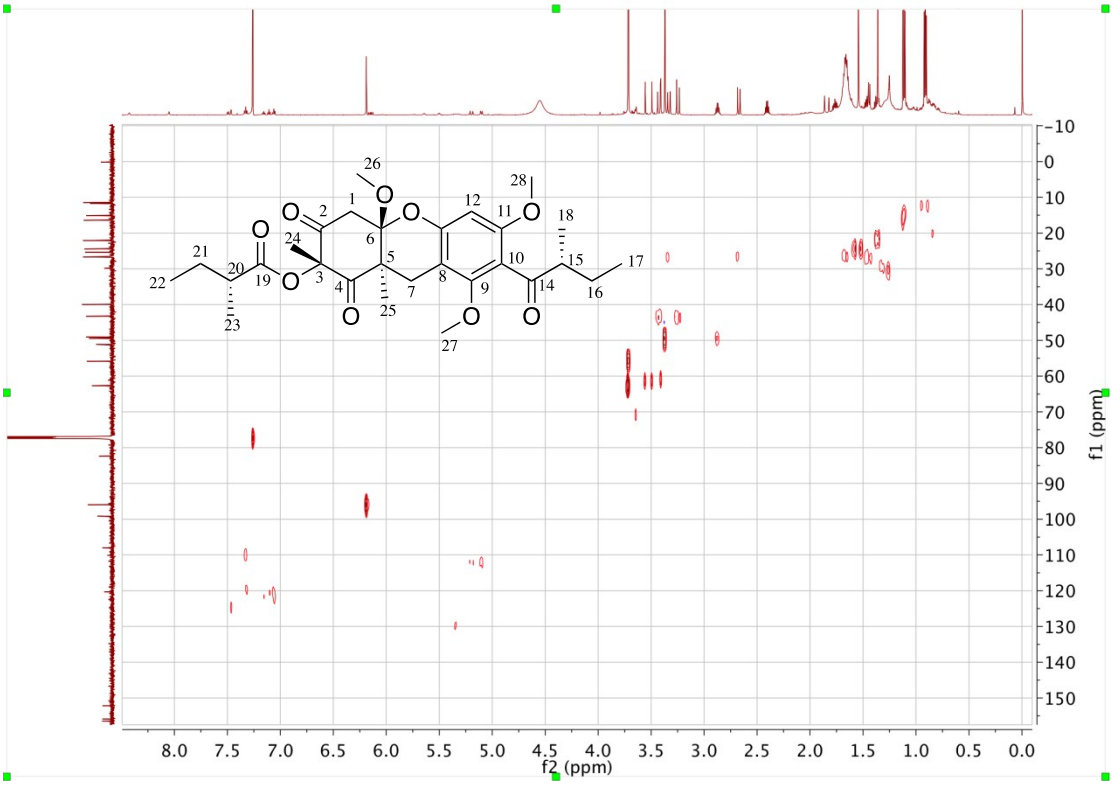


**Figure S21**. The HSQC spectrum of gilluone C (**3**) in $CDCl_3$

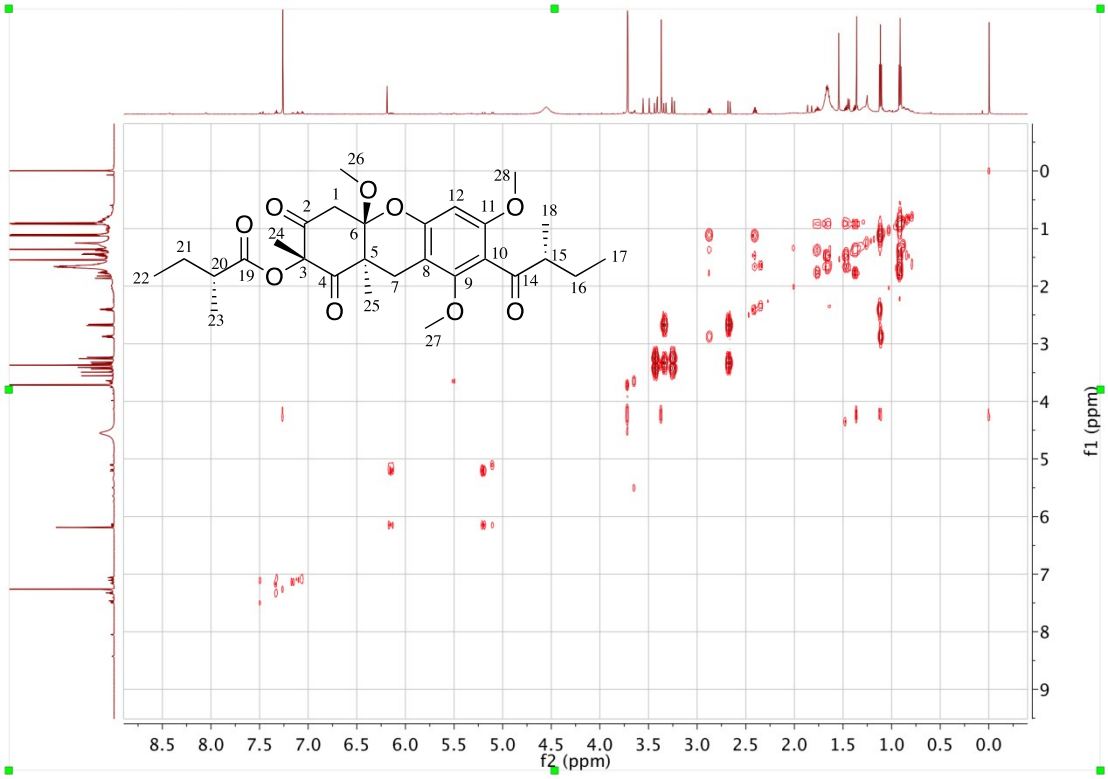


**Figure S22**. The $^{1}H$-$^{1}H$ COSY spectrum of gilluone C(**3**) in $CDCl_3$

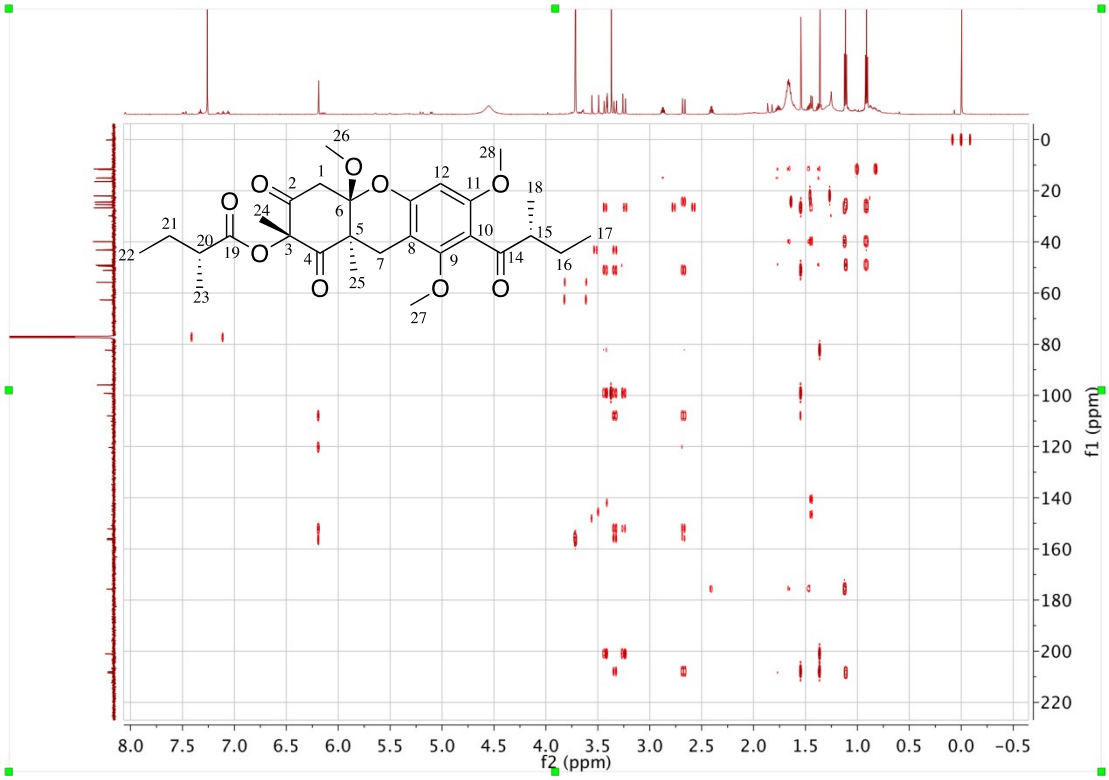


**Figure S23**. The HMBC spectrum of gilluone C (**3**) in $CDCl_3$

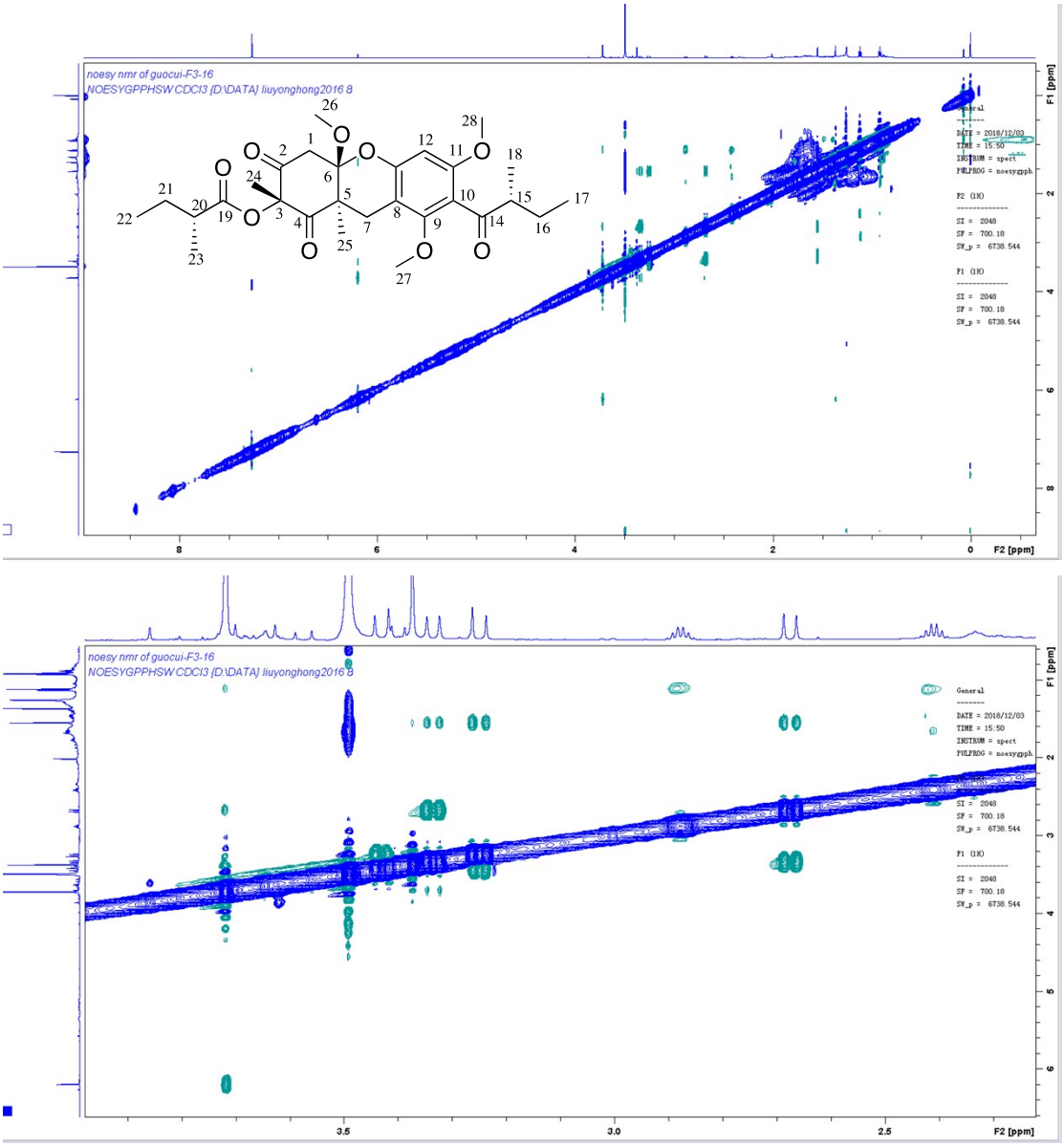


**Figure S24**. The NOESY spectrum of gilluone C(**3)**

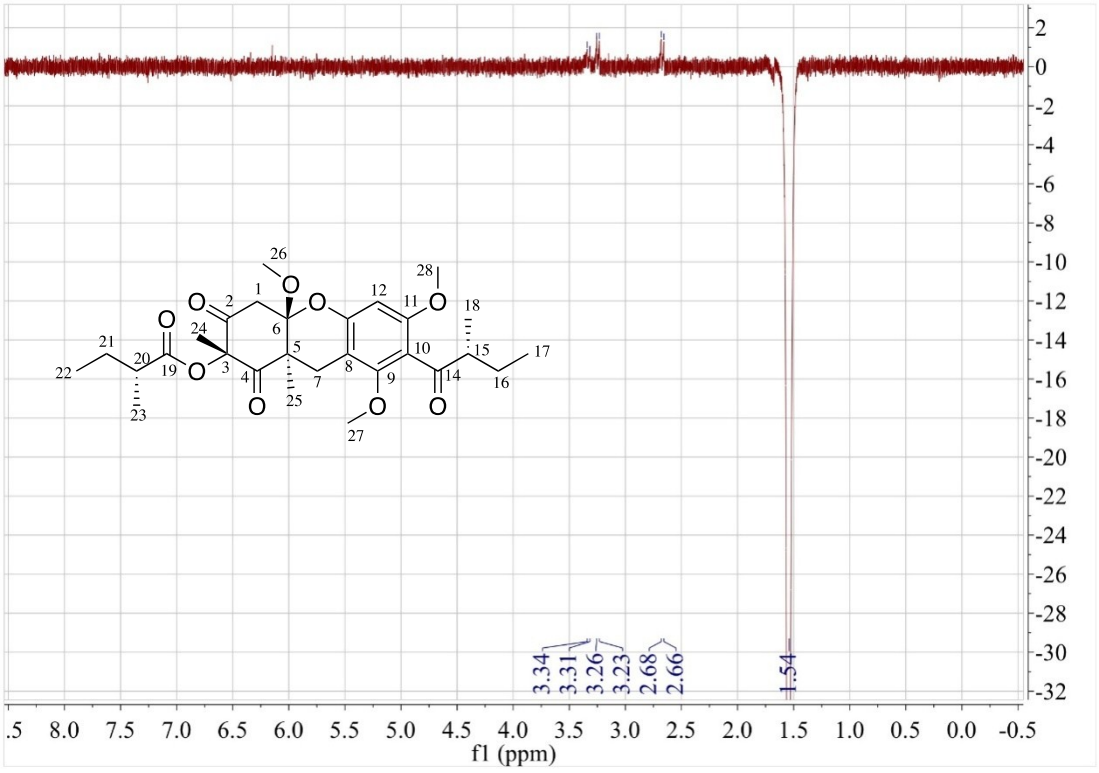


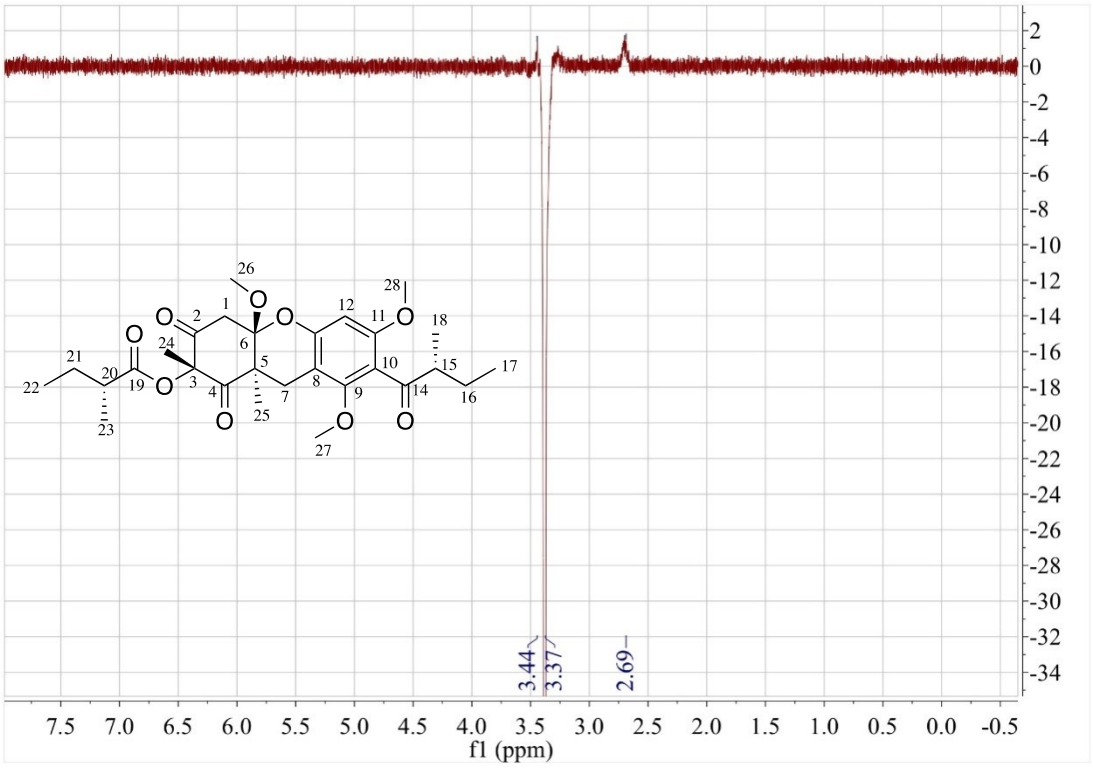


**Figure S25**. The NOE difference experiments of gilluone C (**3**) in $CDCl_3$

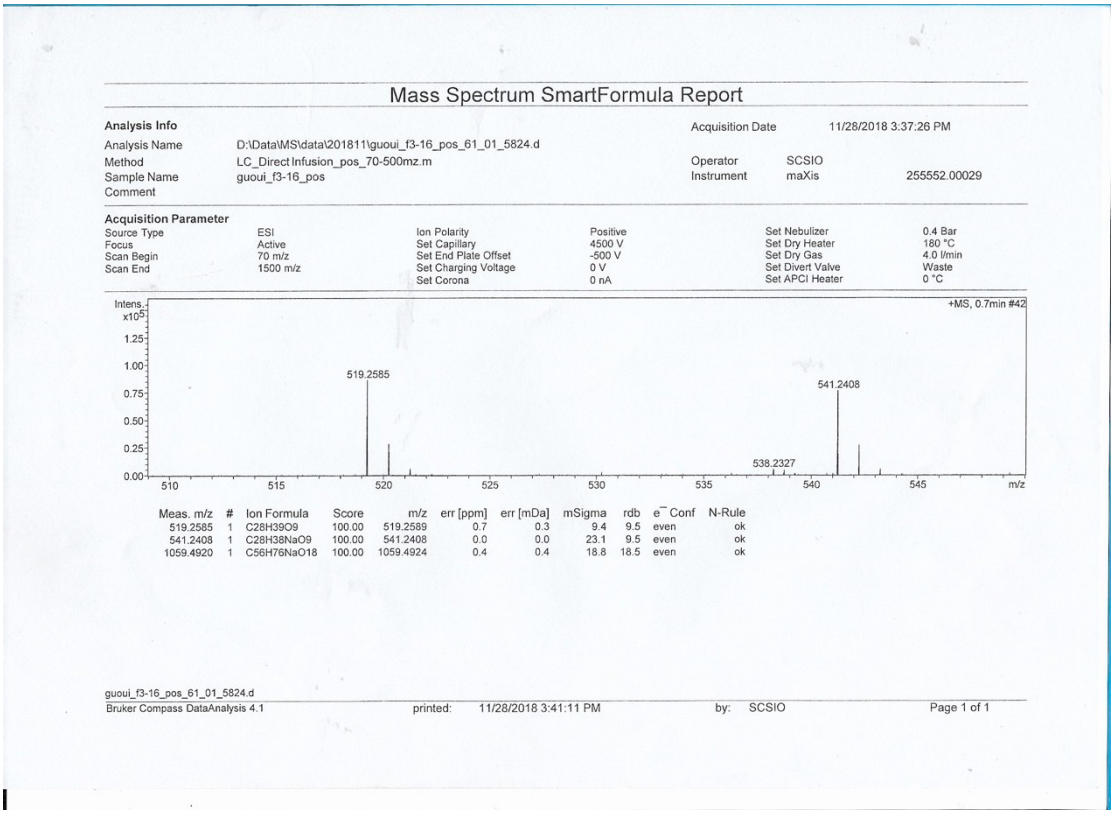


**Figure S26**. The HRESIMS spectrum of gilluone C (**3**)

# 光谱选点检测报告

2018-11-29 11:21:04

数据集: f3-16 - RawData

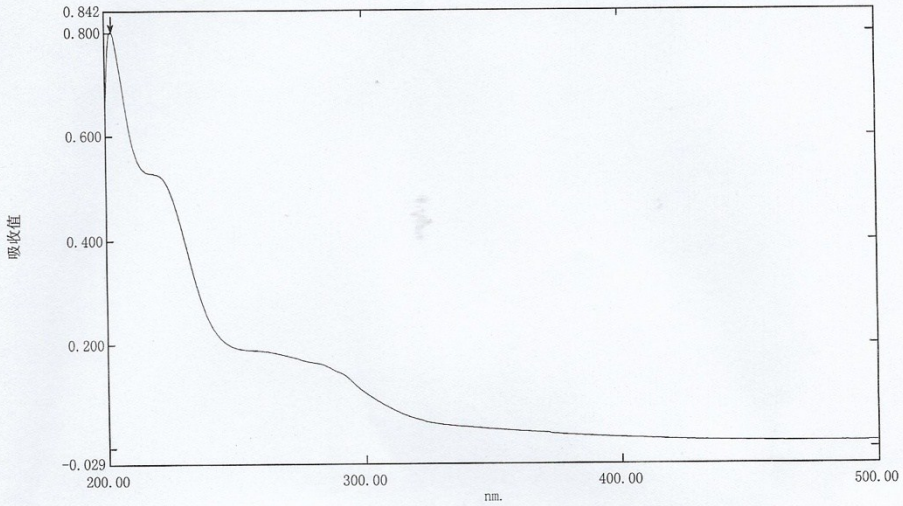


[测定属性]
波长范围 (nm.): 200.00 到 500.00
扫描速度: 中速
采样间隔: 0.2
自动采样间隔: 启用
扫描模式: 单个

[仪器属性]
仪器类型: UV-2600 系列
测定方式: 吸收值
狭缝宽: 2.0
积分时间: 0.1 秒.
光源转换波长: 323.0 nm
检测器单元: 直接
S/R 转换: 标准
阶梯校正: OFF

[附件属性]
附件: 无

[数据处理参数]
阈值: 0.0100000
点: 5
内插: 停用
平均: 停用

[样品准备属性]
重量:
体积:
稀释:
光程长:
附加信息:

| No. | 波长(nm) | 吸收值 | 描述 |
|---|---|---|---|
| 1 | 274.40 | 0.170 | |
| 2 | 218.40 | 0.528 | |
| 3 | 202.80 | 0.801 | |
| 4 | | | |



**Figure S27**. The UV spectrum of gilluone C (**3)**

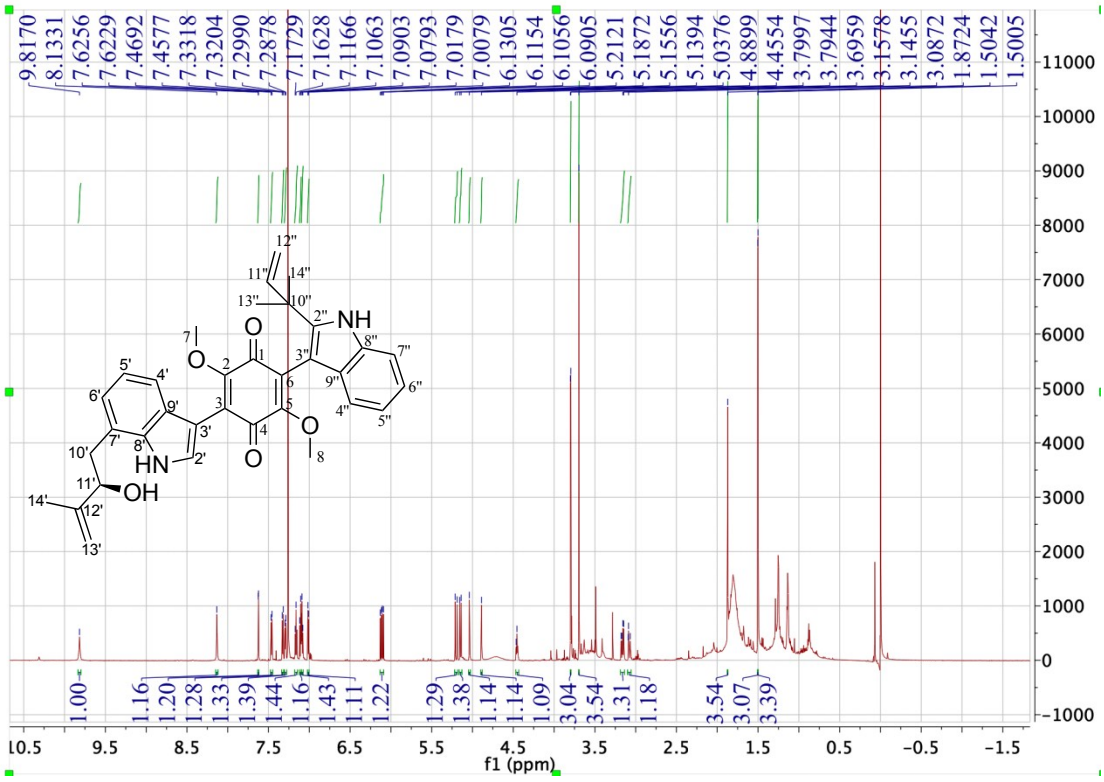


**Figure S28**. The $^{1}$H NMR spectrum of asterriquinone I (**4**) in $CDCl_3$ (700 MHz)

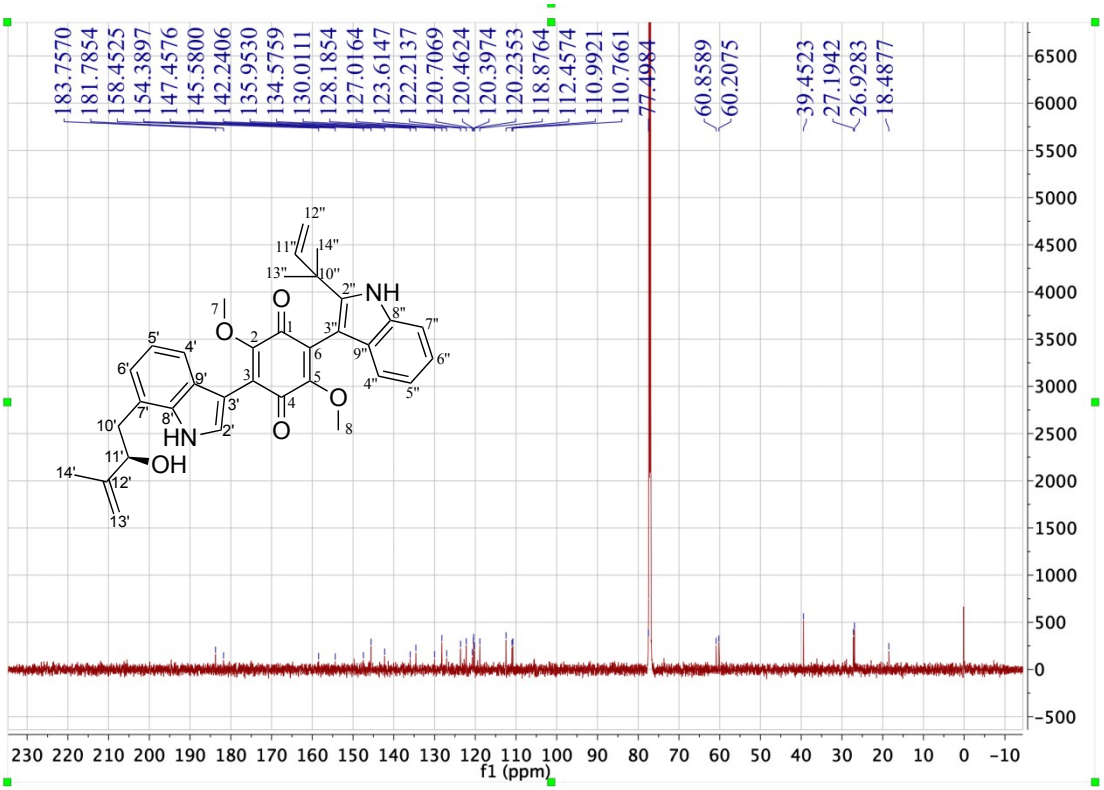


**Figure S29**. The $^{13}$C NMR spectrum of asterriquinone I (**4**) in $CDCl_3$ (175 MHz)

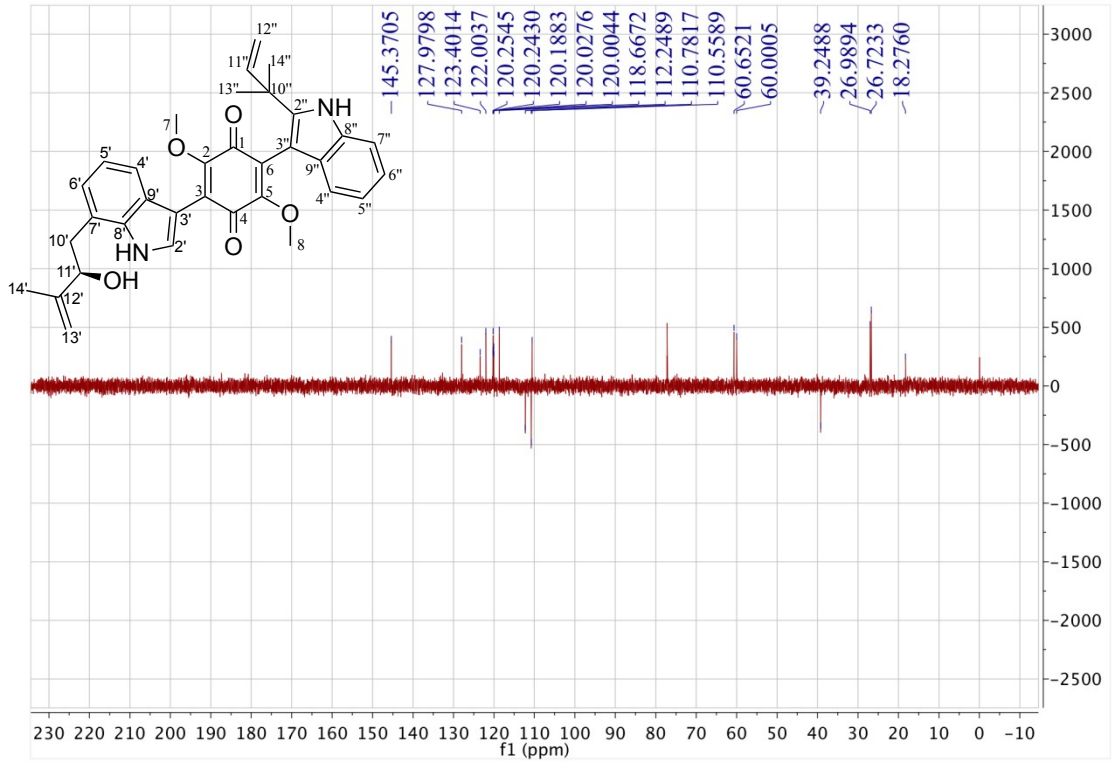


**Figure S30**. The DEPT spectrum of asterriquinone I (**4**) in $CDCl_3$ (175 MHz)

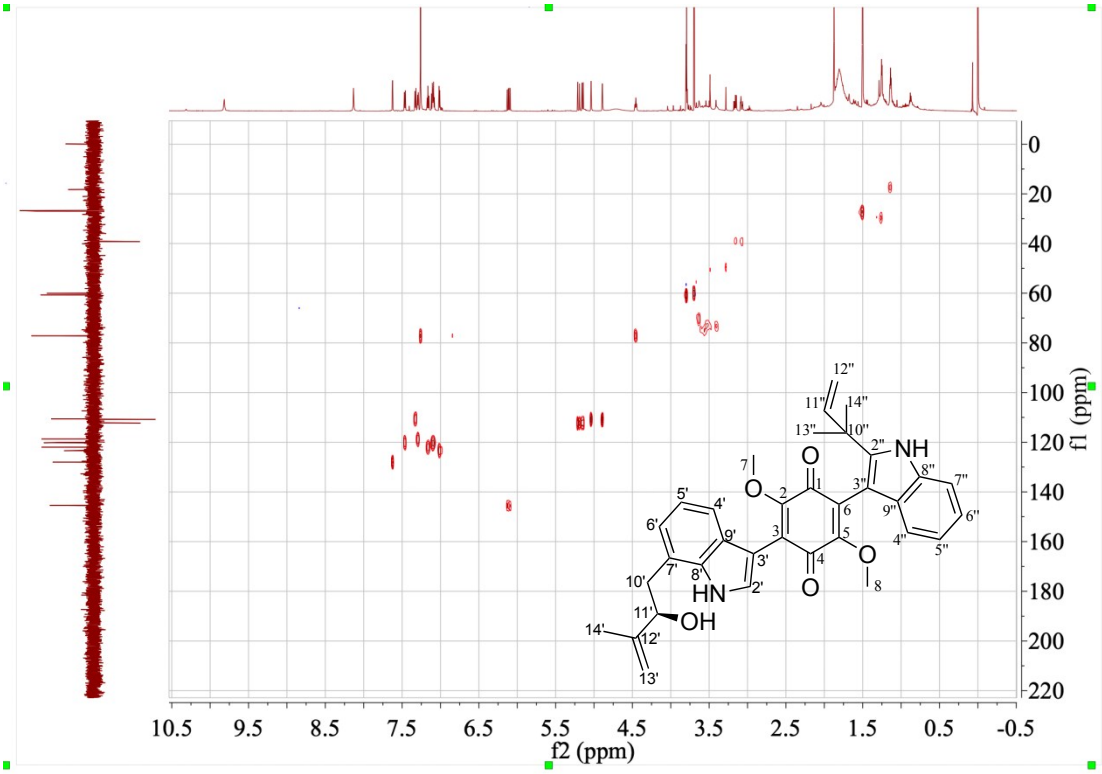


**Figure S31**. The HSQC spectrum of asterriquinone I (**4**) in $CDCl_3$

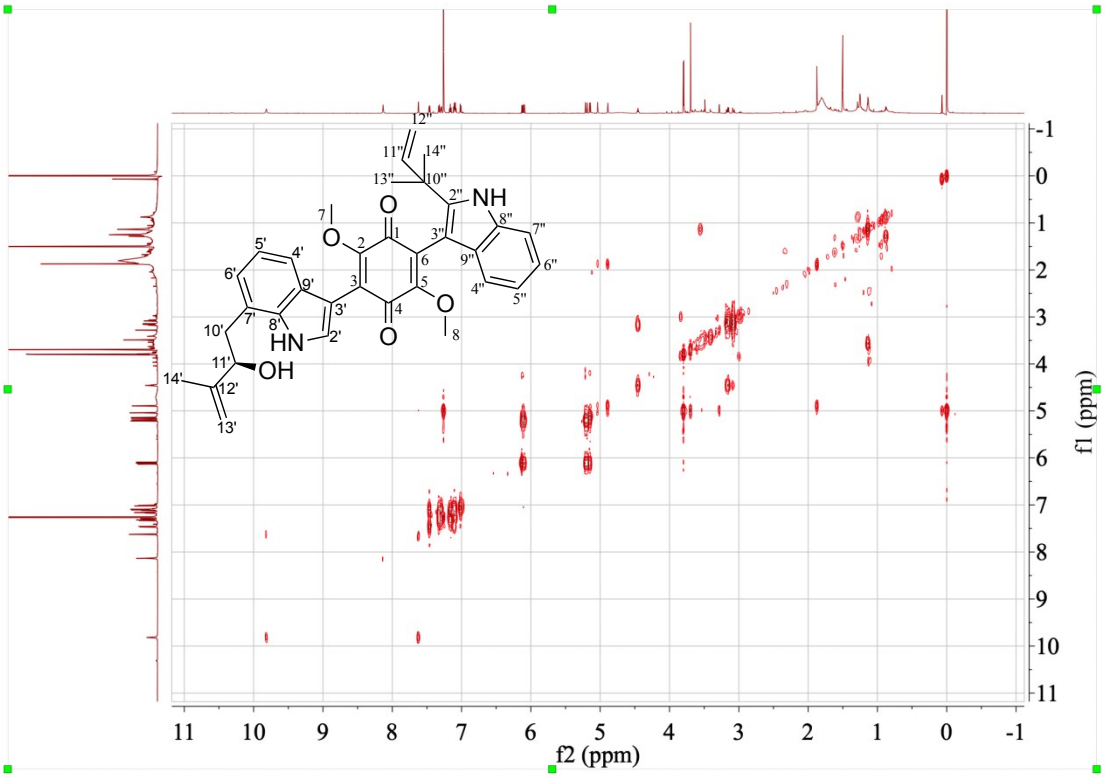


**Figure S32**. The $^{1}H$-$^{1}H$ COSY spectrum of asterriquinone I (**4**) in $CDCl_3$

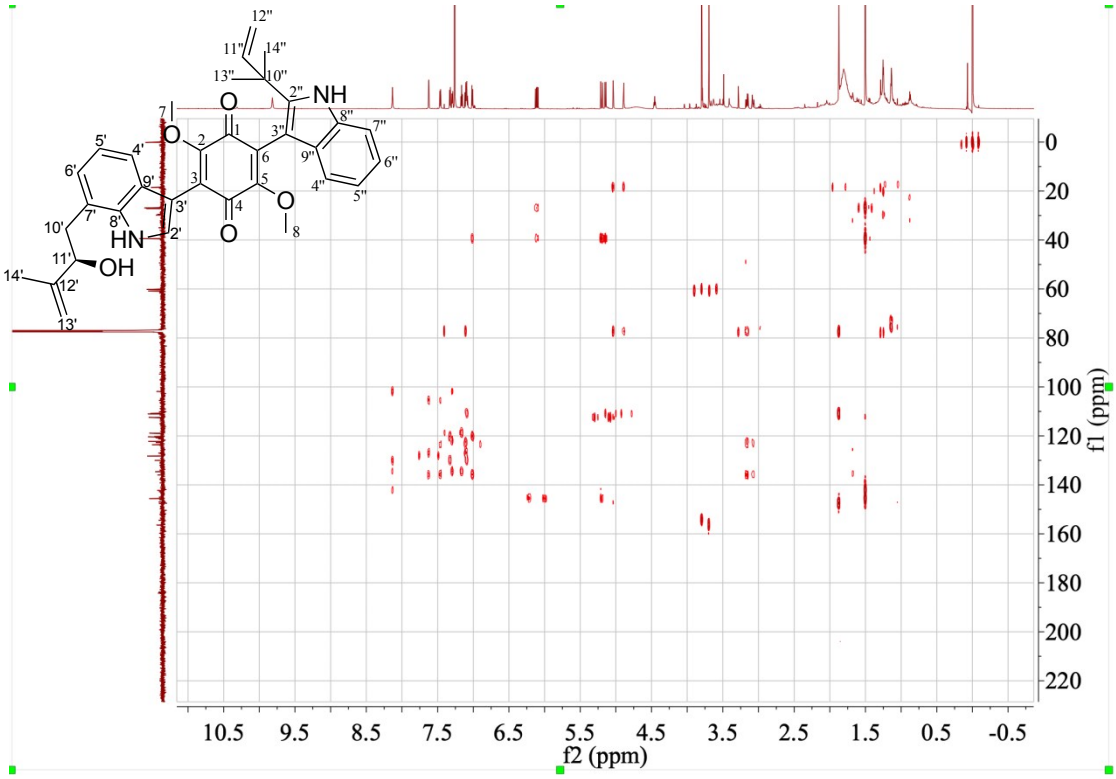


**Figure S33**. The HMBC spectrum of asterriquinone I (**4**) in $CDCl_3$

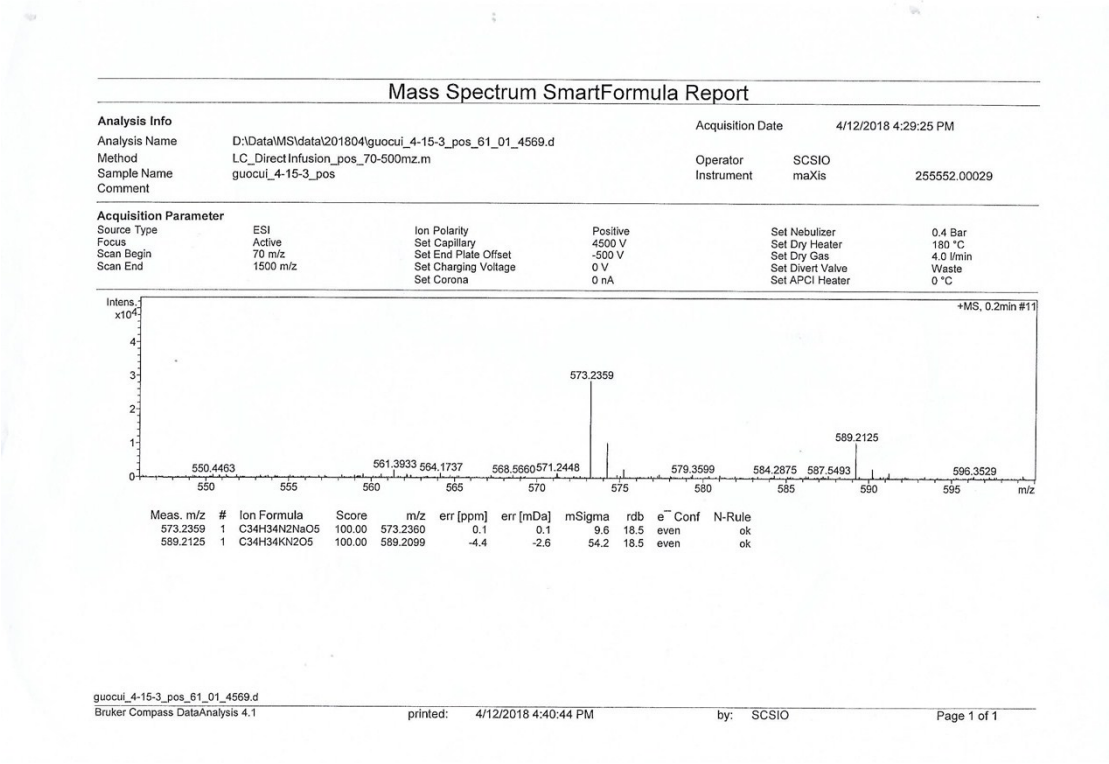


**Figure S34**. The HRESIMS spectrum of asterriquinone I (**4)**

光谱峰值检测报告

2018-06-19 16:33:33

数据集: guocui4-15-3 - RawData

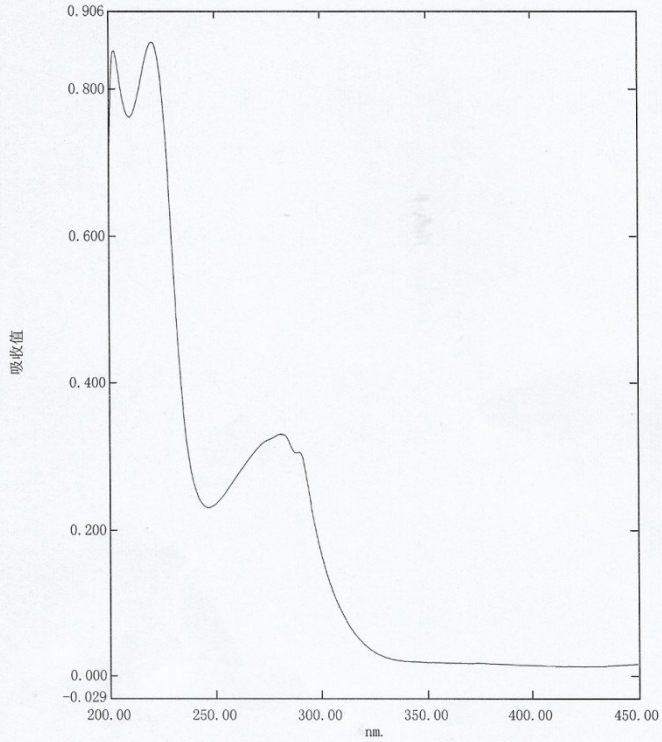


[测定属性]
波长范围 (nm.): 200.00 到 450.00
扫描速度: 中速
采样间隔: 0.2
自动采样间隔: 启用
扫描模式: 单个

[仪器属性]
仪器类型: UV-2600 系列
测定方式: 吸收值
狭缝宽: 2.0
积分时间: 0.1 秒.
光源转换波长: 323.0 nm
检测器单元: 直接
S/R 转换: 标准
阶梯校正: OFF

[附件属性]
附件: 无

[数据处理参数]
阈值: 0.0100000
点: 5
内插: 停用
平均: 停用

[样品准备属性]
重量:
体积:
稀释:
光程长:
附加信息:

| No. | P/V | 波长(nm) | 吸收值 | 描述 |
|---|---|---|---|---|
| 1 | ↑ | 281.00 | 0.330 | |
| 2 | ↑ | 220.60 | 0.864 | |
| 3 | ↑ | 202.60 | 0.852 | |
| 4 | ↓ | 247.00 | 0.230 | |
| 5 | ↓ | 210.00 | 0.762 | |



**Figure S35**. The UV spectrum of asterriquinone I (**4**)

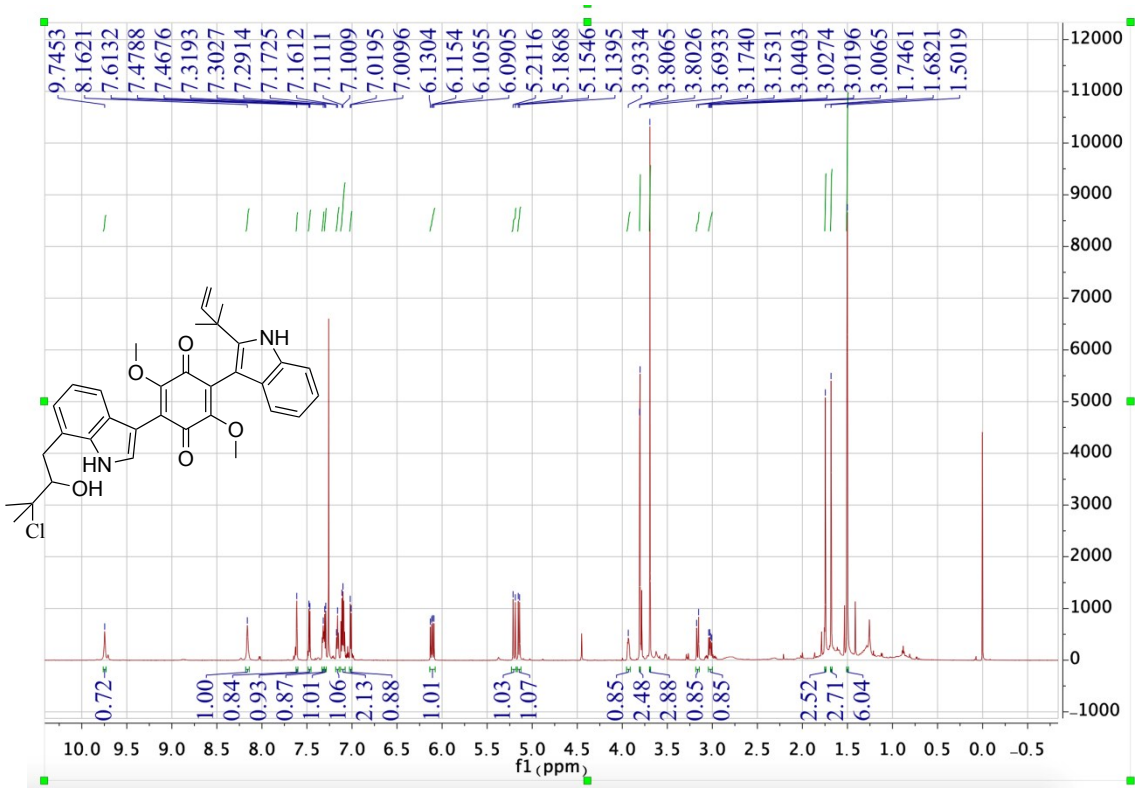


**Figure S36**. The $^{1}H$ NMR spectrum of asterriquinone J (**5**)in $CDCl_3$ (700 MHz)

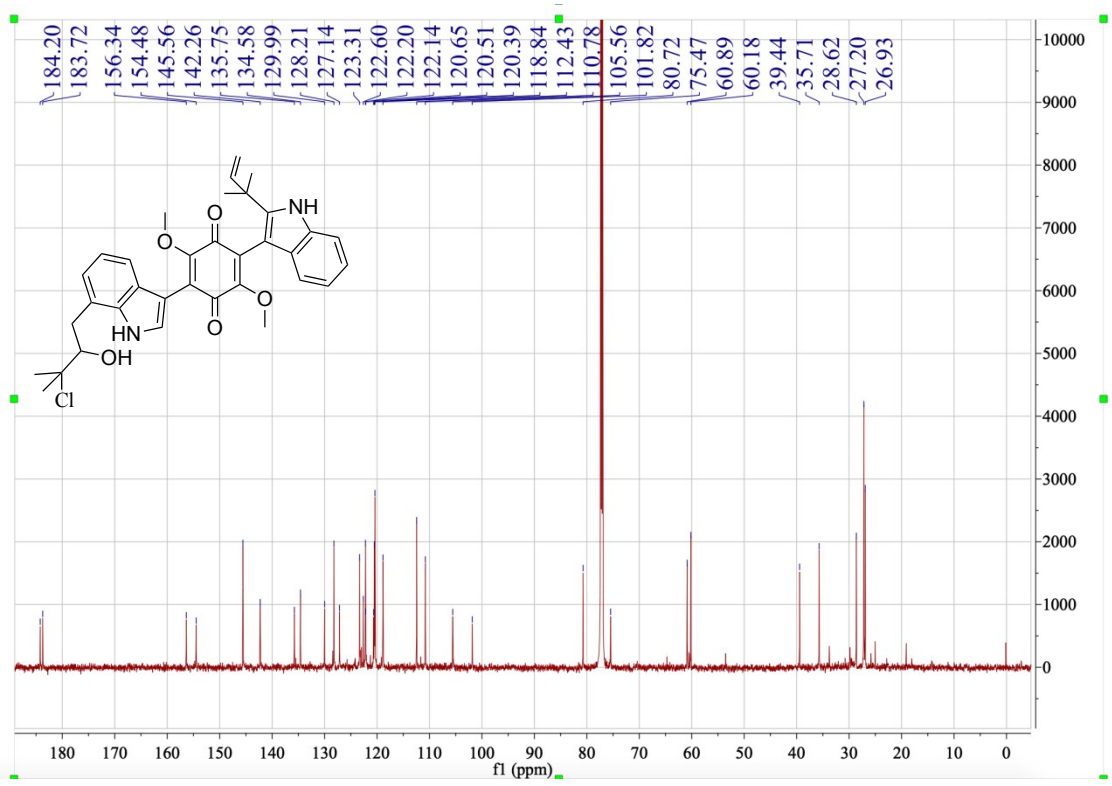


**Figure S37**. The $^{13}C$ NMR spectrum of asterriquinone J (**5**) in $CDCl_3$ (175 MHz)

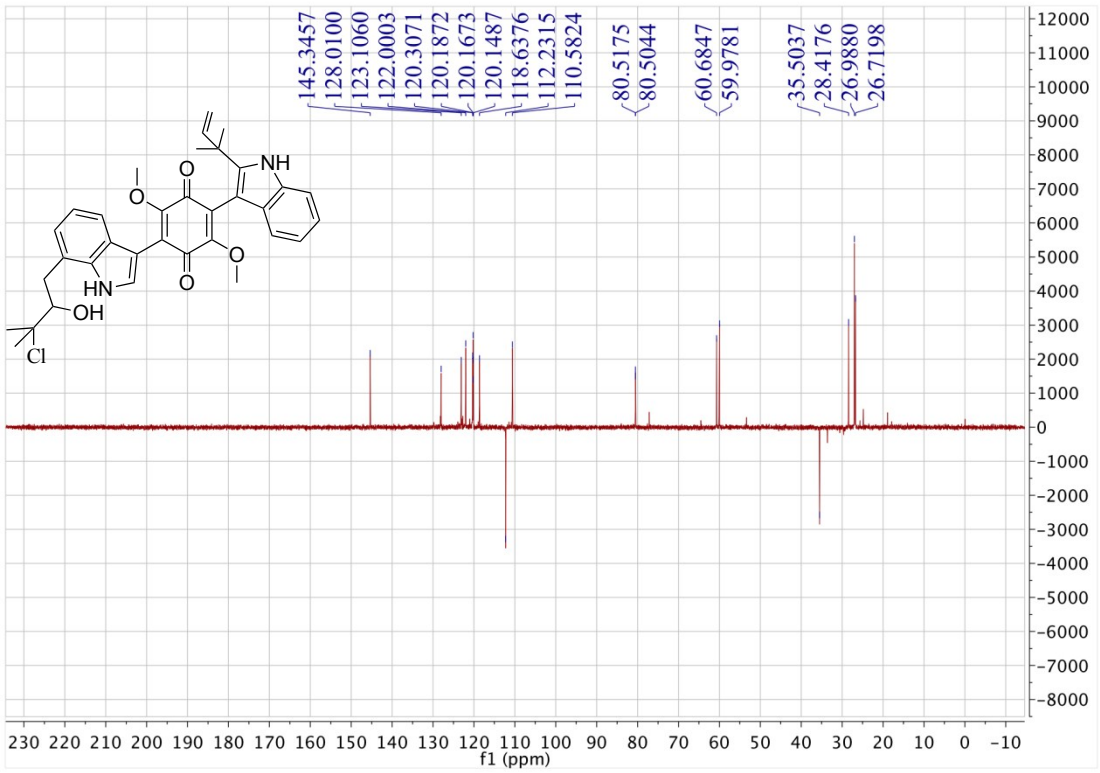


**Figure S38**. The DEPT spectrum of asterriquinone J (**5**) in $CDCl_3$ (175 MHz)

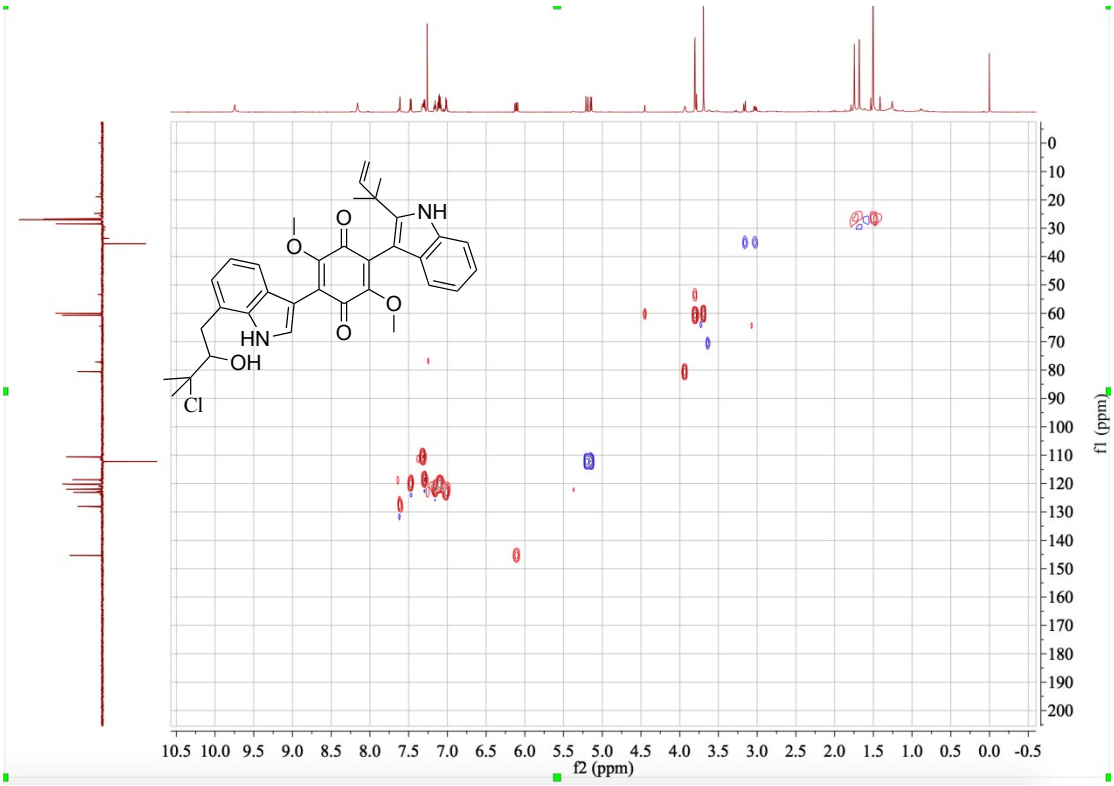


**Figure S39**. The HSQC spectrum of asterriquinone J (**5**) in $CDCl_3$

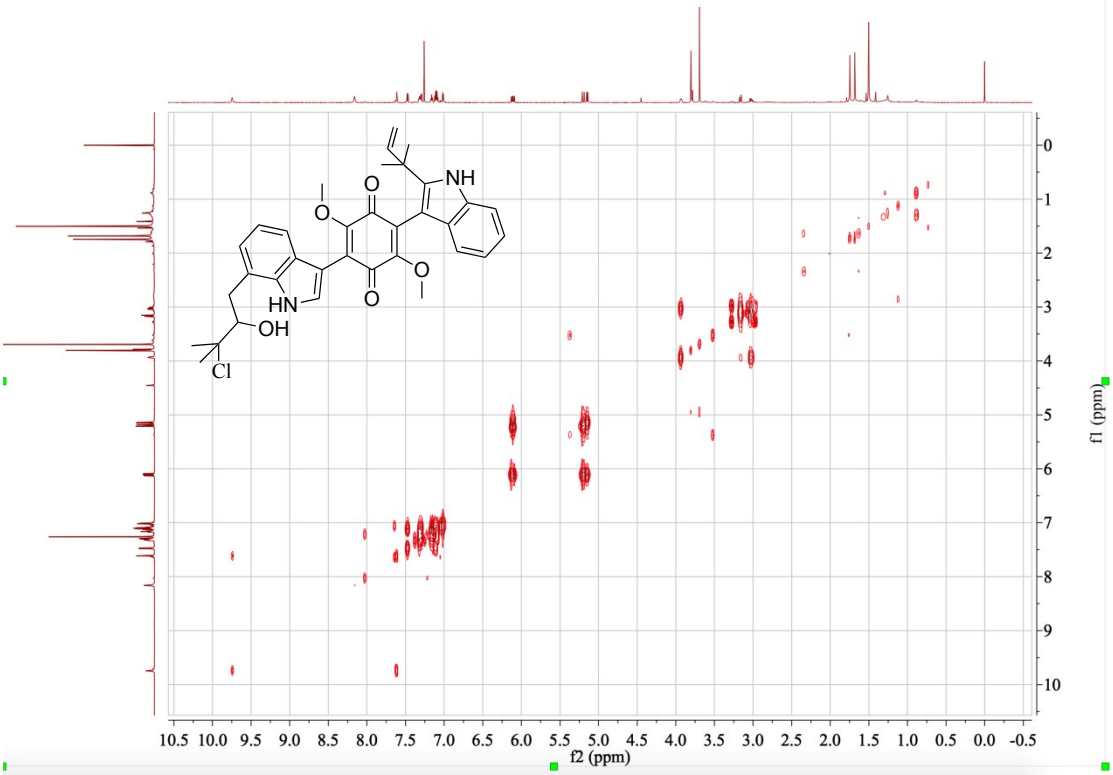


**Figure S40**. The $^{1}$H-$^{1}$H COSY spectrum of asterriquinone J (**5**) in $CDCl_3$

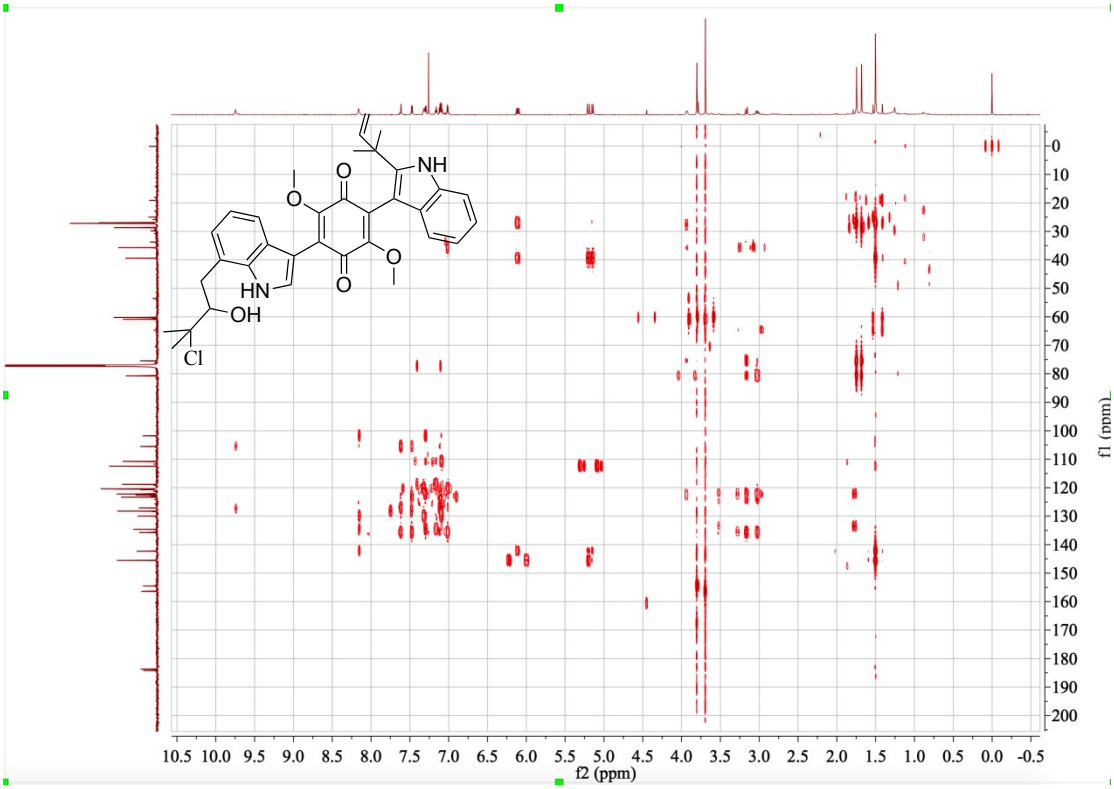


**Figure S41**. The HMBC spectrum of asterriquinone J (**5**) in $CDCl_3$

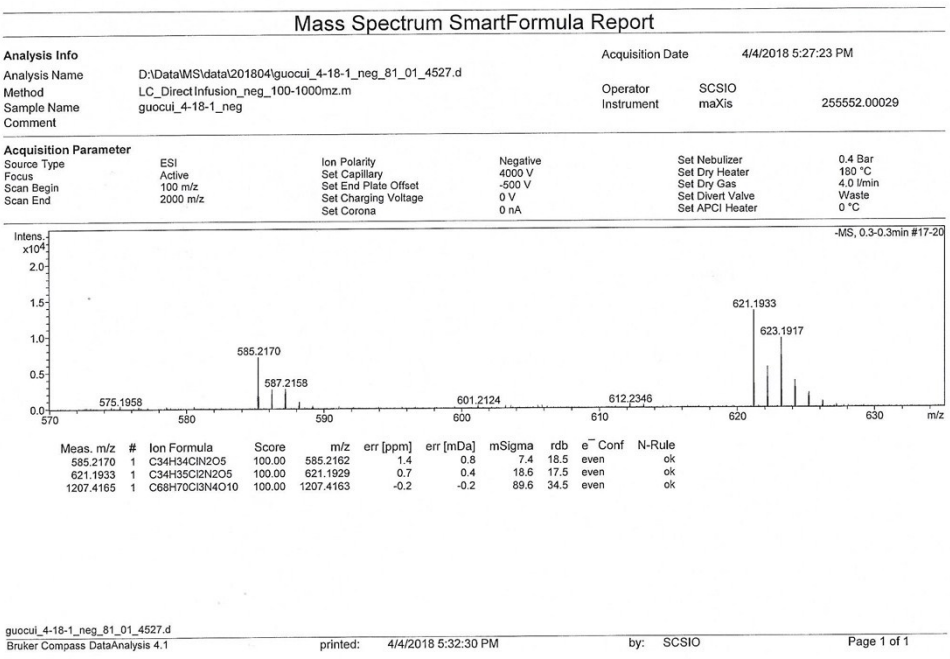


**Figure S42**. The HRESIMS spectrum of asterriquinone J (**5**)

光谱峰值检测报告

2018-06-19 16:48:07

数据集: File4-18-1 - RawData

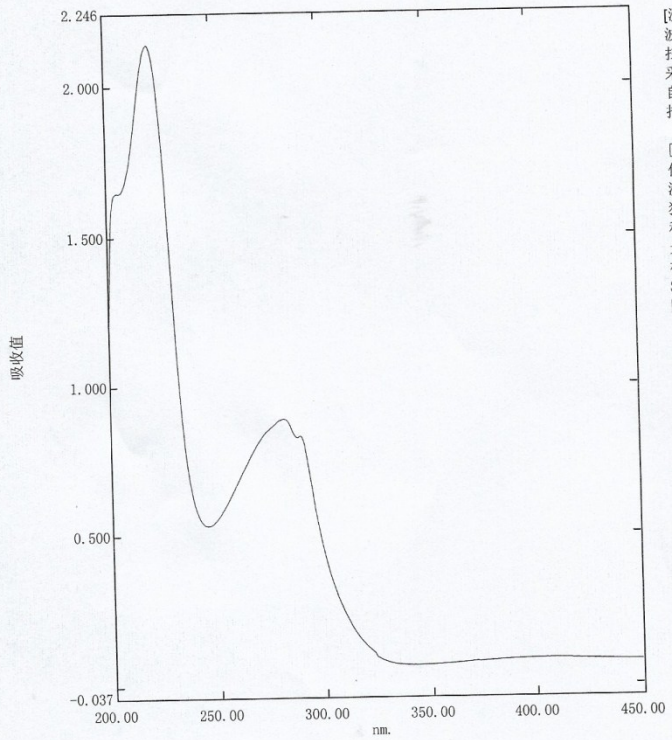


[测定属性]
波长范围 (nm.): 200.00 到 450.00
扫描速度: 中速
采样间隔: 0.2
自动采样间隔: 启用
扫描模式: 单个

[仪器属性]
仪器类型: UV-2600 系列
测定方式: 吸收值
狭缝宽: 2.0
积分时间: 0.1 秒.
光源转换波长: 323.0 nm
检测器单元: 直接
S/R 转换: 标准
阶梯校正: OFF

[附件属性]
附件: 无

[数据处理参数]
阈值: 0.0100000
点: 5
内插: 停用
平均: 停用

[样品准备属性]
重量:
体积:
稀释:
光程长:
附加信息:

| No. | P/V | 波长(nm) | 吸收值 | 描述 |
|---|---|---|---|---|
| 1 | ↑ | 289.60 | 0.832 | |
| 2 | ↑ | 281.80 | 0.890 | |
| 3 | ↑ | 221.00 | 2.142 | |
| 4 | ↓ | 288.00 | 0.828 | |
| 5 | ↓ | 245.20 | 0.533 | |

页 1 / 1

**Figure S43**. The UV spectrum of compound asterriquinone J (**5**)

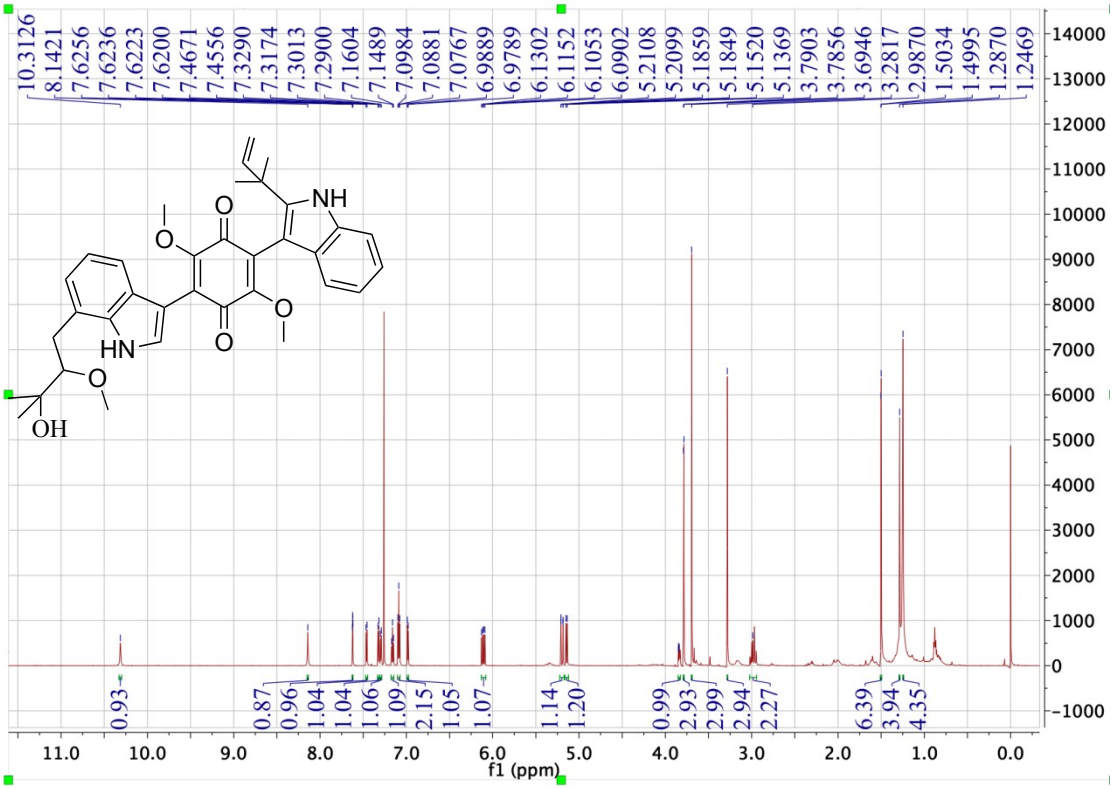


**Figure S44**. The $^{1}$H NMR spectrum of compound asterriquinone K (**6**)in $CDCl_3$

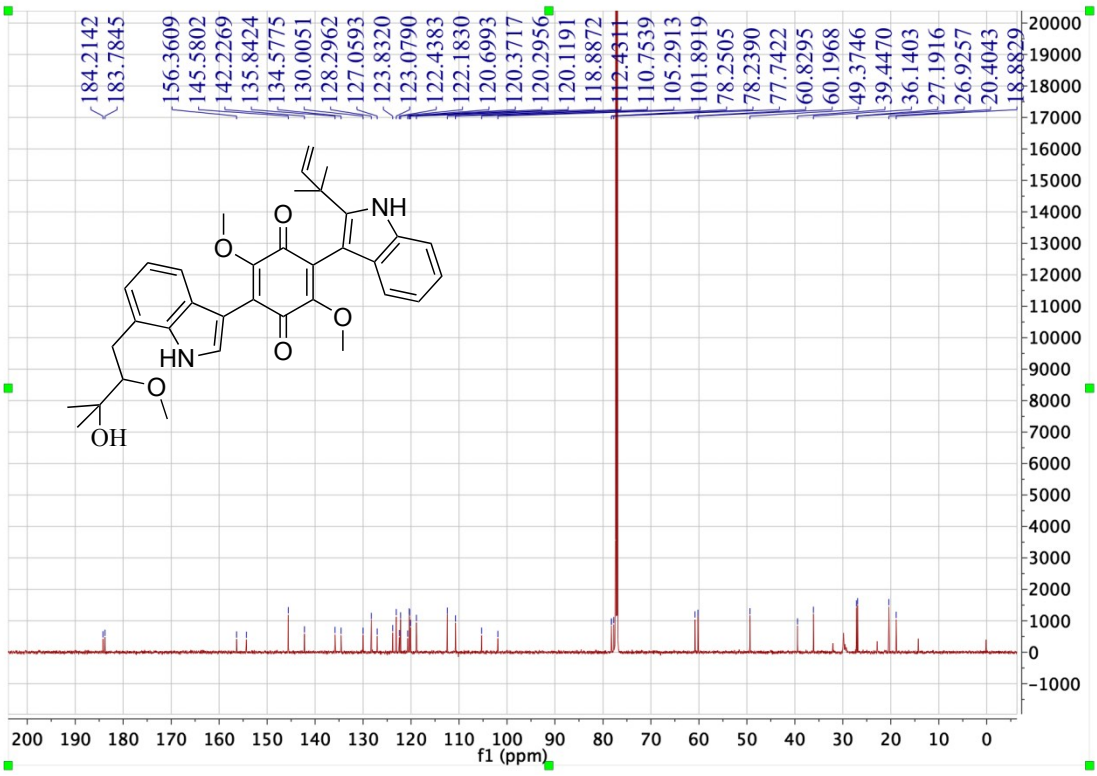


**Figure S45**. The $^{13}$C NMR spectrum of asterriquinone K (**6**) in $CDCl_3$ (175 MHz)

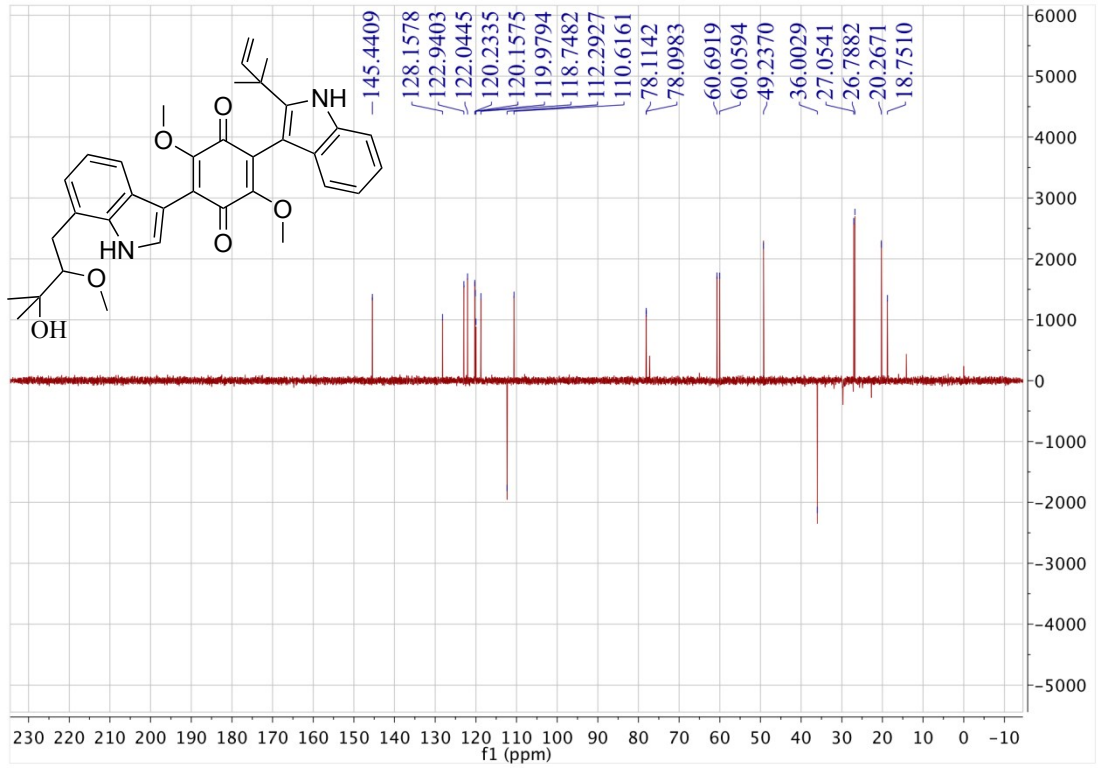


**Figure S46**. The DEPT spectrum of asterriquinone K (**6**) in $CDCl_3$

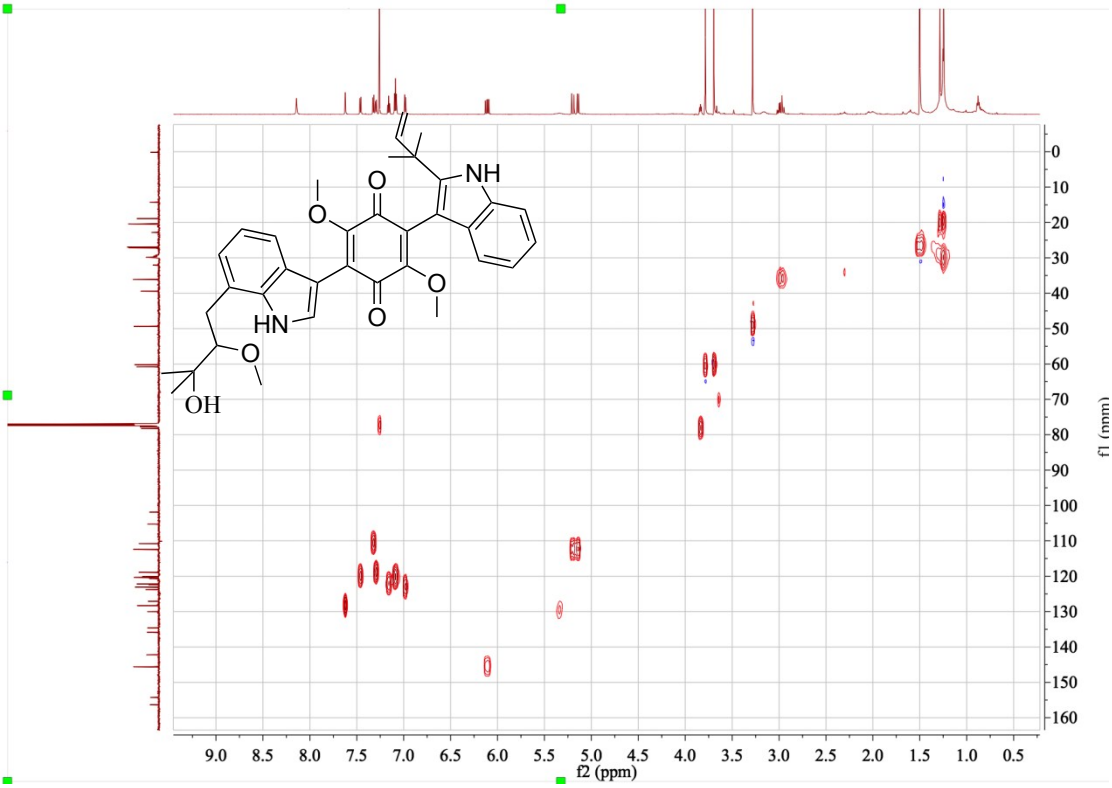


**Figure S47**. The HSQC spectrum of asterriquinone K (**6**) in $CDCl_3$

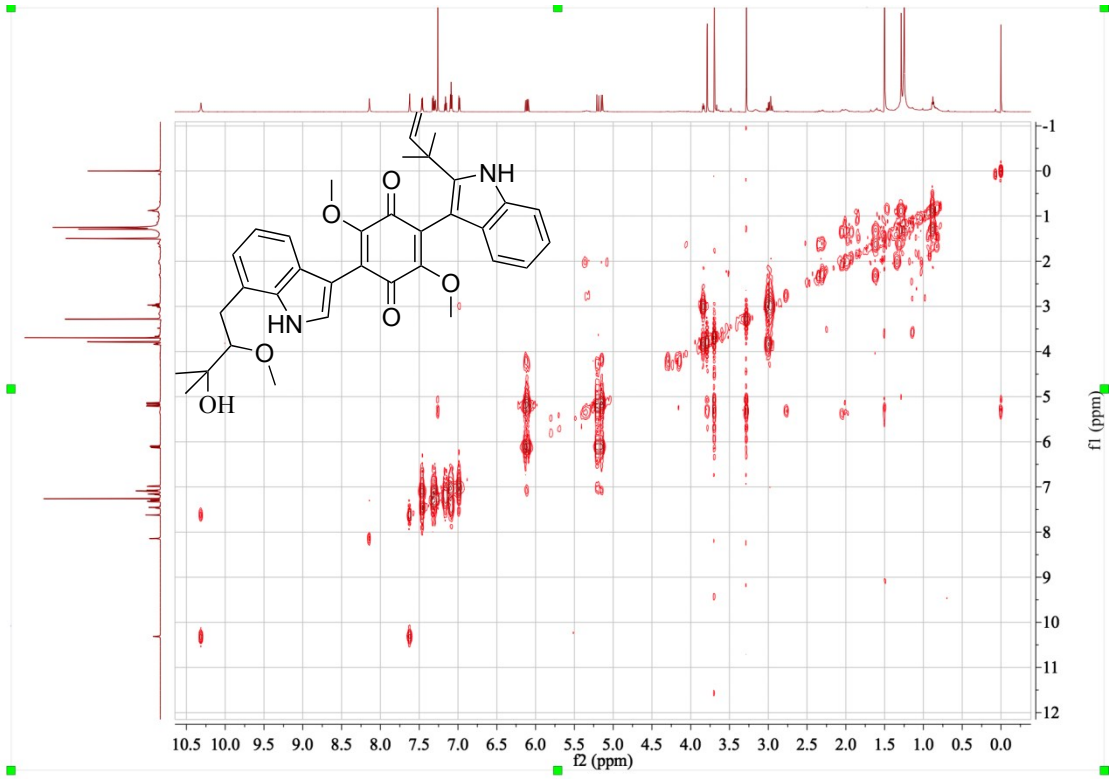


**Figure S48**. The $^{1}H$-$^{1}H$ COSY spectrum of asterriquinone K (**6**) in $CDCl_3$

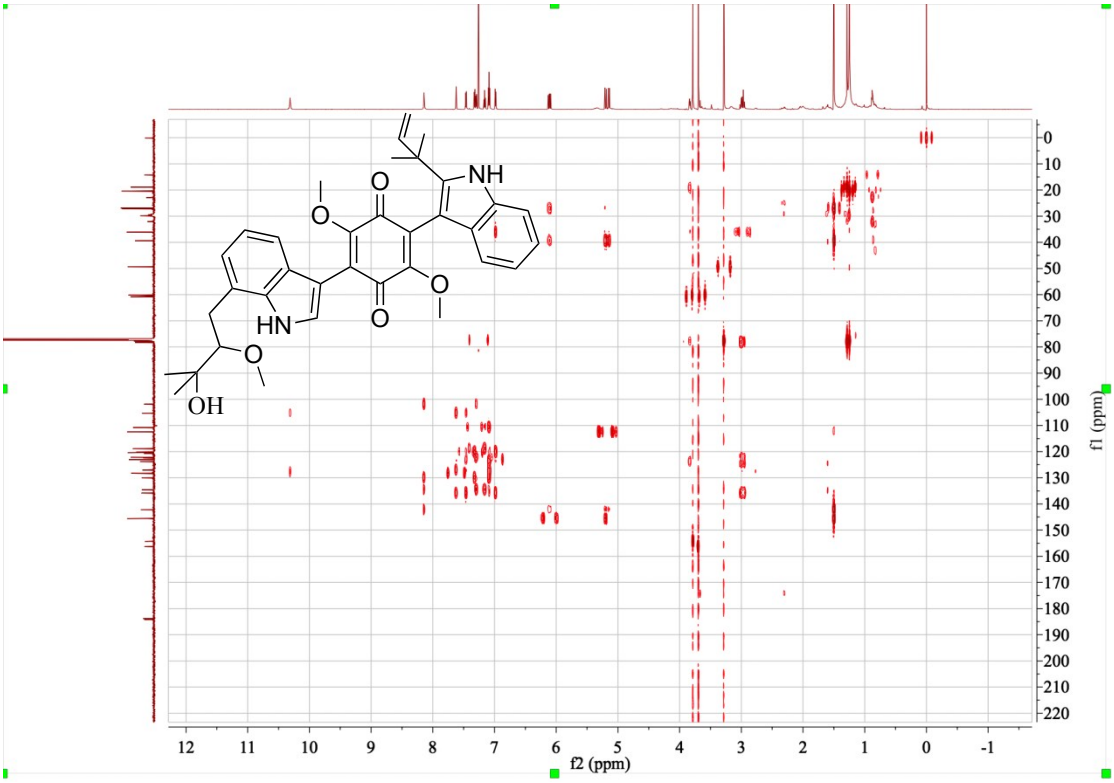


**Figure S49**. The HMBC spectrum of asterriquinone K (**6**) in $CDCl_3$

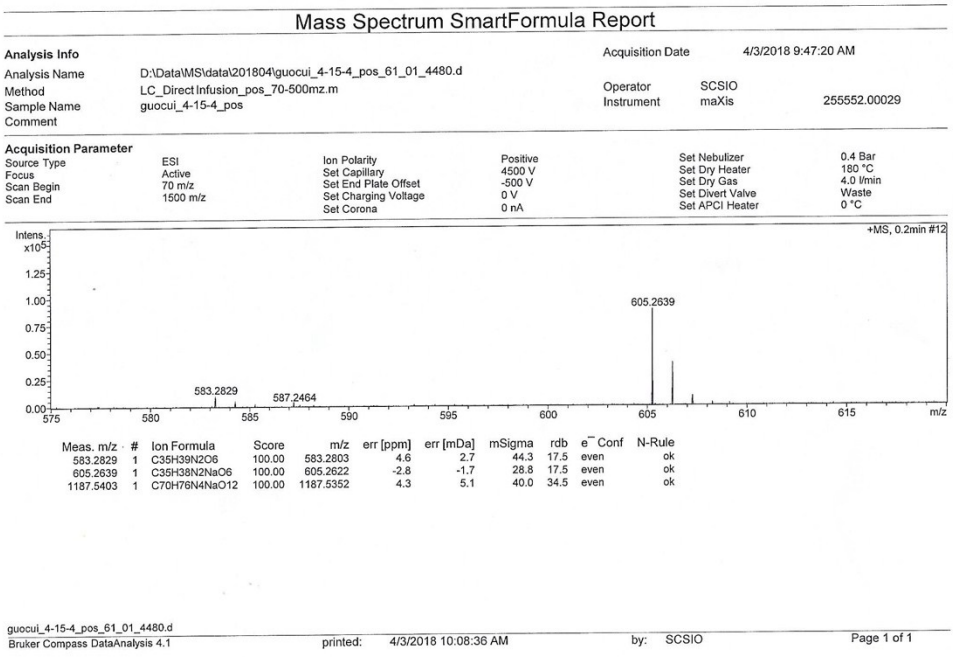


**Figure S50**. The HRESIMS spectrum of asterriquinone K (**6**)

光谱峰值检测报告

2018-06-19 16:39:34

数据集: File4-15-4 - RawData

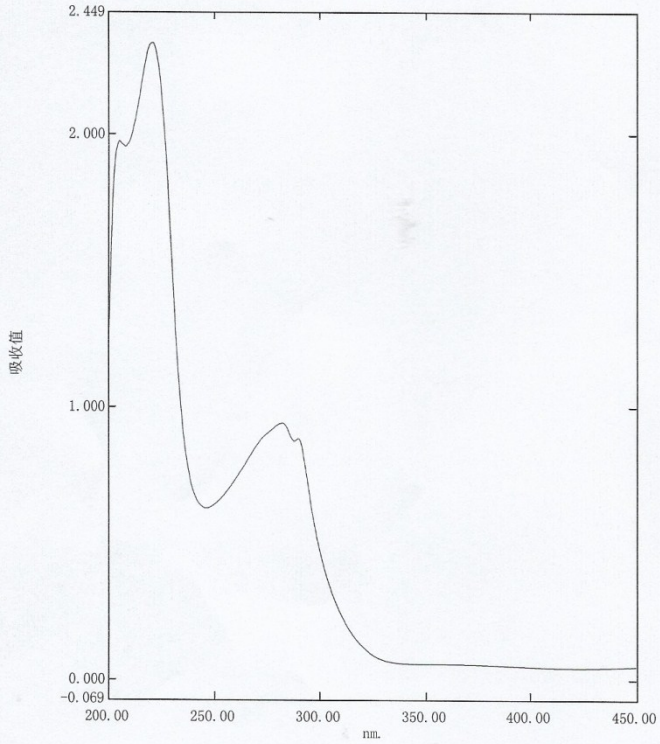


[测定属性]
波长范围 (nm.): 200.00 到 450.00
扫描速度: 中速
采样间隔: 0.2
自动采样间隔: 启用
扫描模式: 单个

[仪器属性]
仪器类型: UV-2600 系列
测定方式: 吸收值
狭缝宽: 2.0
积分时间: 0.1 秒.
光源转换波长: 323.0 nm
检测器单元: 直接
S/R 转换: 标准
阶梯校正: OFF

[附件属性]
附件: 无

[数据处理参数]
阈值: 0.0100000
点: 5
内插: 停用
平均: 停用

[样品准备属性]
重量:
体积:
稀释:
光程长:
附加信息:

| No. | P/V | 波长(nm) | 吸收值 | 描述 |
|---|---|---|---|---|
| 1 | ↑ | 289.60 | 0.885 | |
| 2 | ↑ | 282.20 | 0.943 | |
| 3 | ↑ | 220.80 | 2.335 | |
| 4 | ↑ | 205.20 | 1.974 | |
| 5 | ↓ | 287.80 | 0.878 | |
| 6 | ↓ | 246.40 | 0.631 | |
| 7 | ↓ | 208.00 | 1.954 | |

页 1 / 1

**Figure S51**. The UV spectrum of asterriquinone K (**6**)

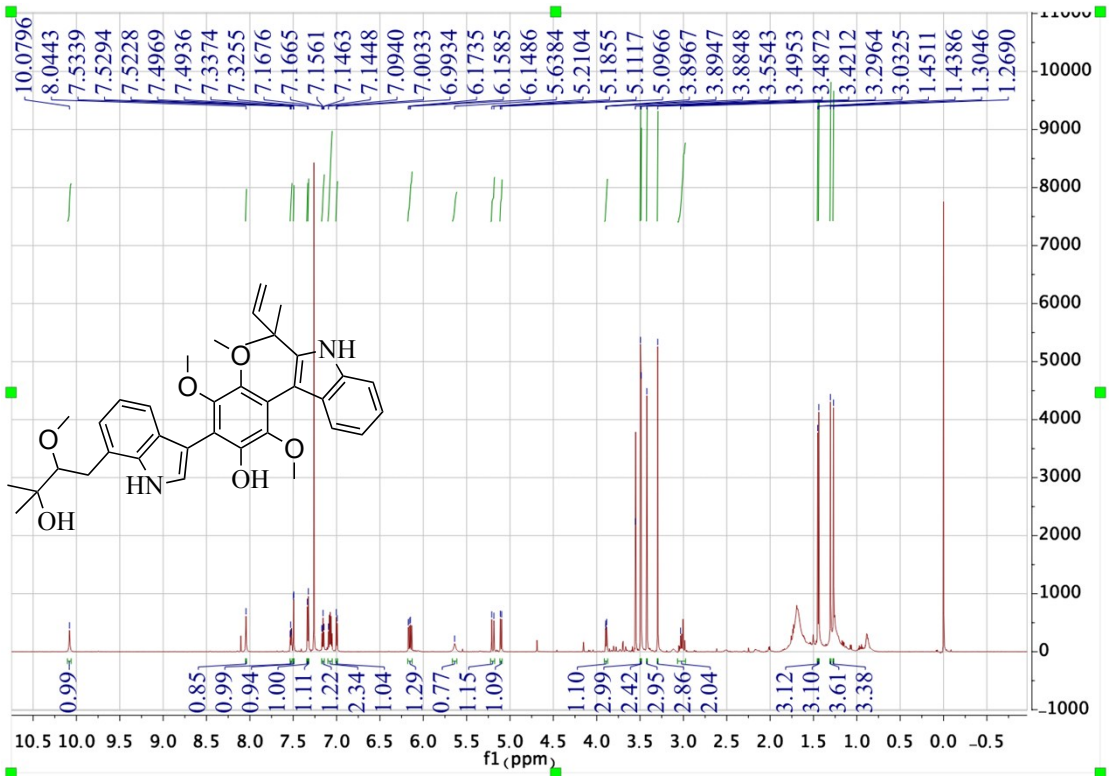


**Figure S52**. The $^{1}H$ NMR spectrum of asterriquinol G (**7**) in $CDCl_3$

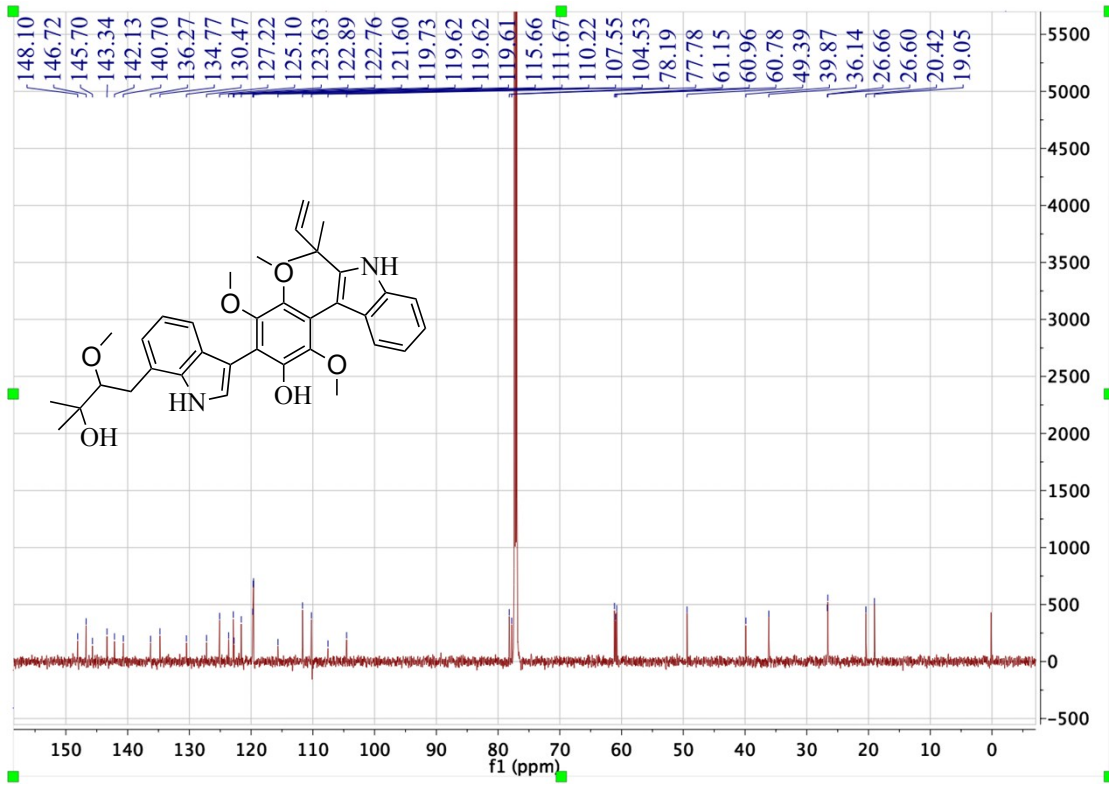


**Figure S53**. The $^{13}C$ NMR spectrum of asterriquinol G (**7**) in $CDCl_3$(175 MHz)

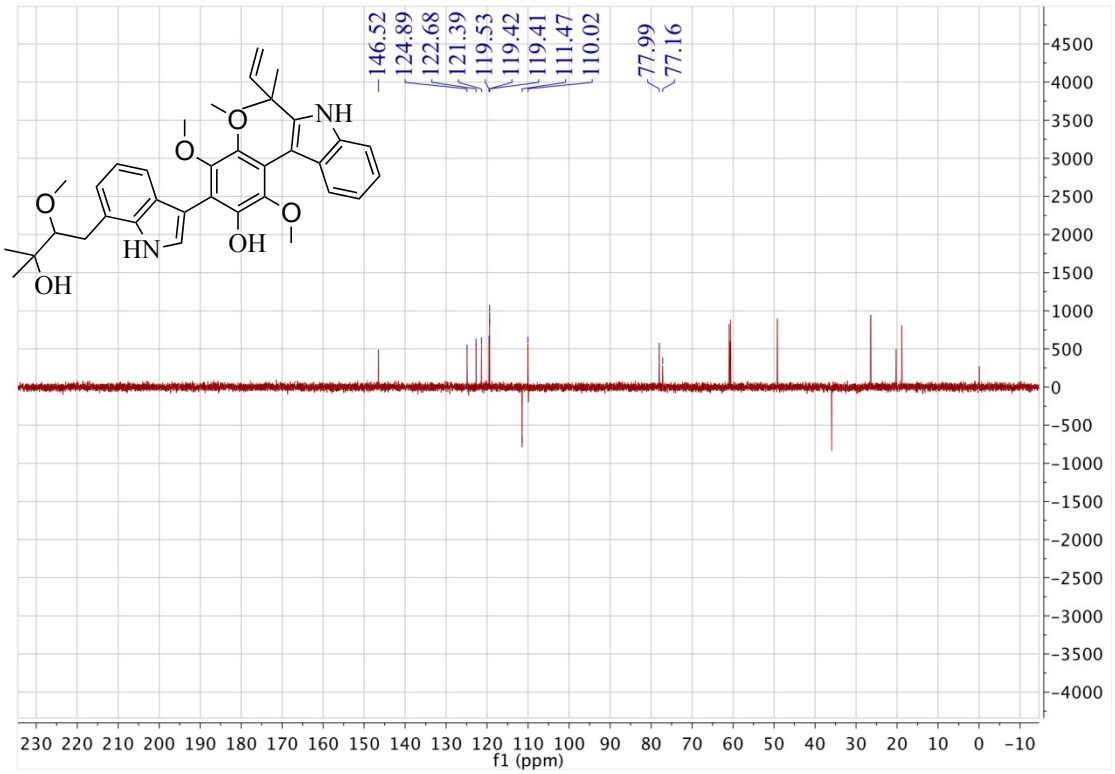


**Figure S54**. The DEPT spectrum of asterriquinol G (**7**) in $CDCl_3$

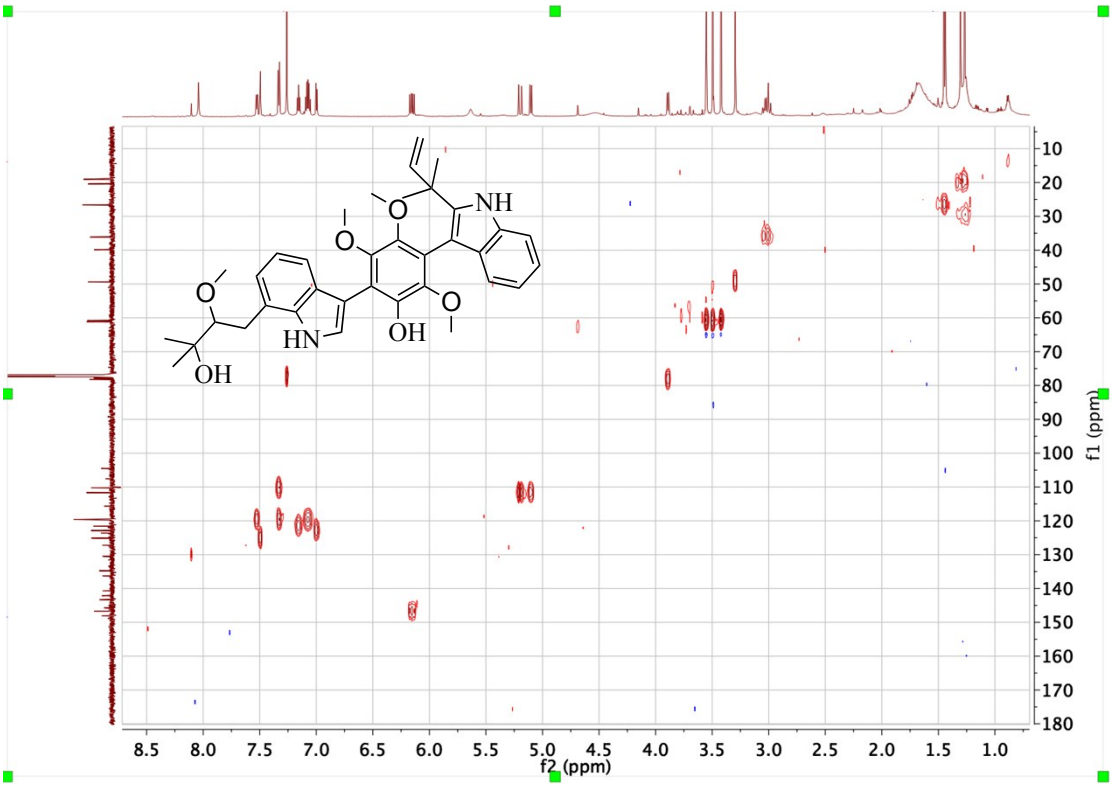


**Figure S55**. The HSQC spectrum of asterriquinol G (**7**) in $CDCl_3$

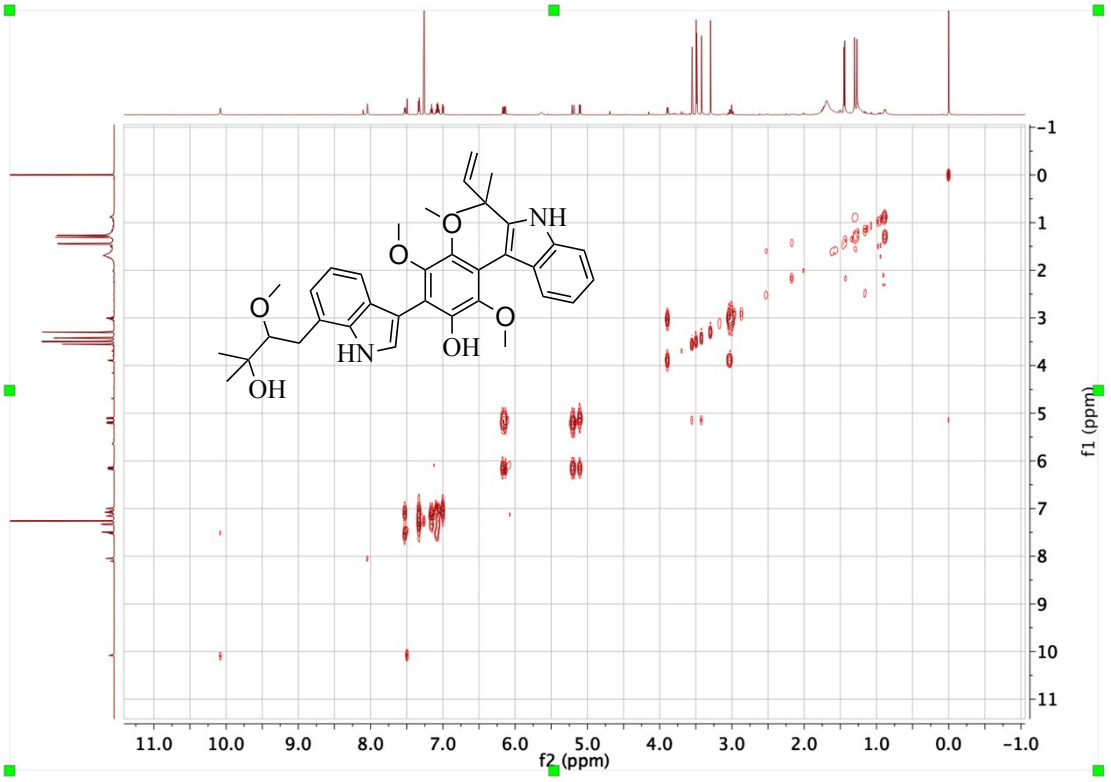


**Figure S56**. The $^{1}$H-$^{1}$H COSY spectrum of asterriquinol G (**7**) in $CDCl_3$

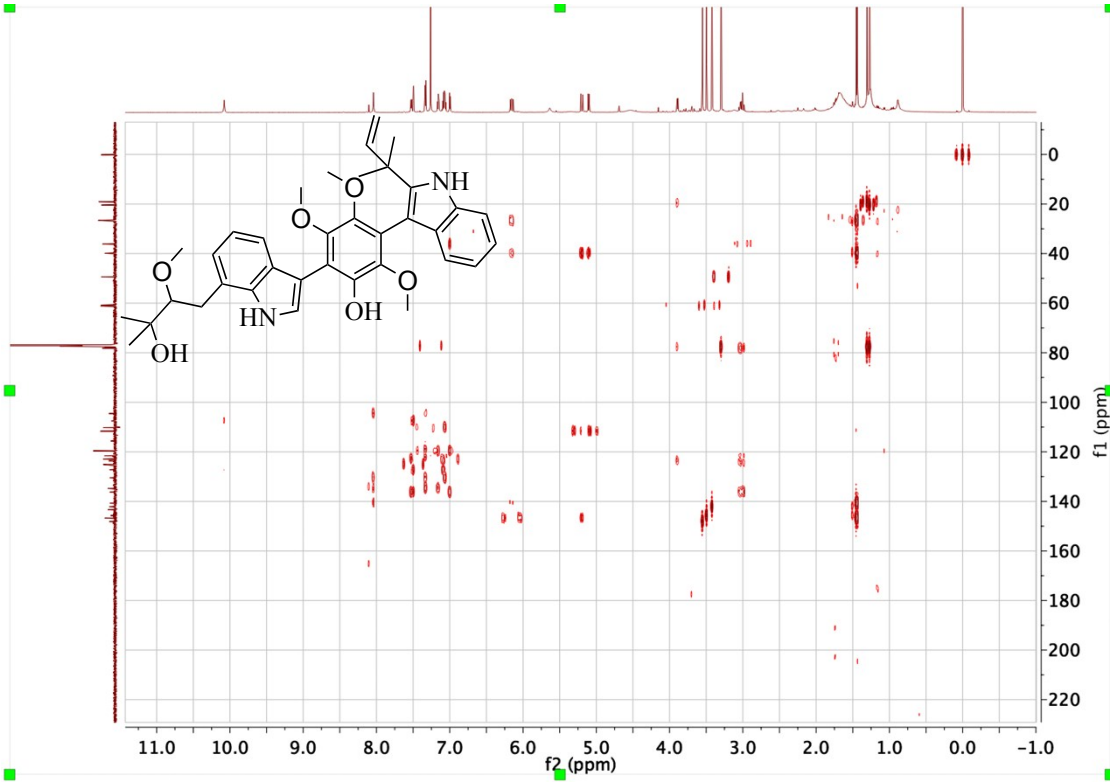


**Figure S57**. The HMBC spectrum of asterriquinol G (**7**) in $CDCl_3$

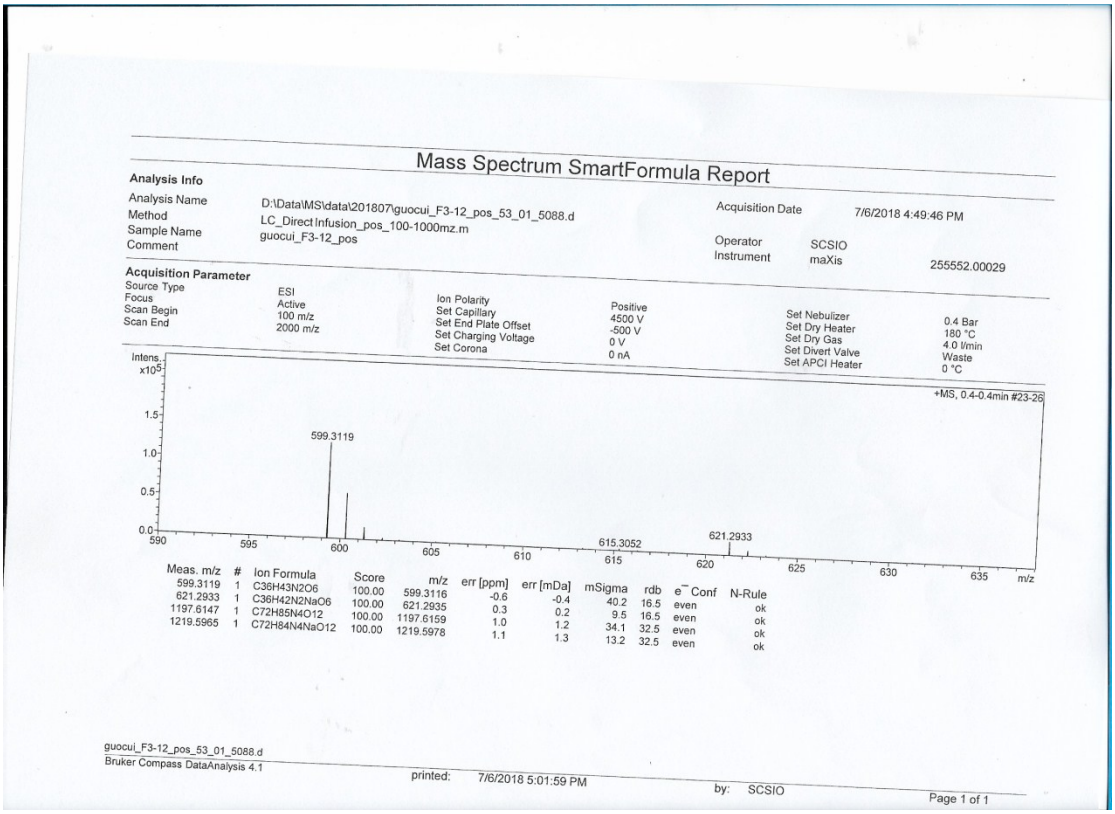


**Figure S58**. The HRESIMS spectrum of asterriquinol G (**7**)

光谱峰值检测报告

2018-09-30 16:59:31

数据集: f3-12- - RawData

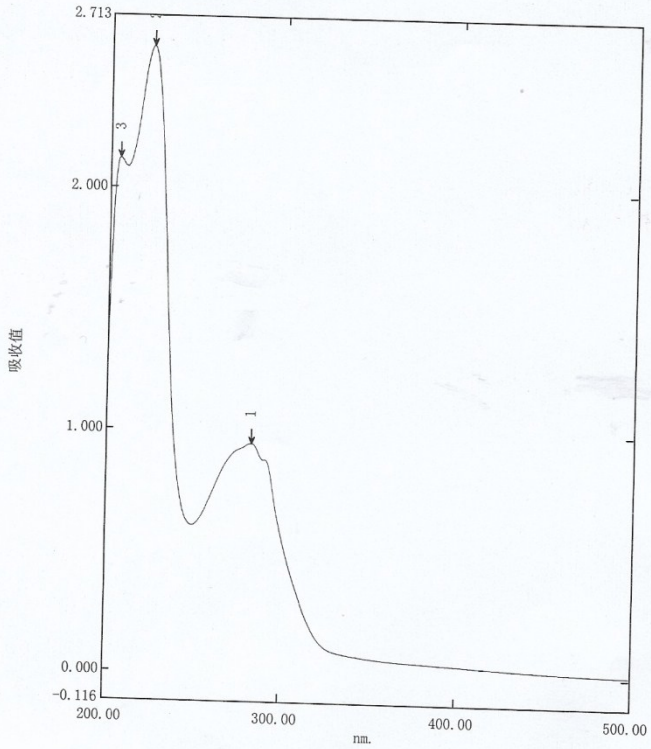


[测定属性]
波长范围 (nm.): 200.00 到 500.00
扫描速度: 中速
采样间隔: 0.2
自动采样间隔: 启用
扫描模式: 单个

[仪器属性]
仪器类型: UV-2600 系列
测定方式: 吸收值
狭缝宽: 2.0
积分时间: 0.1 秒.
光源转换波长: 323.0 nm
检测器单元: 直接
S/R 转换: 标准
阶梯校正: OFF

[附件属性]
附件: 无

[数据处理参数]
阈值: 0.0100000
点: 5
内插: 停用
平均: 停用

[样品准备属性]
重量:
体积:
稀释:
光程长:
附加信息:

| No. | P/V | 波长(nm) | 吸收值 | 描述 |
|---|---|---|---|---|
| 1 | ↑ | 282.60 | 0.947 | |
| 2 | ↑ | 223.80 | 2.584 | |
| 3 | ↑ | 205.60 | 2.119 | |



**Figure S59**. The UV spectrum of asterriquinol G (**7**)

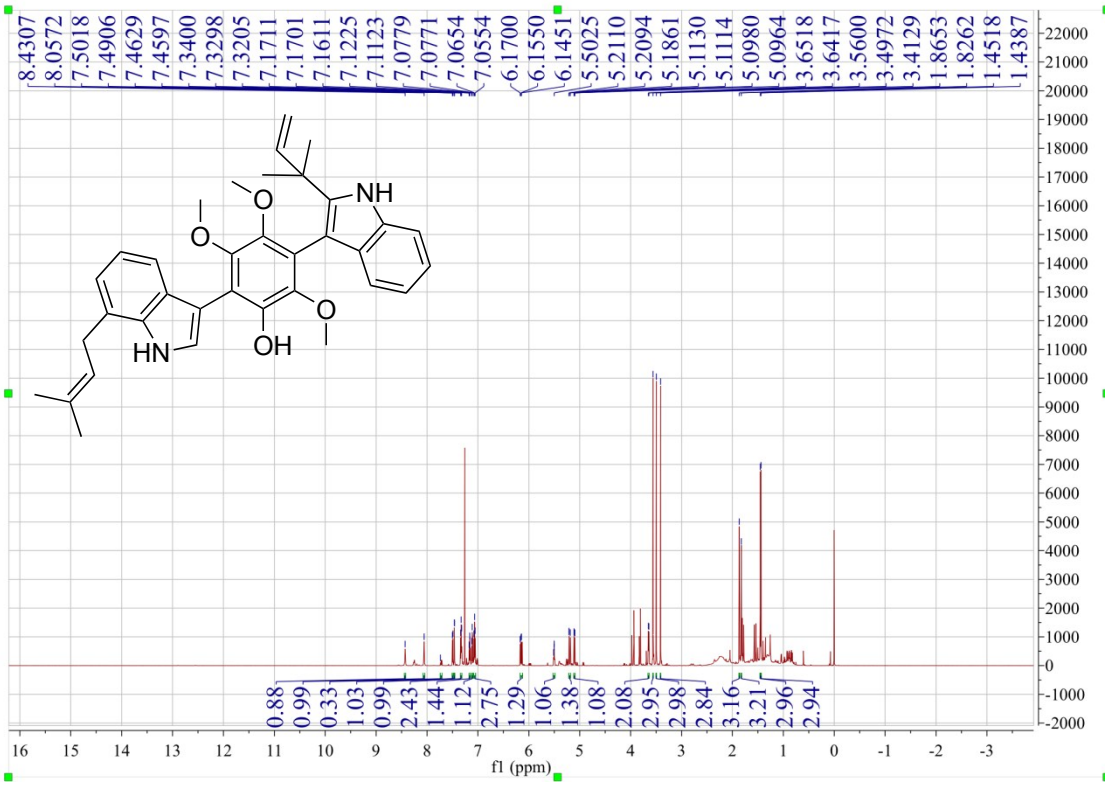


**Figure S60**. The $^{1}H$ NMR spectrum of asterriquinol H (**8**) in $CDCl_3$ (700 MHz)

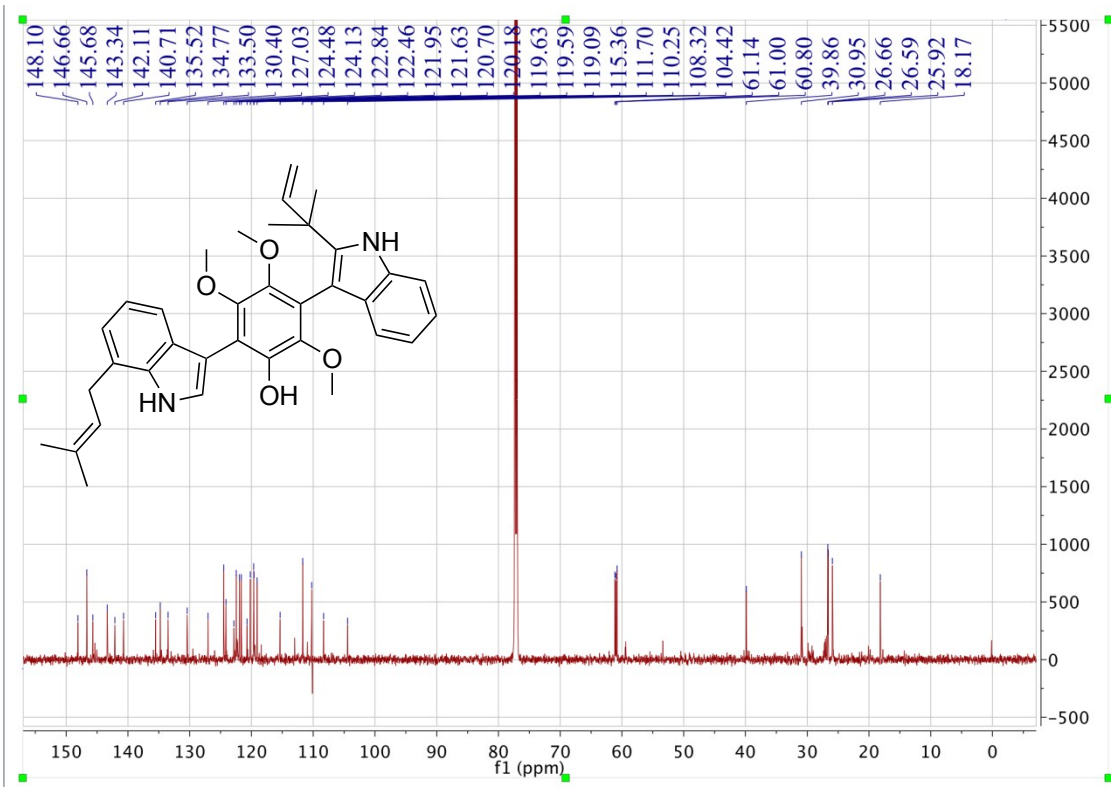


**Figure S61**. The $^{13}C$ NMR spectrum of asterriquinol H (**8**) in $CDCl_3$ (175 MHz)

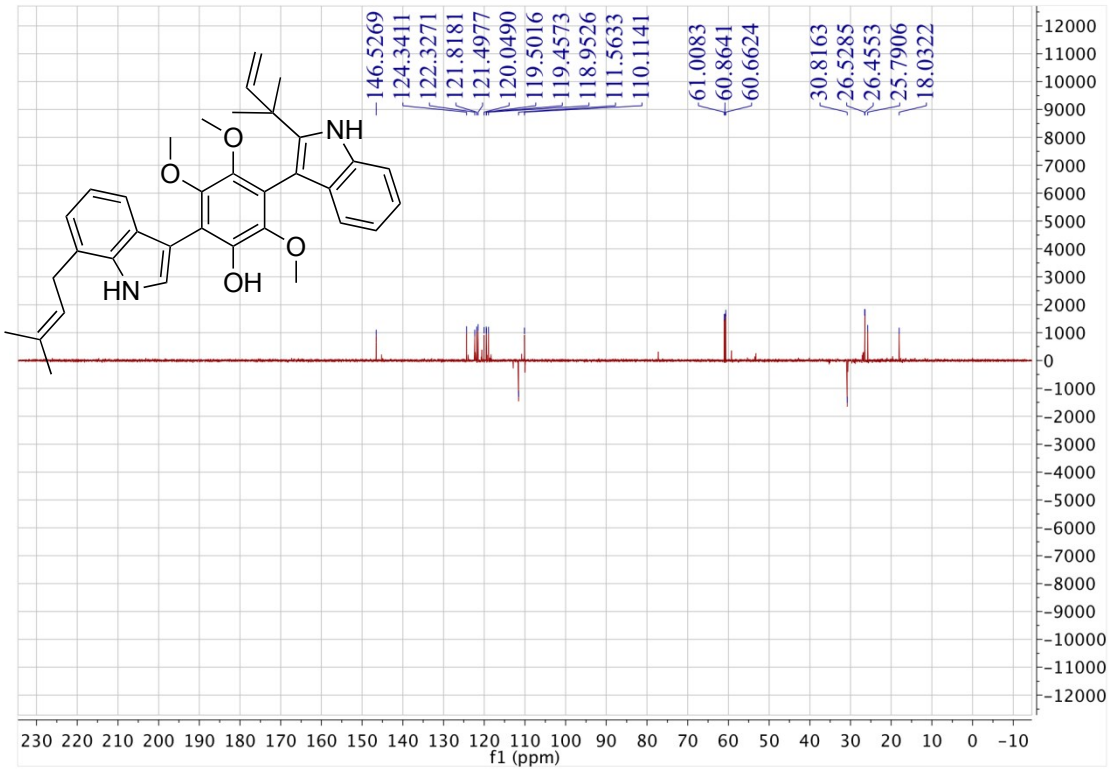


**Figure S62**. The DEPT spectrum of asterriquinol H (**8**) in $CDCl_3$ (175 MHz)

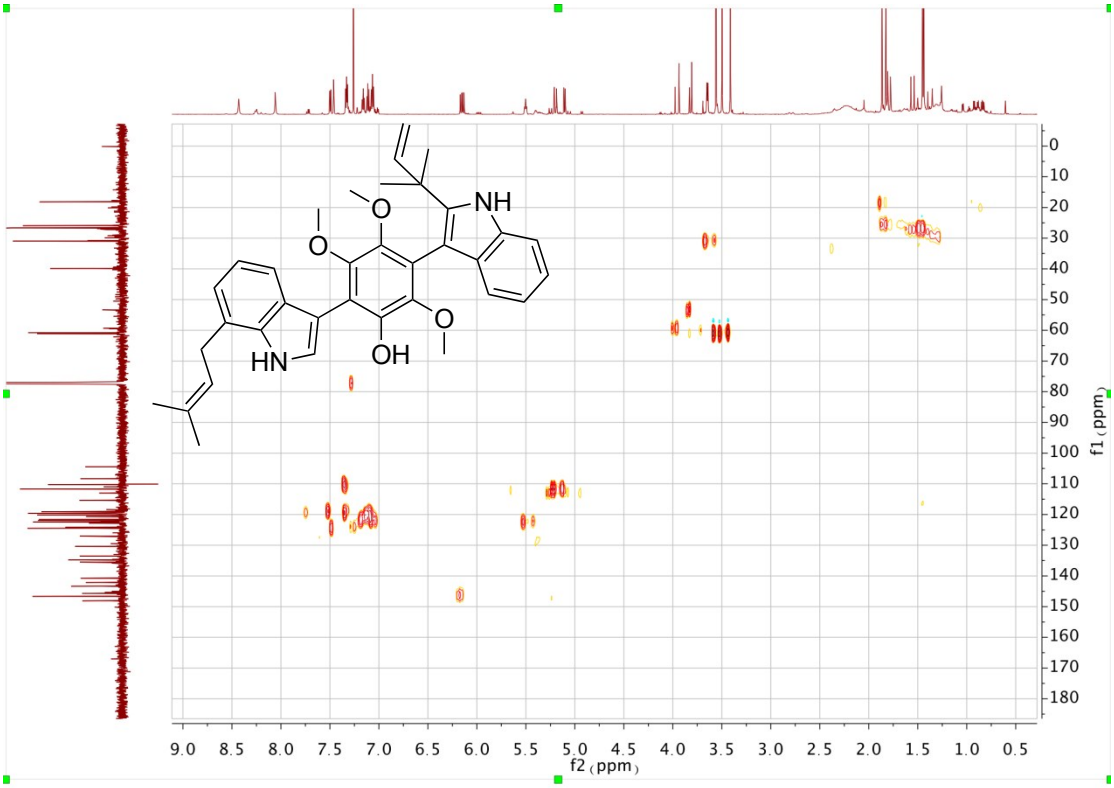


**Figure S63**. The HSQC spectrum of asterriquinol H (**8**) in $CDCl_3$

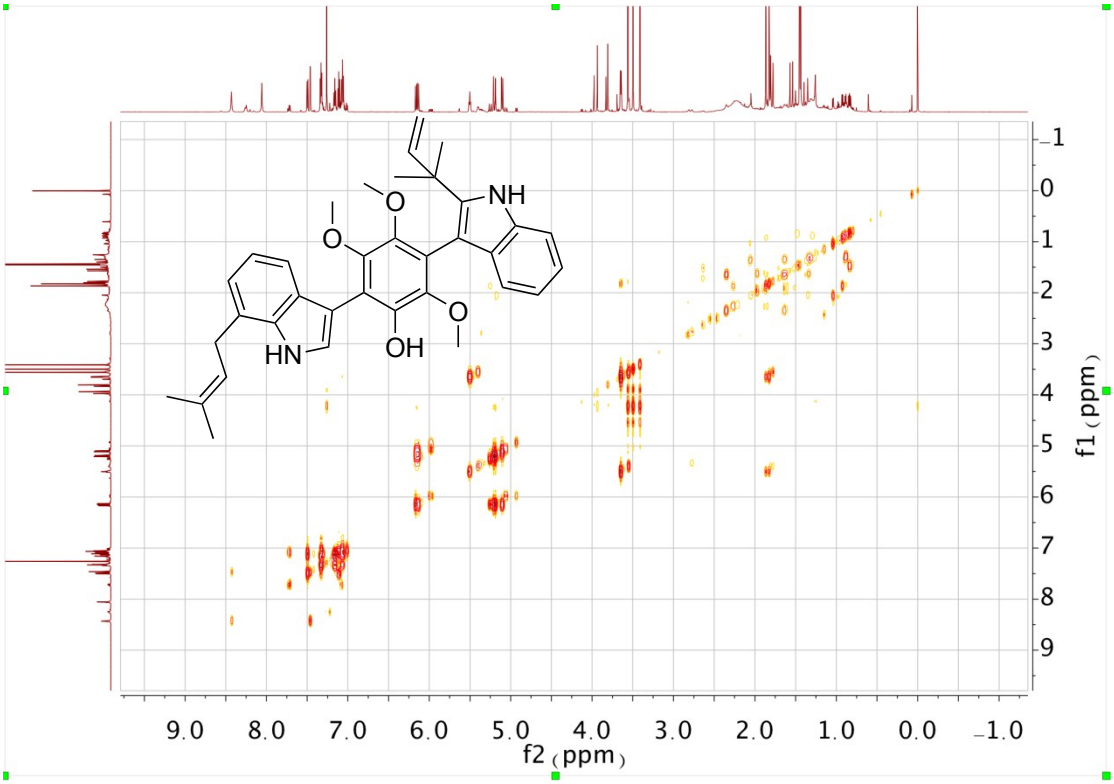


**Figure S64**. The $^{1}$H-$^{1}$H COSY spectrum of asterriquinol H (**8**) in $CDCl_3$

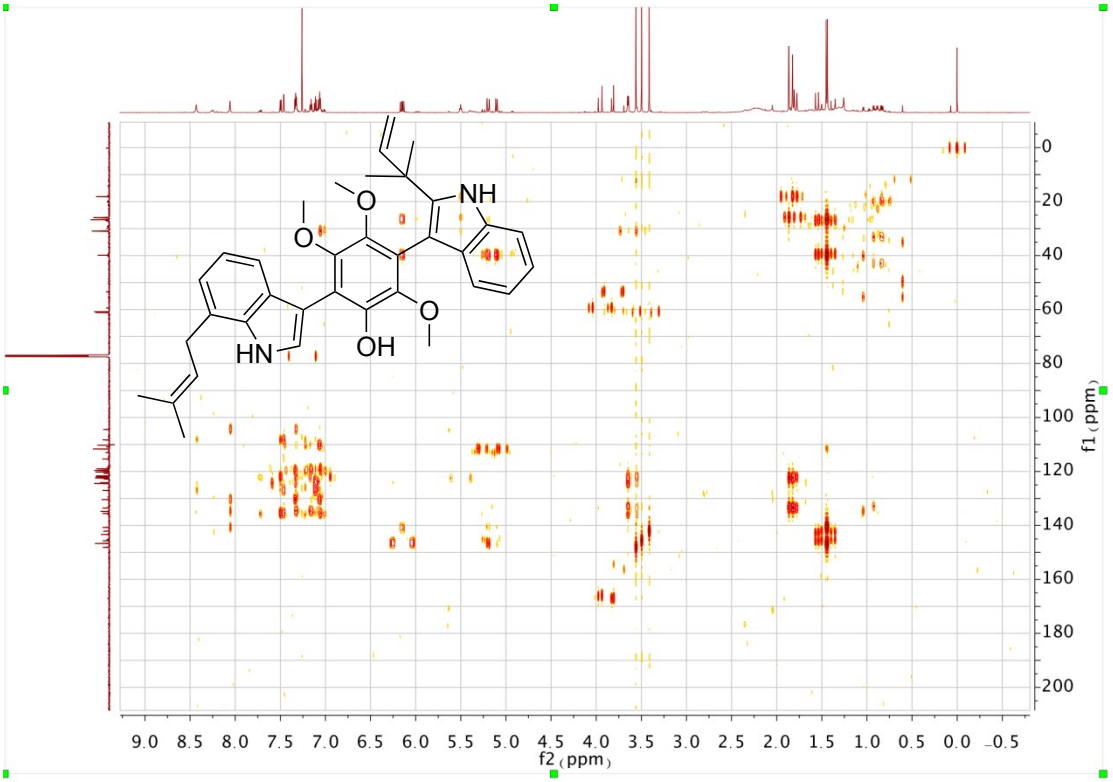


**Figure S65**. The HMBC spectrum of asterriquinol H (**8**) in $CDCl_3$

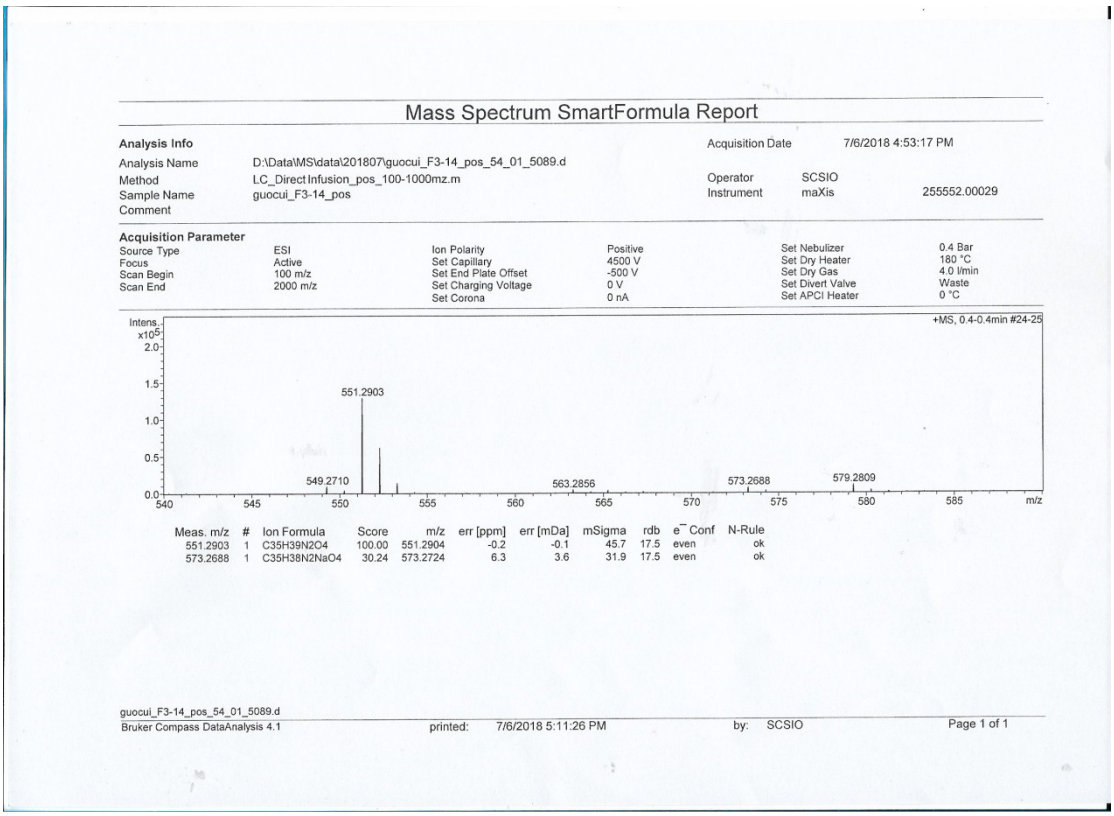
Mass Spectrum SmartFormula Report

**Analysis Info**

| | | | |
|---|---|---|---|
| Analysis Name | D:\Data\MS\data\201807\guocui_F3-14_pos_54_01_5089.d | Acquisition Date | 7/6/2018 4:53:17 PM |
| Method | LC_Direct Infusion_pos_100-1000mz.m | Operator | SCSIO |
| Sample Name | guocui_F3-14_pos | Instrument | maXis 255552.00029 |
| Comment | | | |

**Acquisition Parameter**

| | | | | | |
|---|---|---|---|---|---|
| Source Type | ESI | Ion Polarity | Positive | Set Nebulizer | 0.4 Bar |
| Focus | Active | Set Capillary | 4500 V | Set Dry Heater | 180 °C |
| Scan Begin | 100 m/z | Set End Plate Offset | -500 V | Set Dry Gas | 4.0 l/min |
| Scan End | 2000 m/z | Set Charging Voltage | 0 V | Set Divert Valve | Waste |
| | | Set Corona | 0 nA | Set APCI Heater | 0 °C |



| Meas. m/z | # | Ion Formula | Score | m/z | err [ppm] | err [mDa] | mSigma | rdb | e⁻ Conf | N-Rule |
|---|---|---|---|---|---|---|---|---|---|---|
| 551.2903 | 1 | C35H39N2O4 | 100.00 | 551.2904 | -0.2 | -0.1 | 45.7 | 17.5 | even | ok |
| 573.2688 | 1 | C35H38N2NaO4 | 30.24 | 573.2724 | 6.3 | 3.6 | 31.9 | 17.5 | even | ok |



**Figure S66**. The HRESIMS spectrum of asterriquinol H (**8**)

光谱峰值检测报告

2018-09-30 17:05:52

数据集: f3-14 - RawData

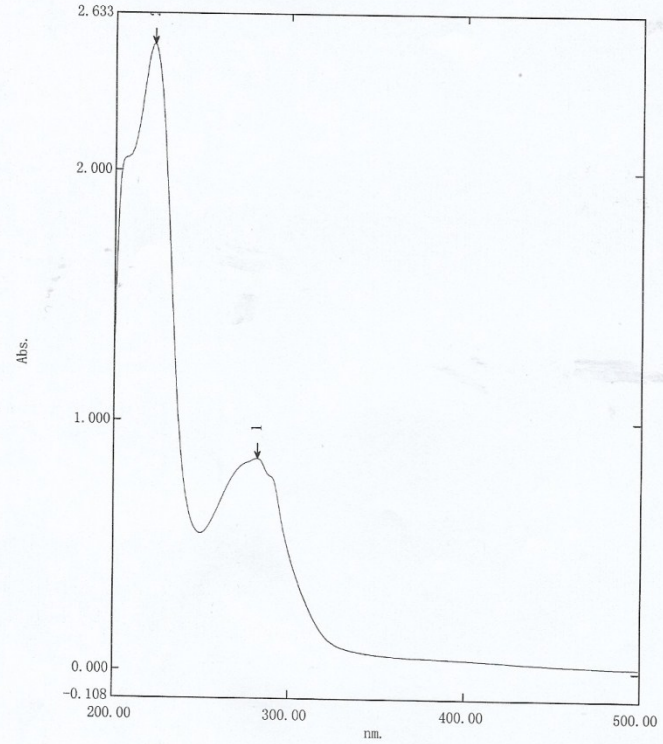


[测定属性]
波长范围 (nm.): 200.00 到 500.00
扫描速度: 中速
采样间隔: 0.2
自动采样间隔: 启用
扫描模式: 单个

[仪器属性]
仪器类型: UV-2600 系列
测定方式: 吸收值
狭缝宽: 2.0
积分时间: 0.1 秒.
光源转换波长: 323.0 nm
检测器单元: 直接
S/R 转换: 标准
阶梯校正: OFF

[附件属性]
附件: 无

[数据处理参数]
阈值: 0.0100000
点: 5
内插: 停用
平均: 停用

[样品准备属性]
重量:
体积:
稀释:
光程长:
附加信息:

| No. | P/V | 波长(nm) | 吸收值 | 描述 |
|---|---|---|---|---|
| 1 | ⊕ | 281.80 | 0.848 | |
| 2 | ⊕ | 222.20 | 2.509 | |



**Figure S67**. The UV spectrum of compound asterriquinol H (**8**)

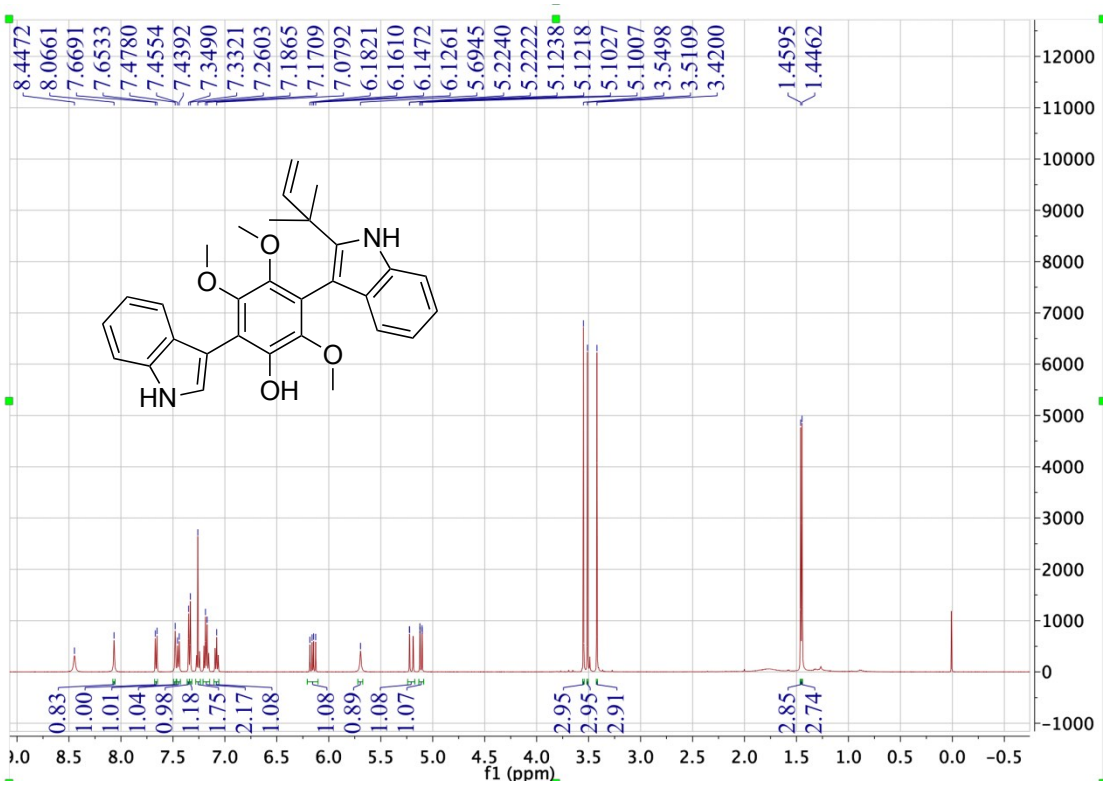


**Figure S68**. The $^{1}H$ NMR spectrum of asterriquinol I (**9**) in $CDCl_3$

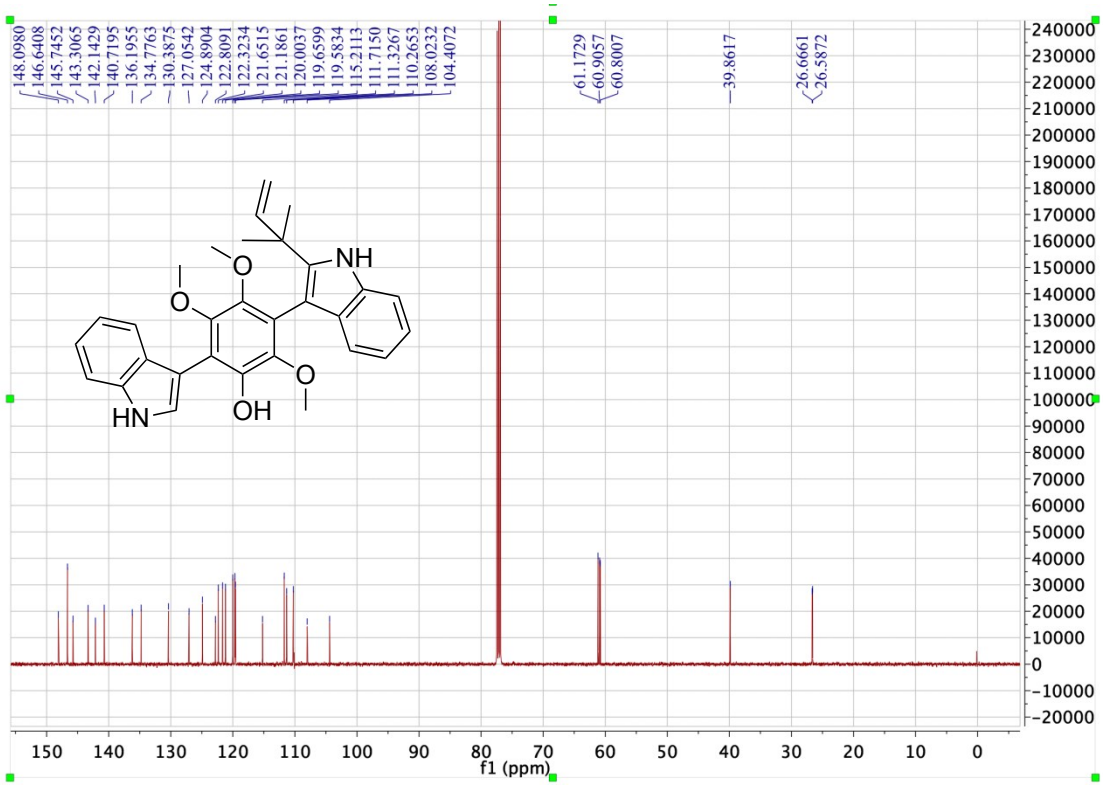


**Figure S69**. The $^{13}C$ NMR spectrum of asterriquinol I (**9**) in $CDCl_3$ (125 MHz)

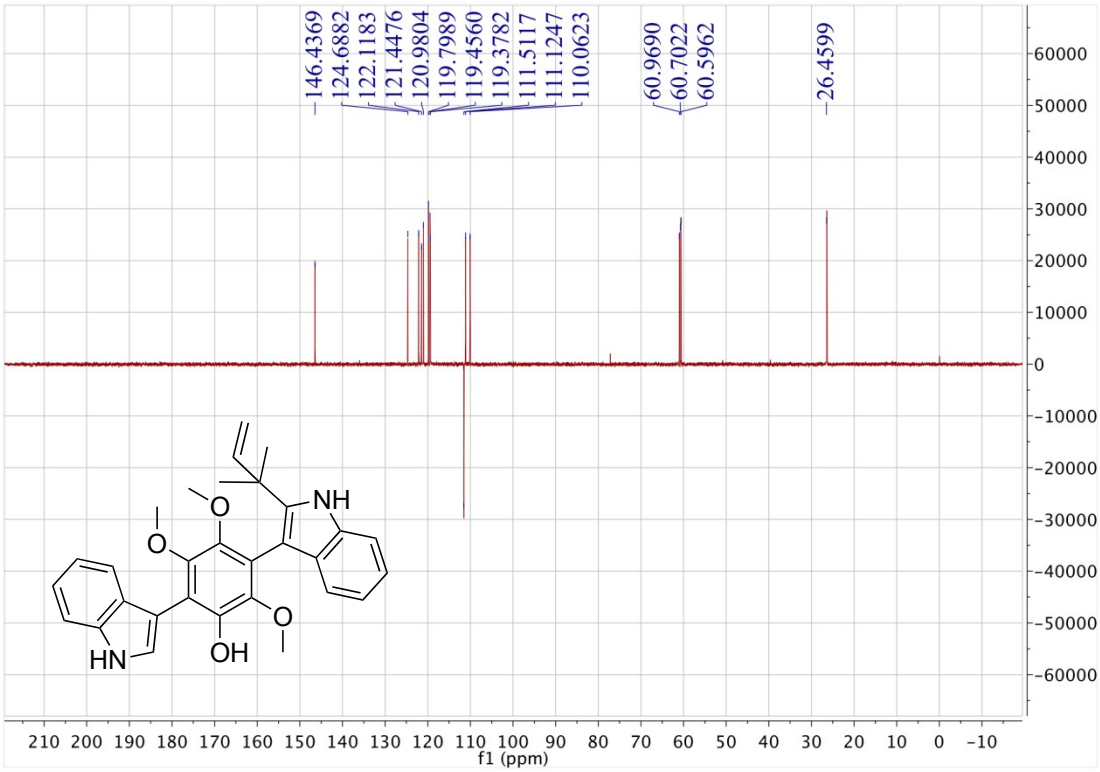


**Figure S70**. The DEPT spectrum of asterriquinol I (**9**) in $CDCl_3$

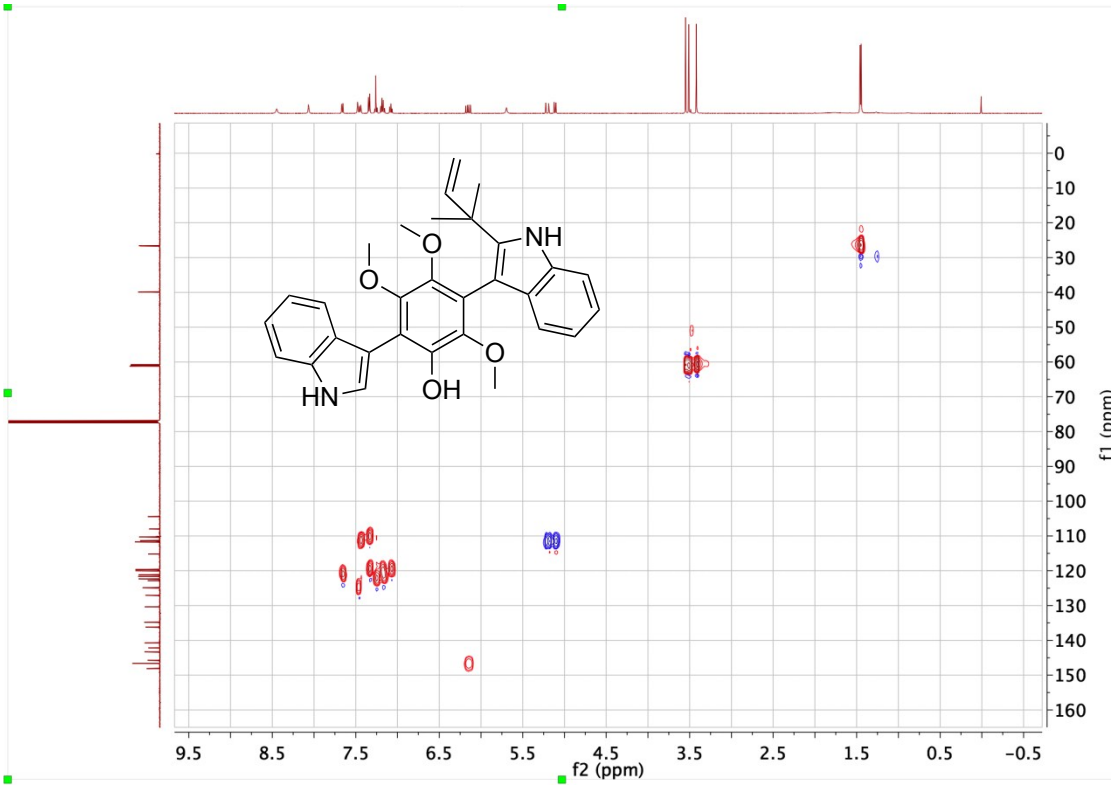


**Figure S71**. The HSQC spectrum of asterriquinol I (**9**) in $CDCl_3$

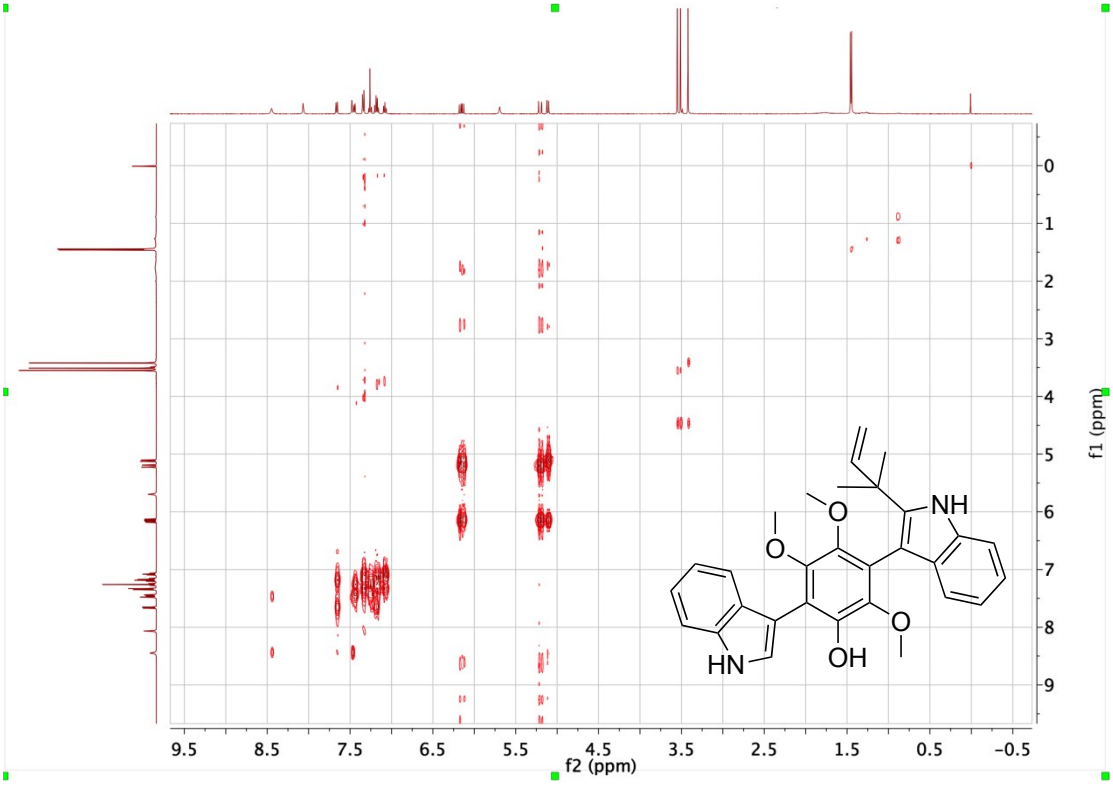


**Figure S72**. The $^{1}$H-$^{1}$H COSY spectrum of asterriquinol I (**9**) in $CDCl_3$

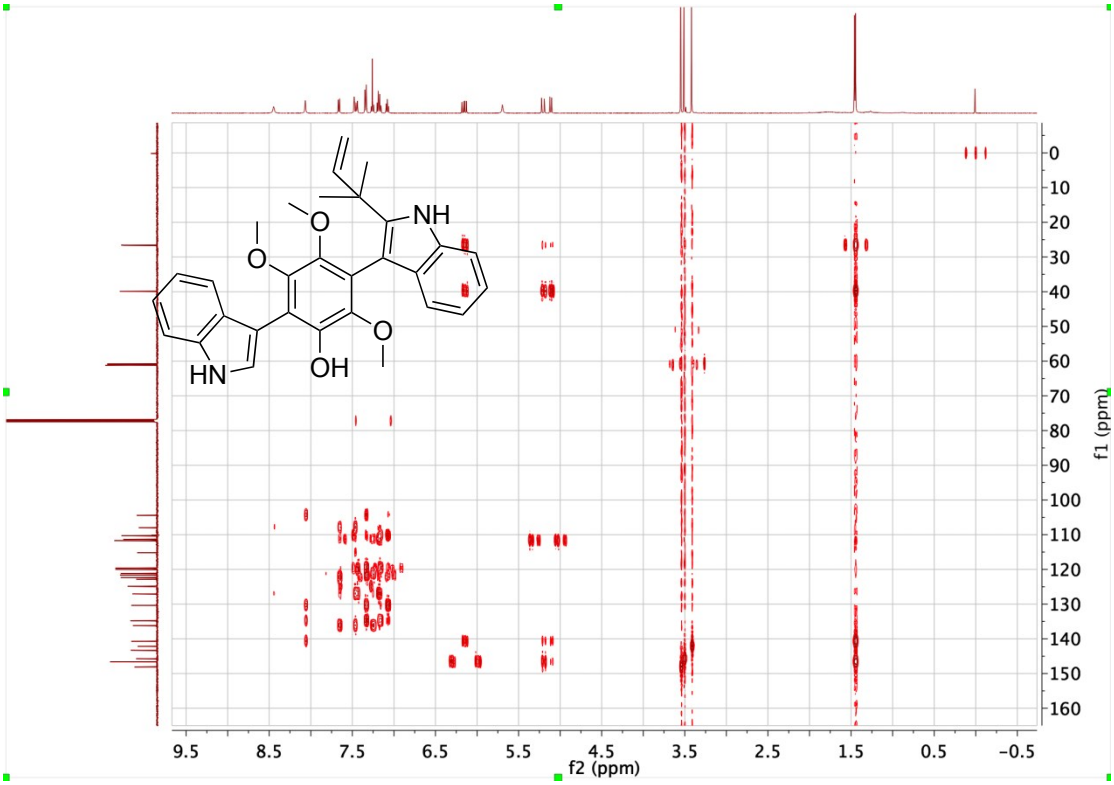


**Figure S73**. The HMBC spectrum of asterriquinol I (**9**) in $CDCl_3$

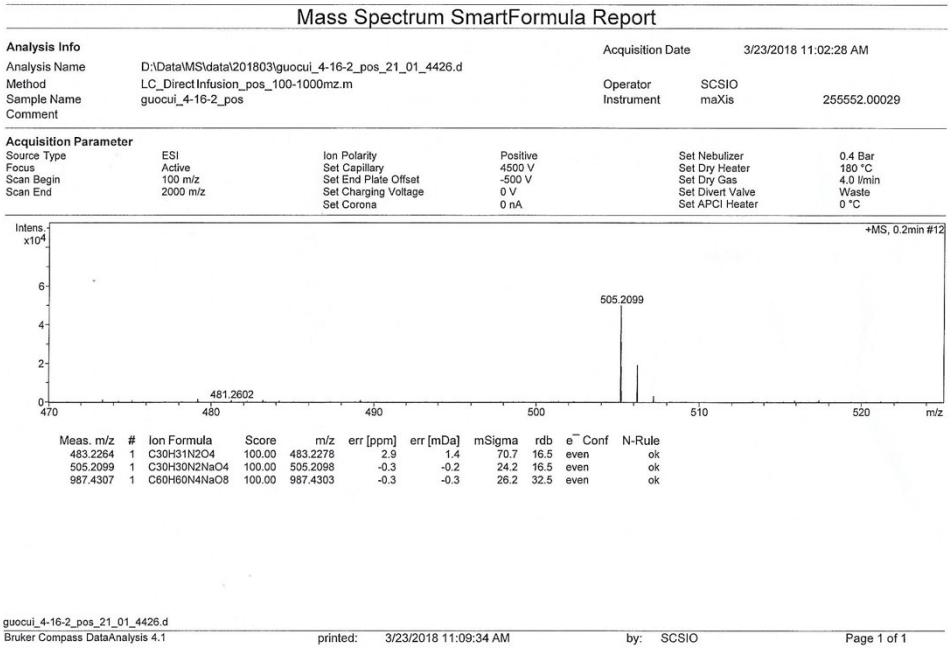


**Figure S74**. The HRESIMS spectrum of asterriquinol I (**9**)

光谱峰值检测报告

2018-09-05 17:33:49

数据集: 4-16-2-1 - RawData

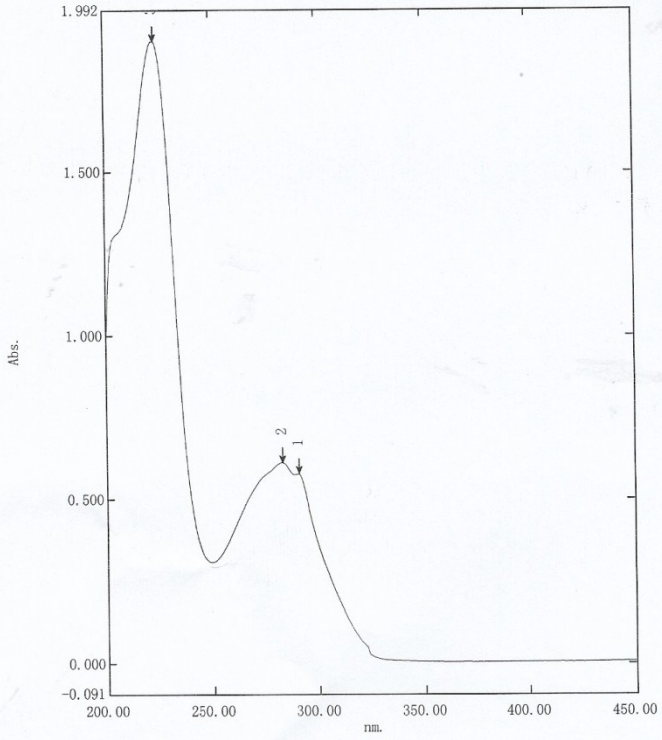


[测定属性]
波长范围 (nm.): 200.00 到 450.00
扫描速度: 中速
采样间隔: 0.2
自动采样间隔: 启用
扫描模式: 单个

[仪器属性]
仪器类型: UV-2600 系列
测定方式: 吸收值
狭缝宽: 2.0
积分时间: 0.1 秒.
光源转换波长: 323.0 nm
检测器单元: 直接
S/R 转换: 标准
阶梯校正: OFF

[附件属性]
附件: 无

[数据处理参数]
阈值: 0.0100000
点: 5
内插: 停用
平均: 停用

[样品准备属性]
重量:
体积:
稀释:
光程长:
附加信息:

| No. | P/V | 波长(nm) | 吸收值 | 描述 |
|---|---|---|---|---|
| 1 | ↑ | 290.60 | 0.577 | |
| 2 | ↑ | 282.80 | 0.612 | |
| 3 | ↑ | 223.80 | 1.897 | |



**Figure S75**. The UV spectrum of asterriquinol I (**9**)